University of Nevada, Reno

Verification of ECPC's Regional Spectral Model Fire Climate and Fire Danger Forecasts

A thesis submitted in partial fulfillment of the requirements for the degree of Master of Science in Atmospheric Science

Hauss J. Reinbold

Dr. Timothy Brown/Thesis Advisor

December 2003

Abstract

The Scripps Experimental Climate Prediction Center (ECPC) has been making extended regional forecasts of atmospheric elements and fire danger indices since September 27, 1997. This study performs a verification of these forecasts in comparison with remote automated weather station (RAWS) observations in the western US. Verification of ECPC validating observations versus RAWS observations is also performed. Bias, root-mean square error, and anomaly correlations are computed for daily 2-meter maximum, minimum, average temperature, 2-meter maximum, minimum, and average relative humidity, precipitation and afternoon 10-meter wind speed, and four National Fire Danger Rating System indices - ignition component, spread component, burning index, and energy release component. Of the atmospheric elements, temperature generally correlates the highest in all three verifications, and relative humidity, precipitation, and wind speed are less correlated. Overall, fire danger indices have much lower correlations, but do show useful spatial structure in some areas such as Southern California, Arizona, and Nevada.

Acknowledgements

As much as I might like to imagine that this thesis was a solo, superhero effort on my part, it was not. A radioactive spider did not bite me, nor was I shipped here from a doomed planet. Coincidentally, my brain is not the result of a mutation that renders me super intelligent. Therefore, as a human not enhanced in any way, I must acknowledge that this paper would not have been finished without the help of others.

First and foremost, Dr. Tim Brown helped make this paper what it is, both in research and editorial aspects. I am grateful for his assistance, without which I might not have made it this far. I consider him Tim, the Wise and Powerful. Dr. John Roads at Scripps has always been very encouraging and I appreciate the times he flew up here to assist me in research directions. Dr. Franco Biondi graciously sat on my committee, and provided valuable feedback.

The rest of the CEFA group contributed in various ways. Beth Hall has always been willing to answer my questions and provide feedback when I barge into her office demanding answers. Charlie Mohrle was always there for commiseration in the lab. Paul Schlobohm is one of the friendliest people I know and continues to put up with me. Crystal Kolden and Ryan Kangas I did not have much contact with for most of the thesis, but have always been friendly, which is nice after a hard night of fighting cri-, um, working on my thesis.

My parents have always encouraged me to get the highest degree of education possible, and I am grateful for their support. My brother showed almost a complete lack of interest, but that's what I love about him. Matt Heinrich and Kaleb Cockrum helped keep me sane during the last month or so. Matt Waters sent me a used baby pacifier as

congratulations for passing the defense, which entertained and worried me. I am grateful to Kara Cockrum for being the first and currently only person to refer to me by my new title, even if it's not technically official yet. Bethany Willison finished her master's first, which made me jealous and gave me additional encouragement to get mine.

There is one non-human acquaintance I would also like to thank. A big thank you to Scalper, the horse who so callously broke my wrist in August of 2000. Had it not been for him, I may never have gotten here. Thanks again Scalper, whenever I use glue, I think of you.

Table of Contents

Figures

CHAPTER 1

INTRODUCTION

The three environmental factors that determine fire behavior are fuel, topography and weather (the fire behavior triangle; e.g., Pyne 1996). Of these, weather varies most over time and space. The effects of various weather elements on fire behavior range from extreme to subtle. High winds can spread a fire quickly, sometimes dominating the influence of fuels or topography. The temperature and relative humidity cycle can enhance fire activity in midday (high temperatures, low relative humidity), while hindering fires at night (low temperatures, higher relative humidity). Precipitation can hinder the propagation and ignition of a fire, but also helps provide fuel moisture content both through the total amount of precipitation in a given time period and the duration of each precipitation event (a small amount of precipitation for ten minutes will not have a strong effect on long-term fuel moistures). There are other natural atmospheric factors important for fire, such as lightning strikes as effective ignition sources for wildfires, and the stability of the air that affects both fire activity and air quality. However, it is the basic elements of atmospheric temperature, moisture and wind, and their relation to fuels that are fundamental for both fire behavior and fire danger.

While fire behavior is the direct fire reaction to the influences of fuel, topography, and weather, fire danger is the resultant descriptor of factors affecting fire initiation, spread and difficulty of control (NWCG 2002). In response to a long history of fire protection programs, the current version of the National Fire Danger Rating System (NFDRS; Bradshaw *el al*. 1983), which incorporates fuel, topography and weather in

calculating fire danger indices, was released in 1978. The primary output indices are used to support strategic fire management decisions. These fire danger indices are relative and can be used locally, but are meant to cover a fire danger rating area on the order of 5,000-200,000 hectares spatial scale. The strategic decisions NFDRS impacts include public awareness, the readiness and staffing levels of an agency, restrictions and closures on public and industrial activity, appropriate suppression resources to dispatch to initiating fires, and the amount of funding or resources for an area (Schlobohm 2003).

Given the relevance of atmospheric inputs into both fire danger and behavior, and the importance of these factors in the fire environment, effective fire management then relies, in part, on the present and future knowledge of weather conditions.

Problem Definition

In order for land managers to allocate fire control resources most efficiently (both for fire use and fire suppression), they need to anticipate the location, timing, and severity of fire danger. The current operational implementation of NFDRS does not provide this knowledge beyond short-range forecasts (some fire weather meteorologists produce 10-day forecasts utilizing a personal computer version of NFDRS calculations). Therefore, identifying fire danger on a weekly, monthly, or seasonal scale requires an implementation of NFDRS that generates fire danger indices at these time scales. There is also an evolving interest in increasing the spatial resolution of NFDRS, as discussed by Schlobohm (2003). The most difficult aspect of predicting fire danger indices at monthly and seasonal time scales is the prediction of the weather elements that NFDRS requires. Developing a climate model that accurately predicts relevant weather elements at

monthly and seasonal time scales is then a necessary part of the accurate prediction of fire danger indices for fire management decisions.

The Experimental Climate Prediction Center (ECPC) at the Scripps Institution of Oceanography has been making extended Regional Spectral Model (RSM) forecasts since September 27, 1997 (Roads 2003a,b). This model produces regional 16-week (four-month) forecasts of common atmospheric elements such as temperature, relative humidity and precipitation every weekend, which are also directly relevant to fire weather meteorologists, fire and fuel specialists and fire management. In addition to these elements, the RSM also calculates fire danger indices for the continental United States. While the skill of the meteorological variables and fire danger indices of this RSM model have been examined (Roads *et al*. 1991, 2003), they have been primarily ascertained against the network of observations used to initialize the model. However, the observations used to initialize the model are taken primarily from urban sites and other locations that are not necessarily representative of fire danger areas.

It is therefore of interest to assess and understand the skill of the RSM in comparison to observed atmospheric measurements and fire danger indices. Land managers will, as a result of this analysis, be able to identify the location, time scale, and time of year where the model is most skillful. This will provide an improved understanding of model forecast skill, and help establish a level of trust or confidence to be placed in an RSM forecast for a given time and location. For research meteorologists, this analysis functions as a performance measure that will be helpful in fine-tuning and further development of the model itself.

Research objectives

Land management agencies retain an observational network of remote automated weather stations (RAWS) for fire weather related measurements. The objective of this study is to assess the accuracy of the ECPC weekly, monthly and seasonal RSM forecasts, as compared to RAWS observations, with emphasis on the elements most related to fire danger (e.g., temperature, moisture and wind), as well as an evaluation of predicted fire danger indices. Specific ECPC forecast atmospheric elements examined include maximum, minimum and average daily surface temperature, maximum, minimum and average daily surface relative humidity, surface wind speed, precipitation amount and precipitation duration. The ECPC forecast fire danger indices that are examined include the Burning Index (BI), Spread Component (SC), Energy Release Component (ERC) and Ignition Component (IC). While ECPC has already performed accuracy tests on both atmospheric and fire danger model output, they have not done so with RAWS data. The analysis in this study complements the skill tests performed by ECPC.

Though the ECPC forecasts cover the continental U.S., the primary RAWS network is currently located in the West. Thus, the western U.S. is the spatial focus of this study. Geographic sub-regions are individually evaluated to increase the spatial resolution of the analysis. Temporally, the study includes year-round model performance, as well as the distinct summer and winter seasons.

Contents

Following the introduction and objectives in Chapter 1, Chapter 2 gives a more detailed examination of the history and operation of the RSM, including a summary of

some of the previous skill tests performed on the model. The NFDRS will also be discussed in greater detail.

Chapter 3 describes the origin and details of the RAWS, ECPC validation and ECPC forecast datasets. The description will include how and when they are generated, as well as what spatial domain they cover.

Chapter 4 outlines the methodology used in preparing and analyzing the data. This includes a section on the statistical measures of skill used in this study.

Chapter 5 presents the analysis in terms of temporal variations. The main focus is on how RAWS observations compare to the RSM forecasts. This is compared and contrasted with how the RAWS observations compare to the RSM validation observations as well as how the RSM validation observations compare to the RSM forecasts.

Chapter 6 discusses the analysis in terms of spatial variations. Again, the main focus is on how RAWS observations compare to the RSM forecasts. This is compared and contrasted with how the RAWS observations compare to the RSM validation observations as well as how the RSM validation observations compare to the RSM forecasts.

Chapter 7 discusses and summarizes the results, including the potential value of the seasonal forecasts to both land managers and interested researchers.

CHAPTER 2

BACKGROUND

The ECPC Regional Spectral Model

Since Sept. 27, 1997, the ECPC has been making experimental long-range forecasts of variables relevant to fire danger, at both global and regional scales (Roads *et al*. 2001, 2002, 2003a,b; Chen *et al*. 2001). As explained by Roads and others (2003a,b), the global model is based on an older version of the global spectral model (GSM; Kalnay *et al*. 1996; Roads *et al*. 1999) used by the National Centers for Environmental Prediction (NCEP) for the NCEP/NCAR reanalysis. This GSM is then used to create boundary conditions for a regional spectral model that is run at varying degrees of resolution over different areas including the United States, the southwestern United States, California, and Brazil (Juang *et al*. 1997), which are run at a spatial resolution higher than the GSM.

The GSM used by ECPC is based on a version of the NCEP medium range forecast model (MRF) used for making 6-14 day predictions and to produce the global data assimilation system (GDAS) that runs four times daily. As of 1995, this GSM is the global model used in NCEP/NCAR reanalysis (Kalnay *et al*. 1996; Roads *et al*. 1999). Caplan and others (1997) describe the improvement of the GSM over a period of several years (1992-1996). The GSM is based on virtual temperature, humidity, surface pressure, mass continuity, vorticity, and divergence prognostic equations, all in a hydrostatic or primitive equation system. It uses terrain following sigma coordinates, where sigma is defined as the ratio of ambient pressure to surface pressure (Roads 2001). The 18

irregularly spaced vertical levels are clustered around the lower boundary and the tropopause. The GSM uses spherical harmonics with a triangular truncation of 62 as the base horizontal spatial functions (Juang and Kanamitsu 1994). Spectral models use continuous wave functions to represent model parameters spatially (usually in the horizontal), but must be transformed to a grid for display. In this case, spherical harmonics with a triangular truncation of 62 translates to a grid with 2-degree (about 200 km) resolution globally. Included in the physics package for the GSM is an in depth land parameterization (Pan 1990; Chen 1996), as well as boundary layer processes, enhanced topography, large-scale condensation, gravity wave drag, and cloud/radiation (shortwave and longwave) interactions (Hong and Leetma 1999; Hong and Pan 1996).

The ECPC GSM makes 7-day forecasts every day, and 16-week forecasts every weekend for atmospheric elements including precipitation, temperature, humidity, surface pressure, 500mb, 700mb and 1000mb heights, wind speed and direction, latent heat, upward and downward longwave radiation, net surface heating, sensible heat, planetary boundary layer height, moisture flux components, evaporation, and wind stress components. According to Roads (2001, 2003a,b), since 1997 the GSM has been initialized nearly every day from the 00 UTC NCEP GDAS operational analysis. Because the vertical and horizontal spatial resolution of the operational analysis is greater than the resolution of the GSM, it must first be transformed to a lower resolution. This is done using a linear interpolation between the vertical levels, reducing the horizontal spectral components to a lower resolution and using a bilinear interpolation method to convert the higher resolution surface grids to the lower resolution ECPC GSM surface grids (this must also be done for the land mask).

Juang and Kanamitsu (1994) developed the current version of the US RSM used in this study. This RSM has a resolution of approximately 60 km and nests within the larger GSM without noticeable errors or influences. Both models use the same mass continuity prognostic equations and primitive hydrostatic system of virtual temperature, humidity and surface pressure based on sigma coordinates. The RSM shares the same 18 sigma levels as the GSM (Roads 2003a,b).

As Roads explains (2003a,b), there are a few small differences in structure between the RSM and the GSM. Instead of using spherical harmonics with a triangular truncation of 62 as its basis functions, the RSM uses sine and cosine waves to simulate regional perturbations from the global values (as translated to the regional grids). Another difference is that the RSM uses momentum equations instead of the vorticity and divergence equations that the GSM uses. The physics packages for the GSM and RSM are essentially identical. However, the scale for horizontal diffusion is obviously smaller, and some of the parameterizations in the RSM have been upgraded. For instance, solar radiation for the RSM is calculated according to Chou and Suarez (1996), although the infrared radiation is still calculated in the same manner as the GSM (Schwartzkopf and Fels 1991). Also, the RSM incorporates convection when the convective available potential energy (CAPE) is great enough (Hong and Pan 1996). The RSM also uses a different method of vertical transport in the boundary layer. Instead of using a Richardson number based diffusion process and the associated eddy diffusion coefficients (Kanamitsu 1989), the RSM uses a prescribed profile shape (a function of boundary layer height and scale parameters) to calculate turbulent diffusion coefficients in the mixed layer (Troen and Mahrt 1986).

As mentioned in Roads and others (2003a,b), the RSM is initialized daily from the global analysis. The essence of an RSM forecast involves nesting the RSM within the GSM, for a period based on the GSM output schedule (in this case, six hours). For this nesting period, the RSM predicts regional deviations from the GSM fields that are then interpolated linearly in time between the six-hour output periods. Computation of the non-linear advection takes place in a series of steps. First, the global and regional spectral components must be transformed to the regional grid points, where the non-linear advection will actually be computed. The global spectral components are transformed to the global grid, which is then bilinearly interpolated to the regional grid. The RSM spectral components are exactly transformed to the regional grid. The benefit of a spectral model is that since these calculations are close to exact (although there is some error associated with the bilinear interpolation of the global grid), the RSM and GSM have no aliasing or phase error. Once the spectral components have been transformed to the grid, the global-scale tendency is removed, leaving only that which affects the regional perturbations. A damping function rapidly reduces the regional perturbations to zero at the lateral boundary, so that the RSM boundaries behave similar to the GSM boundaries (see Roads 2003a,b).

Previous studies using this RSM included an analysis of climate characteristics of regional precipitation forecasts (Chen *et al.* 1999; Hong and Leetma 1999; Anderson and Roads 2002; Roads *et al.* 2002), low-level winds (Anderson *et al.* 2000, 2001), climate simulations for the US (Takle *et al.* 1999; Roads and Chen 2000; Roads *et al.* 2003c), to examine global climate simulations and/or change on a regional scale (Roads *et al.* 2003c; Han and Roads 2002), and climate forecasts for fire danger (Roads *et al.* 1997,

Roads *et al*. 2003). Some of these results can be compared and contrasted with this study. A previous evaluation of seasonal precipitation forecasts for the continental US showed some skill, but only as much as the GSM showed (Roads *et al*. 2003a). When compared to the validating observations, the RSM precipitation forecasts had a week 1 anomaly correlation of 0.4 overall, and an anomaly correlation of 0.13 overall for the seasonal forecasts (Roads *et al*. 2003a). A previous evaluation of the US RSM forecasts of fire danger indices showed good prediction skill at weekly time scales for the continental US. As discussed by Roads and others (2003b), the burning index and energy release component (discussed below) seasonal forecasts showed the greatest skill when compared to validating observations, with overall week 1 forecast anomaly correlations of 0.8 and seasonal forecast correlations closer to 0.4. The spread component and ignition component indices had slightly lower overall week 1 and seasonal forecast correlations of approximately 0.7 and 0.35 respectively. Despite lower overall seasonal forecast correlations, all National Fire Danger Rating System (NFDRS) indices had high seasonal skill over many locations in the western United States (Roads *et al*. 2003b). A fire danger forecast related index, the fire weather index (FWI), has also been assessed by Roads and others (Roads *et al*. 1991; Roads *et al*. 1997, Roads *et al*. 2001) and was found to be predictable at weekly and seasonal time scales.

ECPC developed their forecasts of NFDRS indices in the hopes that land managers might eventually have access to automatic seasonal forecasts that would be useful in making strategic resources (e.g., suppression equipment, personnel) decisions (Roads *et al*. 2003b). In order to understand the difficulty in predicting NFDRS indices,

it must first be understood those factors and considerations used in the calculation of fire danger output.

National Fire Danger Rating System

There are two versions of NFDRS currently in use. The first was developed in 1972 (Deeming *et al*. 1972) and a modified current version was released in 1978 (Deeming *et al*. 1977). Another update was issued in 1988 (Burgan 1988), that increased the usefulness of the system in the eastern US by improving the representation of how fuel moisture changes in response to drought or precipitation (Schlobohm 2003). A complete description of NFDRS has been compiled by NWCG (2002), and is summarized below.

NFDRS was originally developed to provide a consistency in fire danger ratings between land management agencies. The four guidelines for its development indicated that it would be scientifically based, able to adapt to the needs of any local manager, usable anywhere in the country, and inexpensive to implement. The resulting NFDRS, released in 1972, used the physics of combustion as well as coefficients and constants developed in a laboratory to reflect the relationships between weather, topography, fuels, and the risk of fire. Essentially, NFDRS uses the current moisture state of live and dead fuels to reflect previous weather conditions, and then modifies the fuels based on weather predictions.

The outputs of NFDRS are numeric indicators, applied to a large area, of the likelihood a fire will start, spread, or require suppression action. There are four assumptions about NFDRS one must be aware of in order to use it properly. First, NFDRS outputs only indicate the potential for an initiating fire that spreads on uniform

fuels and a uniform slope (does not take crowning or spotting into account). Second, NFDRS outputs address fires from a containment standpoint, not extinguishment. Third, the outputs are considered to be relative, not absolute. Fourth, these outputs represent the near worst-case conditions for an exposed physical location.

NFDRS outputs are best applied on a large spatial scale, usually in predetermined areas known as fire danger rating areas. These predefined areas are typically chosen to be uniform in fuels, topography and climate so that any fire danger ratings computed at a point within the region are assumed to apply to the region as a whole. In other words, this allows land management agencies to assign fire danger ratings to large areas based on relatively few measurements within the area. These areas are typically not chosen on a political basis. In other words, the boundary of a fire danger rating area may not end where an administrative boundary does.

The structure of NFDRS consists of three parts. There is the scientific basis for the equations, the static description of fuels, topography and climate for the site, and the more variable data such as weather. The mathematical models used in NFDRS are based on the physics of combustion. They include representations of ignition temperature and chemical properties of woody materials, the moisture of extinction and rate of combustion for various types of plants, and heat energy potential. Further descriptions and references of the combustion physics used can be found in Deeming and others (1972, 1977) and Burgan (1988).

The second part of NFDRS structure includes the static descriptors for the fire danger rating area. The fuel model represents the size, weight, volume and type (among other physical properties) of the fuel bed. There are twenty fuel models to choose from,

such as trees, slash, bushes, grasses and mosses. The slope represents the slope for the entire area as a percentage, and is divided into five classes: 0-25, 26-40, 41-55, 56-75 and greater than 75%. The grass type indicates whether local grasses are annual or perennial vegetation. There are four climate classes to choose from, arid or semi-arid desert, semi-humid with insufficient summer precipitation, semi-humid with summer precipitation sufficient to sustain plant growth for most of the season, and wet coastal areas. Climate classes contain an inherent assumption on the length of the growing season (shorter for more arid, longer for more humid). In addition to climate class, the annual precipitation must also be input as a static descriptor of the area.

The data needed for computations of NFDRS include daily weather observations and the fuel and topography parameters that control the calculations within NFDRS. Weather data, representing the weather in the fire danger rating area as a whole, is the most significant factor in daily changes of fire danger. Daily observations of temperature, relative humidity, and precipitation are the primary elements. Alternatively, forecasted weather observations can be used to predict fire danger conditions in the future. One such experimental product by the Fire Behavior Research Work Unit at the USDA Forest Service Missoula Fire Sciences Lab and the Missoula Forecast Office of the National Weather Service can be found at http://www.fs.fed.us/land/wfas/wfas26.html.

The NFDRS parameters listed below require constant, if not daily, updates. In order to accurately model elements such as fuel moisture, the state of herbaceous vegetation must be frequently noted. This type of vegetation experiences stages of growing (the start of which is known as “green-up”), curing, and dormant periods.

Woody fuel moisture must also be measured, as the modeled woody fuel moisture in NFDRS is not always accurate. The Keetch-Byram Drought Index (KBDI), a stand-alone index representing drought, can be used with NFDRS for 1978 fuel models and is required for the 1988 fuel models. The 1988 version of NFDRS also requires a few other parameter inputs such as indicating local shrubs as either deciduous or evergreen, the season, and the greenness of grasses and shrubs (i.e., mostly dead or flush with growth).

Processing these inputs and parameters in NFDRS yields two forms of output. Intermediate outputs of fuel moisture function as the basis for the calculations of fire danger. The second type of NFDRS outputs is the fire danger indices themselves.

Fuel moisture outputs include the live fuel moisture of both herbaceous and woody vegetation. Live fuel moisture depends on things like the climate class and what stage of the growing season the plants are in. NFDRS also models the dead fuel moistures, which are entirely dependent on environmental conditions. There are four categories of dead fuel moisture. The 1-hour fuel moisture represents the fuel moisture content for the dead fuels of herbaceous plants and round-wood less than 0.635 cm in diameter. It is very responsive to current atmospheric conditions (e.g. temperature, relative humidity, and precipitation). The 10-hour fuel moisture content represents dead fuel moisture for round-wood with a diameter of 0.635 cm to 2.54 cm and changes with day-to-day changes in the weather. The 100-hour fuel moisture content measures dead round-wood moisture content with a diameter of 2.54 cm to 7.62 cm. It is largely dependent on the weather of the preceding two days. The 1000-hour fuel moisture content represents the moisture in dead woody fuels with a diameter of 7.62 cm to 20.32

cm. This fuel moisture largely reflects the atmospheric conditions of the past week, but is also an indicator of seasonal drought (Bradshaw *et al*. 1983).

A flowchart illustrating the inputs, processing and outputs for NFDRS is shown in Figure 2-1. The four fire danger indices output by NFDRS that are examined in this study are the Burning Index (BI), the Ignition Component (IC), the Energy Release Component (ERC) and the Spread Component (SC). These indices are summarized below, and the technical documentation is provided by Bradshaw and others (1983), Deeming and others (1972, 1977) and Burgan (1988). These are not the only four indices output by the NFDRS, but they are the indices used most by land managers.

1. BI predicts the upper limit of the flame length, should a fire occur. Important components of the burning index are the SC and the ERC. It is intended as a measure of how difficult a fire will be to contain.
2. SC is the potential rate of spread of a fire. It is largely dependent on the wind speed and slope of the area in question.
3. ERC is a measure of how much energy per square foot will be released from the time the front of the fire line enters a specific spot to the time the rear of it passes by. It can also be used as a measure of drought conditions, as dryer fuels will release more energy when burned.
4. IC measures the probability that a firebrand will ignite a fire and that the resulting fire will spread. Consequently the SC and the probability of ignition are important components of the IC. As a probability, the IC ranges from 0 to 100 (unlike the other three indices, all of which are open ended). For example, an IC of 100, indicates 100 percent of firebrands will start a fire that

will spread. Whereas an IC of zero means no firebrand will start a moving fire.

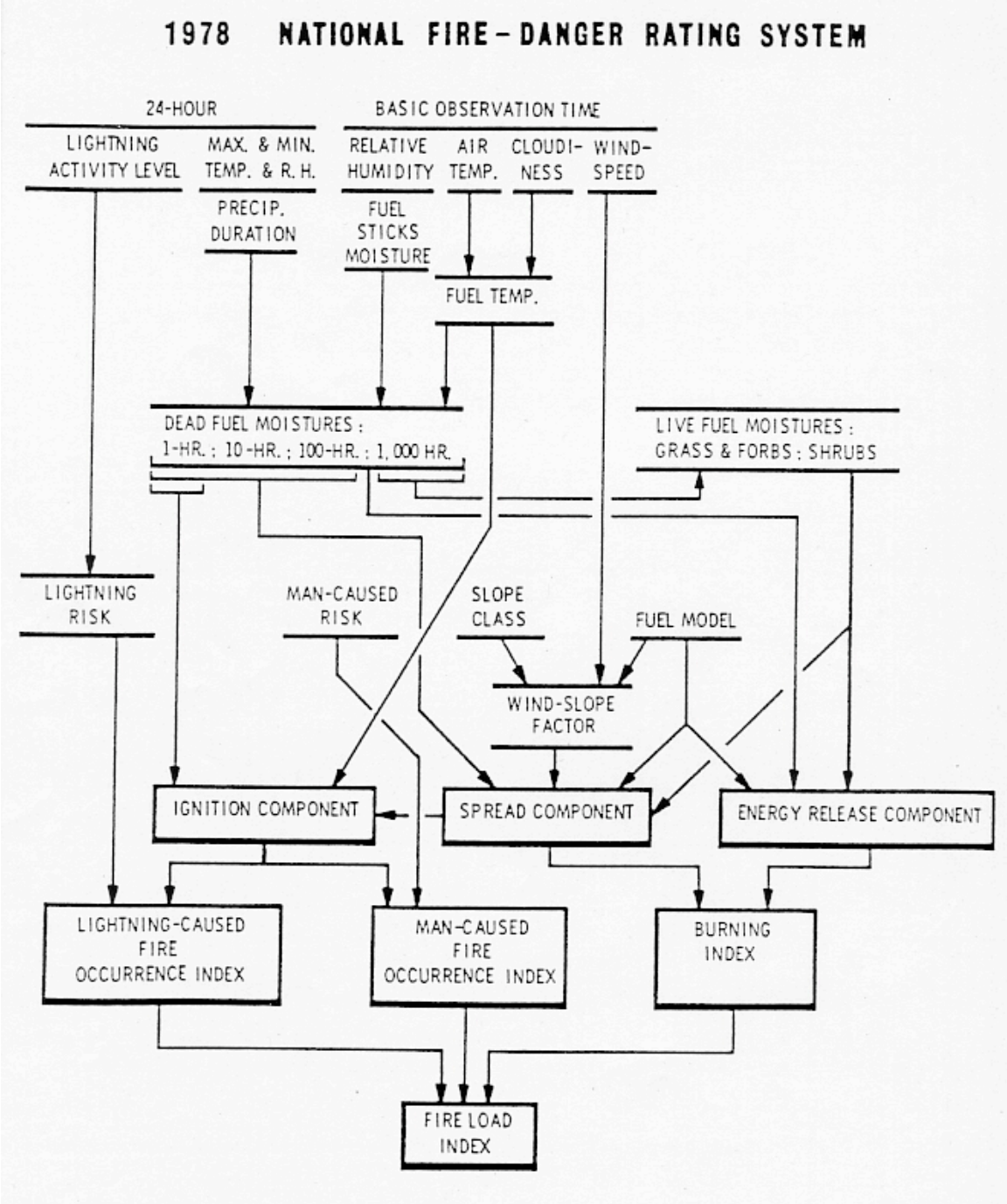

Figure 2-1 A flow chart illustrating the weather and fuel moisture components used to compute NFDRS output indices.

CHAPTER 3

DATA

Three primary data sets will be used in this study: ECPC RSM forecasts, ECPC RSM validation, and RAWS observations. The spatial domain for all datasets covers the western United States and includes approximately 100ºW to about 125ºW, and 30ºN to 50ºN. All data sets are inclusive of the period from September 27, 1997 through December 31, 2002. The primary atmospheric elements used in the study include RAWS 2-m maximum, minimum and average temperature, 2-m daily maximum, minimum and average relative humidity, daily precipitation amount, daily precipitation duration and daily mean afternoon 10-m wind speed (1200-1800). The RSM output atmospheric elements used are 2-m daily maximum, minimum and average temperature, 2-m daily maximum, minimum and average relative humidity, daily precipitation amount, daily precipitation duration and daily mean afternoon 10-m wind speed (1200-1800).

ECPC RSM forecast dataset

Every weekend, ECPC makes a 16-week RSM forecast for surface temperature (daily minimum, maximum and mean), relative humidity (daily minimum, maximum and mean), precipitation amount, hours of precipitation, mean afternoon wind speed (defined as 1200 to 1800 hours), IC, SC, ERC, and BI. Model output consists of daily values that are averaged to create weekly means that can then be combined into monthly (four-week) and seasonal (12-week) means. Each extended forecast examined in this study (275 total from September 27, 1999 through December 28, 2002) is evaluated in the form of twelve one-week means, three one-month means and one seasonal mean. These forecasts have a

spatial resolution of approximately 0.6 degrees (approximately 60 km) and comprise 58 x 97 grid nodes (covering the entire contiguous U.S.), where each node represents the spatial position of the forecast output elements. Because the majority of RAWS are located in the western US (see Figure 3-1), only the 43 x 39 grid nodes over the West will be used in this study.

ECPC RSM validation dataset

Every day, ECPC makes one-day RSM forecasts based on the 00 UTC NCEP operational analysis initial conditions. These are known as the ECPC validation forecasts. The validation forecasts are not identical to the operational analysis (which uses the latest high-resolution global model) or reanalysis data (created using the same model as ECPC), which are based on 6-hour forecasts made four times daily, but can be considered a useful approximation (Roads, *et al.* 2003). Similar to the extended forecasts, they contain all thirteen atmospheric elements used in this study and are contained within an identical spatial grid. They are archived as weekly averages of daily values and essentially function as validating observations. There were 286 weekly averages of validation data used in this study, including the first eleven weeks of data from 2003. Acquisition of the 2003 data was necessary to evaluate the extended forecasts made in late 2002.

RAWS

Land and fire management agencies retain an observational network of remote automated weather stations (RAWS) for fire weather related measurements (see http://www.fs.fed.us/raws). They are typically located in wilderness, forest and rangeland areas where it is desired to monitor fire danger. The hourly observations are

transmitted to the National Interagency Fire Center (NIFC) using a geostationary operational environmental satellite (GOES) operated by the National Oceanic and Atmospheric Administration (NOAA). These data are forwarded to the Weather Information Management System (WIMS) for agency use distribution, and to the Western Regional Climate Center (WRCC) for historical archiving. The RAWS data used in this study were obtained from WRCC. From this dataset, RAWS surface measurements of daily minimum temperature, daily maximum temperature, daily mean temperature, wind speed, daily minimum relative humidity, daily maximum relative humidity, daily mean relative humidity, precipitation and hours of precipitation were extracted and used in the analysis. WIMS provides site descriptors (fuel model, slope, climate class, etc.) for each RAWS, which, combined with the above atmospheric elements, allows for the calculation of relevant fire danger indices (BI, IC, ERC, SC) used in this study. Larry Bradshaw, U.S. Department of Agriculture Missoula Fire Sciences Laboratory, provided the original NFDRS computer software code for calculating the indices that was then adapted to fit the RAWS data format used in this project.

There were 262 RAWS sites in the western U.S. (shown with ECPC output grid nodes in Figure 3-1) that had sufficient quality data for the years 1997-2003. Again, observational data through 2003 was needed to verify the seasonal RSM forecasts made in late 2002. Sites were chosen based on three criteria regarding completeness of the data set – 1) no more than two months of missing data in any year, 2) availability of year-round operational measurements, and 3) availability of historical data for the period September 1997 through March 2003. Measurements that were clearly in error (e.g.,

relative humidity over 100 percent, negative wind speed) were considered missing and excluded from the analysis. There were 477 RAWS with data histories from September 1997 through March 2003 that were missing weeks, months or years of data, mostly due to instrument error or seasonal operation, and therefore were unsuitable for use in this study.

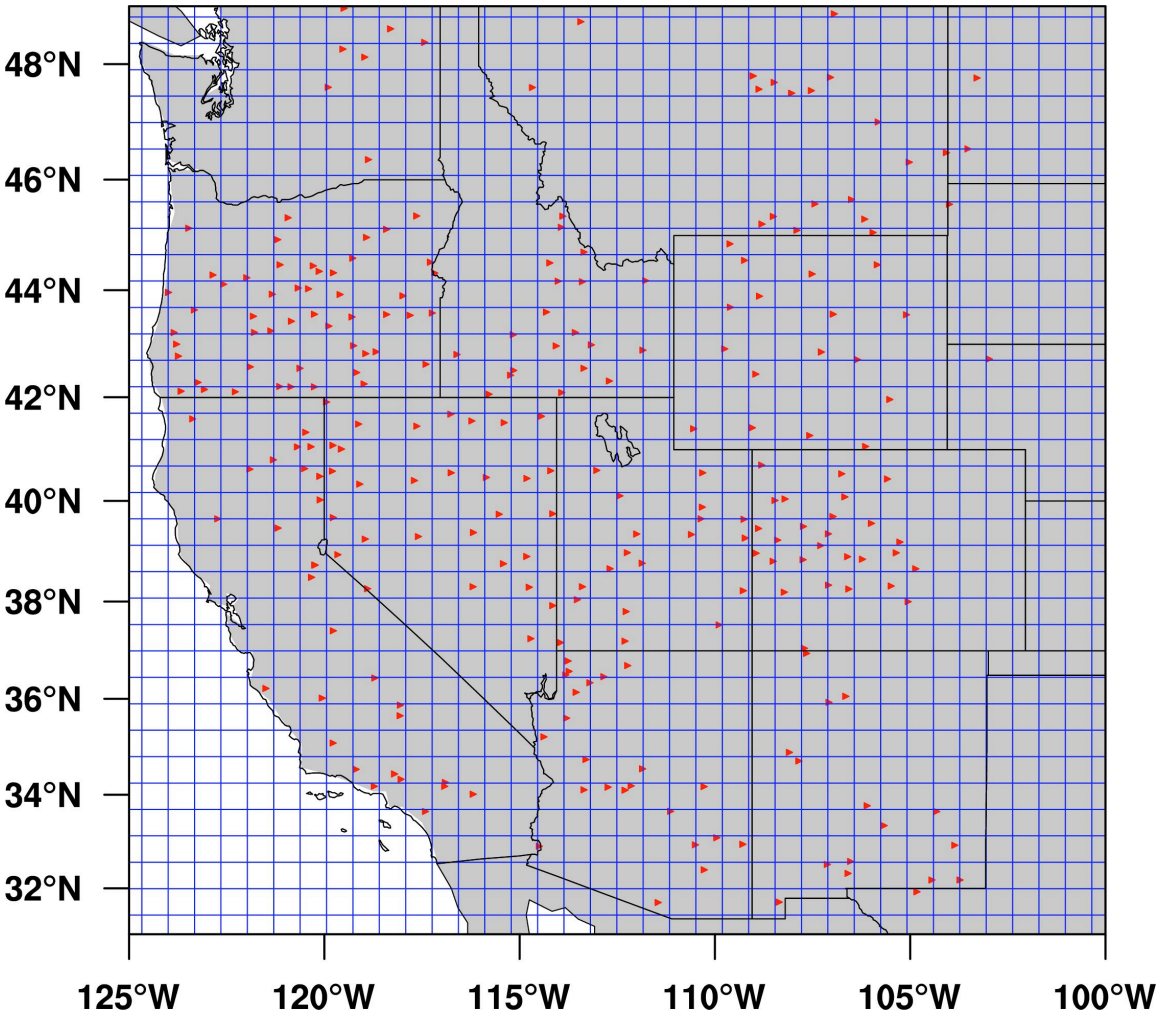

Figure 3-1 RAWS locations (red triangles) with RSM output grid overlay (blue lines).

CHAPTER 4

METHODS OF ANALYSIS

There are three major components to this study. The first is a comparison of the RAWS observations to the RSM forecast output. The second is a comparison of the RAWS observations to the RSM validating observations. The third is a comparison of the RSM forecasts to the RSM validating observations. Each of these components examines the results for the western U.S. as a whole and then for regions within the western U.S. In addition, these studies are done for the twelve one-week, three one-month and one seasonal mean for every forecast. Comparing the RSM observations to the RSM validations will only involve a weekly, monthly and seasonal mean (no forecasted values, just comparing two sets of observations). For all three cases analyses are done for surface temperature (daily minimum, maximum and mean), relative humidity (daily minimum, maximum and mean), precipitation amount, hours of precipitation, mean afternoon wind speed (1200 to 1800 hours), IC, SC, ERC, and BI.

A quality control (QC) analysis was performed on the RAWS data for 263 stations that met the initial acceptance criteria described in Chapter 3. The data were checked for suspicious values (spikes) through a visual inspection of the time series for each variable and RAWS site. Measurements that were clearly in error (e.g., relative humidity over 100 percent, negative wind speed) were considered missing and excluded from the analysis. One RAWS was removed from the study as a result of this process (leaving 262 total stations for analysis), as it appears to have been physically moved at some point in the last five years. The RSM forecast and validation files did not require a

similar QC process, but were visually examined via time series plots to ensure their sufficient internet file transfer from ECPC to local files.

In order to compare the RAWS observations to the RSM forecast or validation data, it was necessary to match the data sets both temporally and spatially. The RSM forecasts are output as weekly averages of daily values out to sixteen weeks (although this study will only be examining the first twelve weeks of these forecasts for a seasonal emphasis), and are produced every weekend. The RAWS observations include the 1300 local time observations of temperature, humidity and wind speed needed for the calculation of the NFDRS indices, as well as the daily values for maximum and minimum temperature and relative humidity, precipitation, and the mean afternoon wind speed (1200 to 1800).

The first step in matching the datasets is to transform these daily values into weekly averages of daily values. The 1300 local time observations are used to calculate daily values for the four NFDRS indices, while the daily maximums and minimums of temperature and relative humidity are used to calculate daily averages. The weekly mean of these daily values is then calculated with the dates for each weekly mean matching exactly the dates for the RSM forecast weekly means. Weekly means with missing values for 3 consecutive or 4 nonconsecutive days were considered missing. The weekly means of all three datasets are then transformed into monthly and seasonal means. For the forecasts, monthly means are calculated by taking the means of weeks 1-4, weeks 5-8, and weeks 9-12 of each twelve-week forecast. Monthly means for the RSM validation and RAWS datasets are computed in the same manner, but using the weekly means for the twelve-week period matching each 12-week forecast. Likewise, forecast seasonal

means are computed by taking the mean of all twelve forecast weeks. RAWS and RSM validation seasonal means are computed by taking the mean of the twelve weeks matching each 12-week forecast.

Once the three datasets were matched on a temporal scale, the next step was to match them spatially. The RSM forecast and validation data are output as a grid of values separated by a distance of roughly 60 km. RAWS observations are spatially dissimilar in that they are spaced in an irregular pattern that is not in any way aligned with the model grid output. Extrapolation of the RAWS station data to a grid matching that of the RSM output was ruled out due to potential error in the extrapolated values at grid nodes with no nearby RAWS sites. In this case, interpolating the forecast grids to RAWS locations seems a more accurate method of comparing the datasets. The values in the RSM validation and forecast grids were bilinearly interpolated to match each of the 262 RAWS locations used in this study. This bilinear interpolation algorithm determines values between grid nodes by calculating a distance-weighted average of values at the nearest four nodes. For the sake of consistency, the ECPC validation versus ECPC forecast comparison uses the forecast and validation grid values as they are interpolated to RAWS sites, rather than a direct comparison of the forecast and validation output grid nodes.

Rather than assessing model performance for each individual RAWS, regional model performance is assessed by dividing stations into eight geographic regions based on similar climate patterns. The divisions (Figure 4-1) were found through a cluster analysis of the RAWS data. As explained by Wilks (1995), a cluster analysis sorts data into groups based on the similarities between the individual observations of chosen

datasets. In this case, the annual climatologies of daily average temperature and precipitation of each RAWS station were the observations used. Cluster analysis functions by grouping data values such that the differences, or distances, between values within each cluster are less than the distances between clusters. While there are several specific methods of defining the distances between clusters, Ward's minimum variance method is the one used in this study. Ward's minimum variance method computes the sum of the squared distances between a cluster's points and the centroid (mean) of the cluster. The cluster closest to a given cluster is then defined as the cluster that increases the sum of squared distances the least when combined with the given cluster.

Region 1 depicts the area most affected by the Southwest Monsoon. Region 2 encompasses the area where the monsoon has a lesser impact in the four-corner states. Region 3 represents the mid-northwestern coast, which typically receives the brunt of wintertime storms in the West. Region 4 captures most of the Great Basin, along with the eastern portions of Washington and Oregon (not dissimilar in Great Basin characteristics). Region 5 closely outlines the Rocky Mountains and region 6 includes eastern Montana and portions of adjoining states. Southern California is the focus of regions 7 and 8, where the RAWS in region 7 are all at a higher elevation than those in region 8. Also, the overlap between regions 2 and 5 seems largely due to differences in elevation. In the overlap area, the elevations of the region 5 RAWS exceed 2256 m, and most of the elevations of the region 2 RAWS range from 1829 to 2256 m.

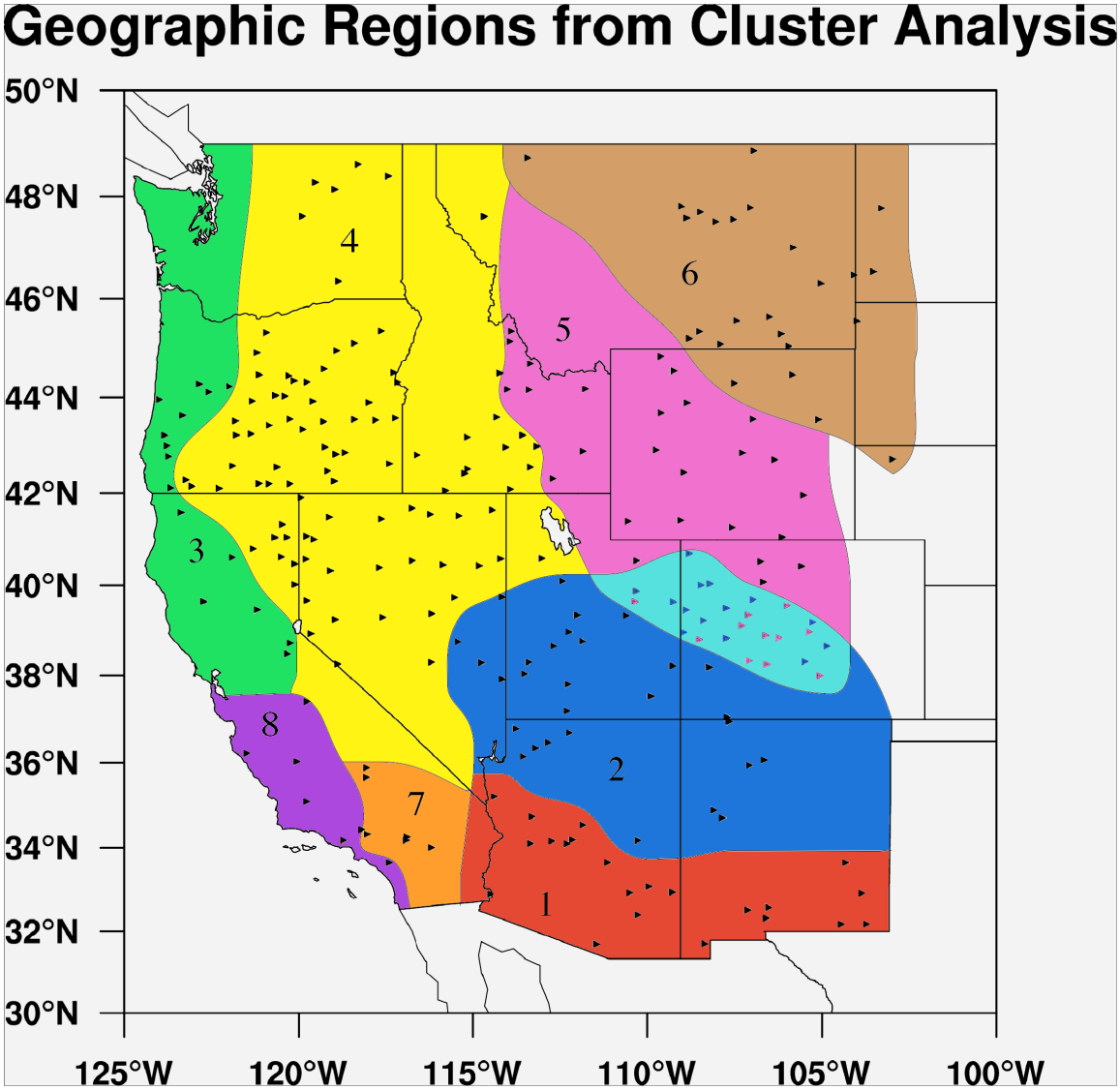

Figure 4-1 Eight geographic sub-regions, chosen using cluster analysis. Note that regions 2 and 5 overlap.

The purpose of forecast verification is to determine the quantitative accuracy of the forecast. The statistical methods employed in this study as a means of forecast verification are bias, root mean square error, anomaly correlation, and standard deviation.

Bias is a simple calculation of forecast minus observation (Wilks 1995), or

$$bias = f - o, \qquad \text{Equation 4-1}$$

where *f* is the forecast value and *o* is the value of the observation. When shown in graphical form, this calculation has the benefit of revealing under what situations the model is over or under forecasting and by how much. It is also useful in determining potential seasonal characteristics in the errors between the datasets.

Another quantitative measure of forecast accuracy is the Root Mean Square Error (RMSE; Wilks 1995). This measure is defined by

$$\text{RMSE} = \sqrt{\frac{1}{M}\sum_{m=1}^{M}(f_m - o_m)^2}, \qquad \text{Equation 4-2}$$

where *M* is the total number of stations in a region, *f* are the forecast values and *o* are the observational values. The RMSE shown in graphical form can be interpreted as a typical error magnitude, and is also useful in determining possible seasonal influences on the error of the model (i.e., does the model typically perform better in the winter versus summer?).

Anomaly Correlation is commonly used to evaluate extended forecasts. It is designed to reflect good forecasts in the pattern of an observed field, not necessarily the magnitude of the values (Wilks, 1995). There are two different equations, representing the two types of anomaly correlation used in this study. The first is for judging the spatial variation and correlation of the anomalies (equation 4-5; Roads *et al*. 2003). In other words, equation 4-5 calculates the year-round ensemble correlations for each individual RAWS station. The second equation is better described as temporal variations in spatial correlations (equation 4-6; Wilks 1995). Conversely to equation 4-5, equation 4-6 calculates the overall correlation of multiple RAWS stations for one forecast. Anomalies are computed by taking the difference between the total forecast (either by

region or for the entire Western U.S.) and the climatological monthly means. In other words,

$$A = f - C_f, \qquad \text{(Equation 4-3)}$$

where A is the anomaly, f is the forecast and C_f is the climatological mean for that forecast type (weekly, monthly or seasonal mean). The anomalies will then have a statistical distribution characterized by the standard deviation

$$SD = \left(\frac{1}{n-1}\sum A^2\right)^{1/2}. \qquad \text{(Equation 4-4)}$$

Given that A is a forecast anomaly of any type (weekly, monthly or seasonal mean) and that B is the validating anomaly from observation, then the spatial variation in the anomalies is represented by

$$corr(x,y) = \frac{\sum_{n=1}^{N} A_n B_n - \sum_{n=1}^{N} A_n \sum_{n=1}^{N} B_n \Big/ N}{\left(\sum_{n=1}^{N} A_n^2 - \left(\sum_{n=1}^{N} A_n\right)^2 \Big/ N\right)^{1/2} \left(\sum_{n=1}^{N} B_n^2 - \left(\sum_{n=1}^{N} B_n\right)^2 \Big/ N\right)^{1/2}}, \qquad \text{(Equation 4-5)}$$

where N is the total number of forecasts (N = 275 for each forecast type in the complete time period). Similarly, the temporal variations in the spatial anomaly correlations (sometimes known as pattern correlation) are calculated using

$$\text{Anomaly Correlation} = \frac{\sum_{m=1}^{M} [A_m B_m]}{\left(\sum_{m=1}^{M} A_m^2 \sum_{m=1}^{M} B_m^2\right)^{1/2}}, \qquad \text{(Equation 4-6),}$$

where M is the total number of RAWS in the current region (M = 262 for the western U.S.). Missing values in the observational anomalies for either equation 4-5 or equation

4-6 reduce the anomaly summations for both datasets by the number missing (the missing RAWS values and matching interpolated validation or forecast values are removed).

Computing the anomalies for each dataset requires a calculation of the climatologies for each variable and forecast type in the three separate datasets. Computing and using climatologies for use in determining the anomaly correlations is difficult in that the RSM forecast periods do not reset at the beginning of every year, they just continue making the same forecasts every weekend no matter what time of year it is. This means that the first forecast of one year will not quite match the same dates as the first forecast of another year.

The climatologies for each variable and forecast type were calculated in a manner to solve or at least mitigate this date matching problem. First, rather than try to somehow compare weekly averages that do not span the same dates from year to year, it was decided to compute monthly climatologies for all forecasts beginning in a given month. Thus, the climatology for any given week contains twenty values as opposed to just five. For example, a one-week forecast made in mid-June will be compared to a climatology consisting of all one-week forecasts made in the month of June during the five-year period. Likewise, the fifth week of a twelve-week forecast would be compared to a climatology consisting of all fifth-week forecasts made in June, a one-month forecast mean compared to a climatology of all mean one-month forecasts made in June, and so forth. Of course the two observational datasets (RAWS and RSM validation) do not contain extended forecasts, but the climatologies for the weekly, monthly and seasonal means matching the forecast dates are computed in the same manner.

Finally, the climatologies for each variable and time-span are smoothed in order to increase the accuracy of the anomaly correlation. In other words, the twelve climatologies (January to December) for a given variable and forecast type are interpolated (in this case linearly) to each individual day within each month. For instance, if the March climatology of daily maximum temperature for seasonal forecasts made in March has a value of 70°F and the April value for the same climatology is 80°F, each day between March 15 and April 15 increases by a regular amount from 70°F to 80°F. Therefore, the anomaly computed for a seasonal forecast of maximum temperature made on March 23rd would then use the smoothed climatology value for March 23rd (in this case about 72.66 °F).

Comparisons were also done involving the summer and winter months separately. The performance of the model in summer months is of obvious interest from a fire danger aspect since this is when for most areas in the West the fire season occurs. Wintertime performance of the model, while still having relevance to fire danger in areas with warmer climates (i.e., Arizona and southern California), is done here mostly for comparison and contrast with the summer forecasts. In summer cases, the study included all weekly forecasts made in June, July or August (JJA), all monthly forecast means that fall within JJA, and the seasonal forecast for each summer (the seasonal mean from the first forecast week in June). The winter analysis likewise included all weekly forecasts made in December, January or February (DJF), all monthly forecast means that fall within DJF, and the seasonal forecast for each winter (the seasonal mean from the first forecast week in December).

CHAPTER 5

TEMPORAL ANALYSIS

This temporal analysis investigates possible variations in the accuracy and precision of the model forecasts over time. Analysis of the US West average performance (the average performance of all 262 RAWS) of the model forecasts over time should reveal important temporal characteristics, such as seasonal variations in forecast accuracy.

Figure 5-1 plots the average weekly and seasonal means of atmospheric observations for all RAWS used in this study. The vertical dashed lines in each graph represent the first (January) and 26th (mid-July) forecast dates of every year for reference. The temperature curves show the seasonality one might expect (highest temperatures in summer, lowest in winter, with seasonal means leading the weekly means because each seasonal mean incorporates the upward or downward trend of the next twelve weeks). Relative humidity has an inverse relationship to temperature and therefore the overall pattern is the opposite of the temperature curves (higher in winter and lower in summer). However, the annual relative humidity pattern is not as regular as temperature because on longer time scales relative humidity is affected by air circulation patterns as well as temperature. For instance, it is a change in circulation patterns that brings air with more moisture (and higher relativity) into Arizona and New Mexico during the summer. Both precipitation amount and precipitation duration show higher values in the winter, which makes sense since most places in the West receive the majority of yearly precipitation during the winter. Wind speed is clearly seasonal, with highest values occurring in the

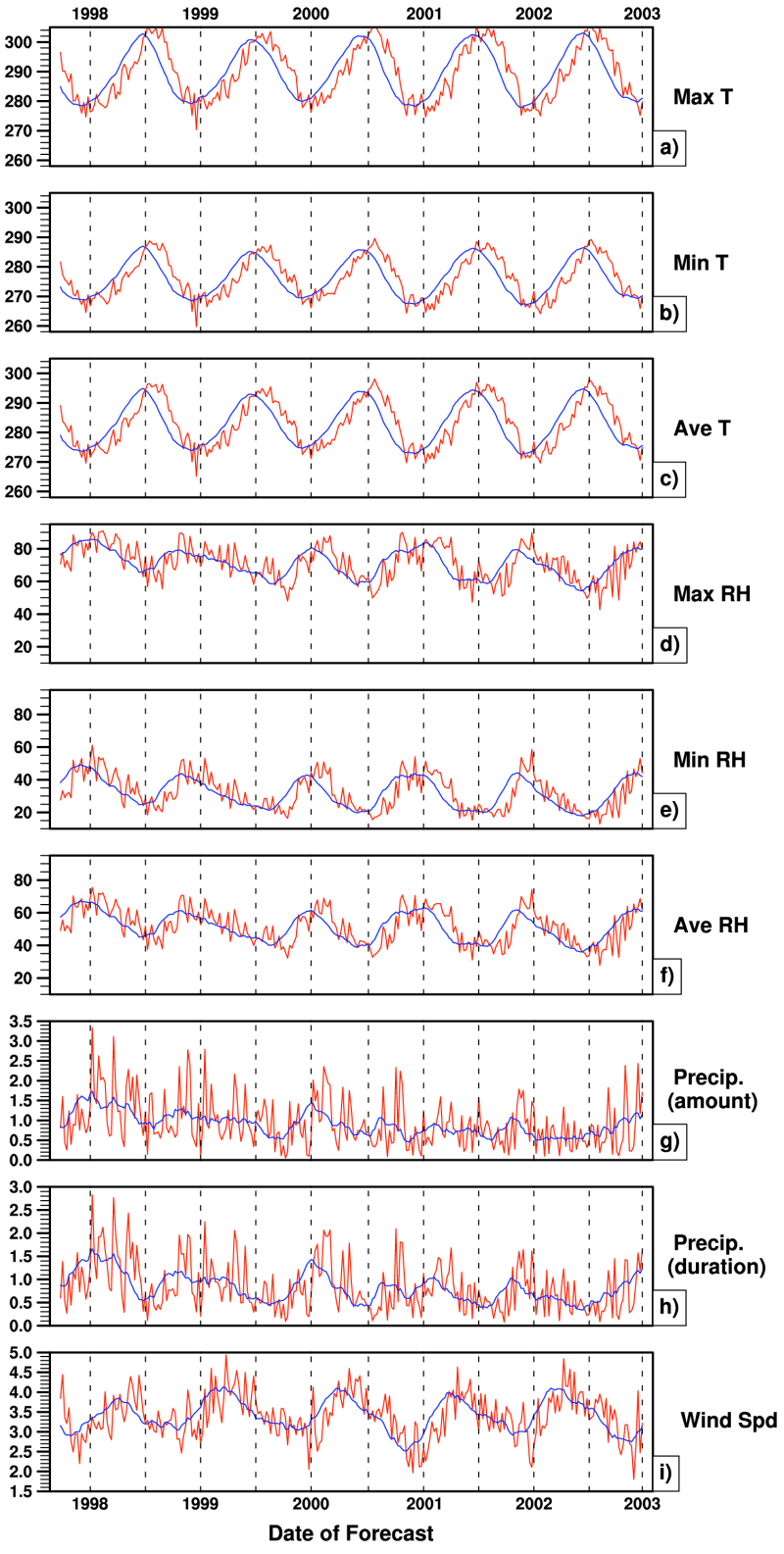

Figure 5-1 RAWS seasonal (blue line) and weekly (red line) means for (a) Max T (K); (b) Min T (K); (c) Ave T (K); (d) Max RH (%); (e) Min RH (%); (f) Ave RH (%); (g) Precip Amt (mm); (h) Precip Dur (hrs); (i) Wind Spd (m/s).

spring. The fire danger indices (Figure 5-2) all show a clear seasonal variation. BI, ERC and IC all have their respective peak values in the summer months, but SC peaks in the spring likely in response to the higher spring winds. The rapid decline of these indices in the fall is likely attributable to the start of winter precipitation. Likewise, the slow spring increase in the fire danger indices is probably the result of declining precipitation, which leads to a gradual decline in fuel moisture.

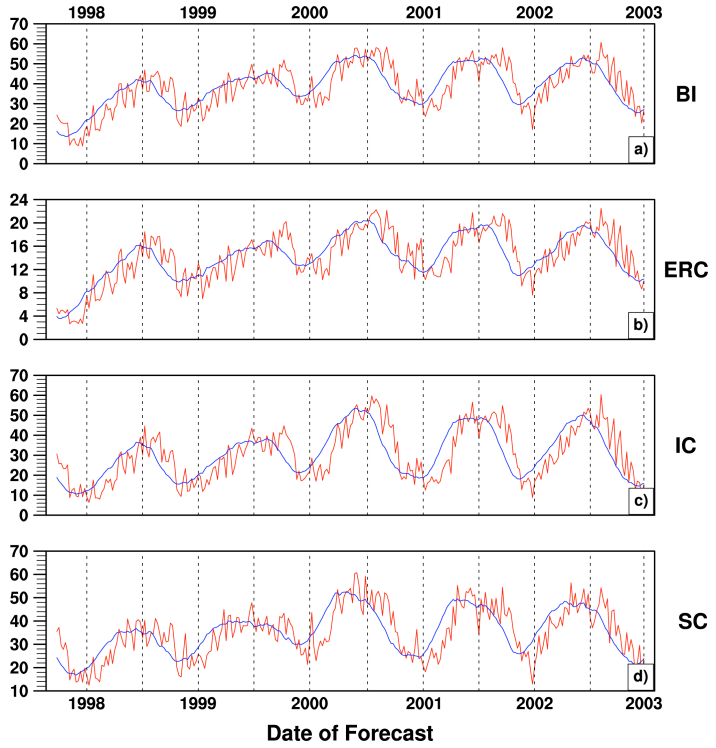

Figure 5-2: RAWS seasonal (blue line) and weekly (red line) means for (a) BI; (b) ERC; (c) IC; (d) SC.

Figure 5-3 shows the average weekly and seasonal means for the interpolated atmospheric RSM forecasts. All indices indicate seasonal cycles that are generally more defined than the seasonal cycles in the RAWS observations, especially when compared to the relative humidity indices. Precipitation amount and duration show a clear seasonality (both are higher in winter), and the wind speed again peaks in spring. The four NFDRS

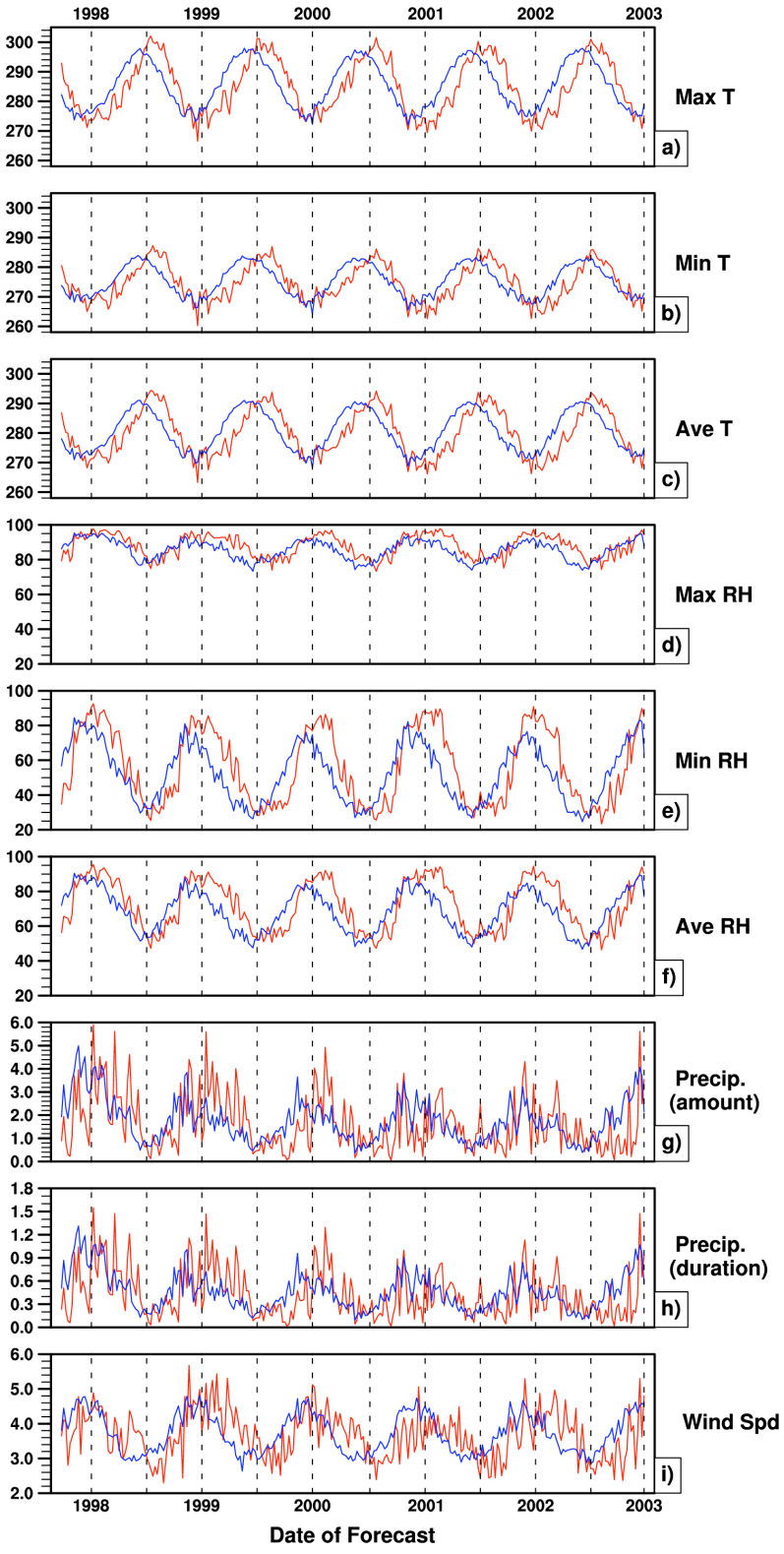

Figure 5-3 RSM forecast seasonal (blue line) and week 1 (red line) means for (a) Max T (K); (b) Min T (K); (c) Ave T (K); (d) Max RH (%); (e) Min RH (%); (f) Ave RH (%); (g) Precip Amt (mm); (h) Precip Dur (hrs); (i) Wind Spd (m/s).

indices (Figure 5-4) show seasonality, peaking in late summer. This is similar to the RAWS fire danger indices, except for RAWS SC, which peaks in the spring.

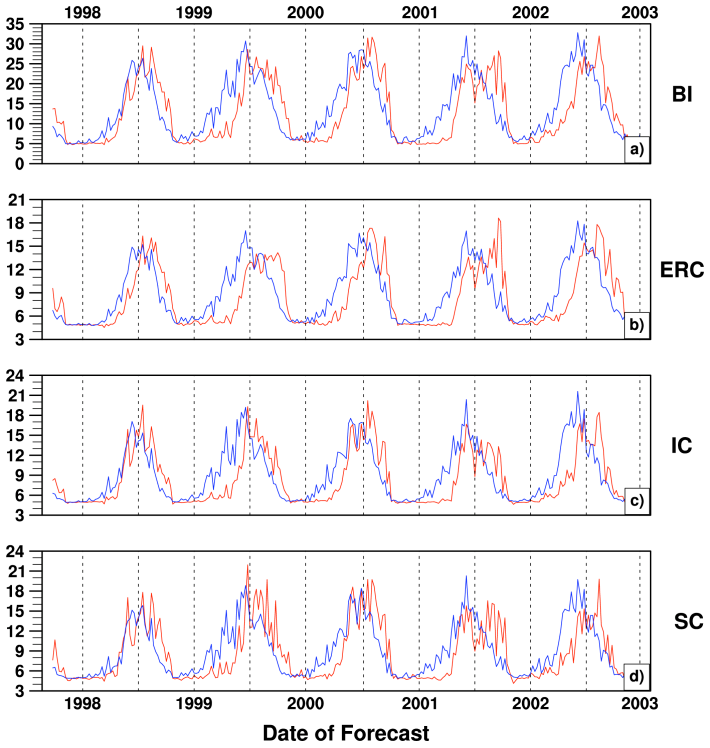

Figure 5-4 RSM forecast seasonal (blue line) and week 1 (red line) means for (a) BI; (b) ERC; (c) IC; (d) SC.

The average time series for interpolated RSM validations (Figures 5-5 and 5-6) closely resemble the forecast time series. The precipitation and NFDRS indices are generally of greater magnitude in the forecast time series.

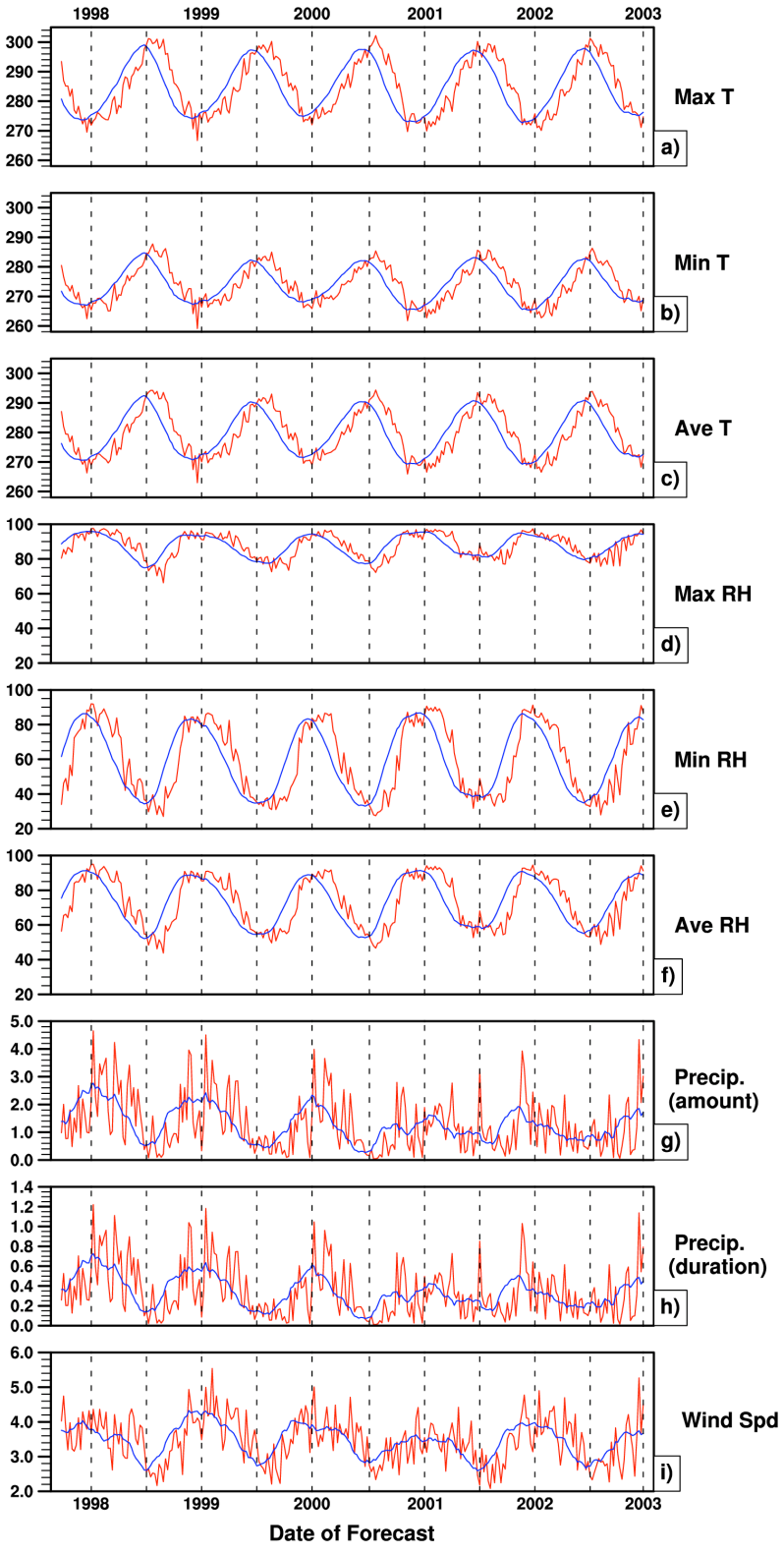

Figure 5-5 RSM validation seasonal (blue line) and week 1 (red line) means for (a) Max T (K); (b) Min T (K); (c) Ave T (K); (d) Max RH (%); (e) Min RH (%); (f) Ave RH (%); (g) Precip Amt (mm); (h) Precip Dur (hrs); (i) Wind Spd (m/s).

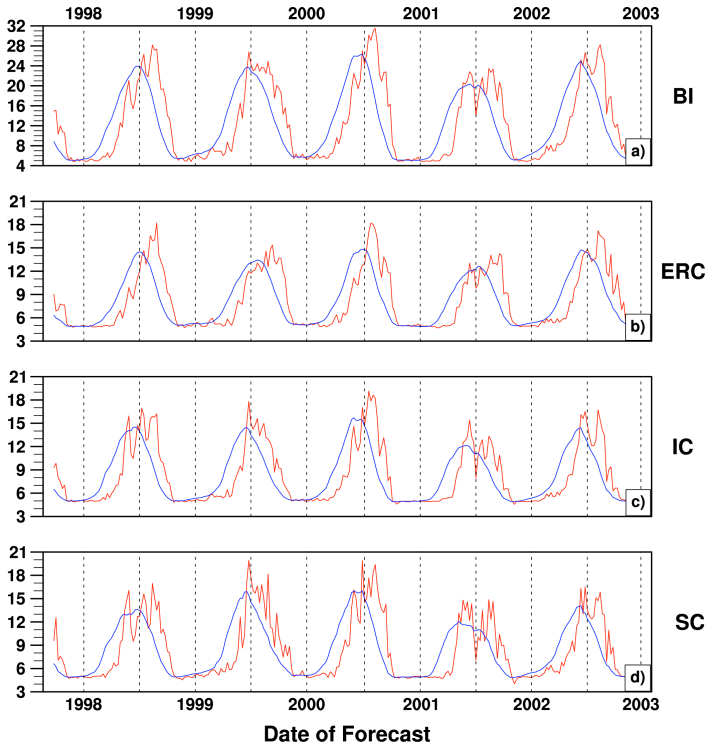

Figure 5-6 RSM validation seasonal (blue line) and weekly (red line) means for (a) BI; (b) ERC; (c) IC; (d) SC.

It is clear from simple visual inspection of these time series that the magnitude of the fire danger indices in the RAWS dataset is at least double that of the ECPC fire indices, although ERC is typically comparable between all three. This is most likely due to differences in the calculation of the fire danger indices between the RAWS and ECPC datasets. Recall from Chapter 2 that weather elements are not the only factors that affect the calculation of NFDRS indices. The fuel model, slope and carry over of fuel moisture values are similar but not the same between ECPC and the values used to calculate fire danger from the RAWS observations. However, because these plots represent averages over all locations used in this study, the average values of the RSM and RAWS fire danger indices are not realistic. While this averaging is useful for the skill assessment of

this model, the average index values themselves are probably of little use to fire managers. The atmospheric elements are much more comparable between the datasets, although there are some biases. In particular, the relative humidity values are generally 10-20 percent greater in the ECPC datasets than in the RAWS observations.

The time series of variability (standard deviation; SD) for the RAWS observations (Figures 5-7 and 5-8) show the greatest seasonal variation during the spring and fall for the average and maximum temperature. Minimum temperature variability peaks in winter. The relative humidity elements typically have slightly higher variability in fall. Precipitation and wind speed vary more during the winter. The variability in these elements seems to concur with known climate patterns in the West. The burning index and energy release component show little to no seasonal variation, while the ignition and spread components seem to peak in the summer. In all cases, the seasonal variability is less than the weekly variability, as expected (week to week variations are minimized in a seasonal mean).

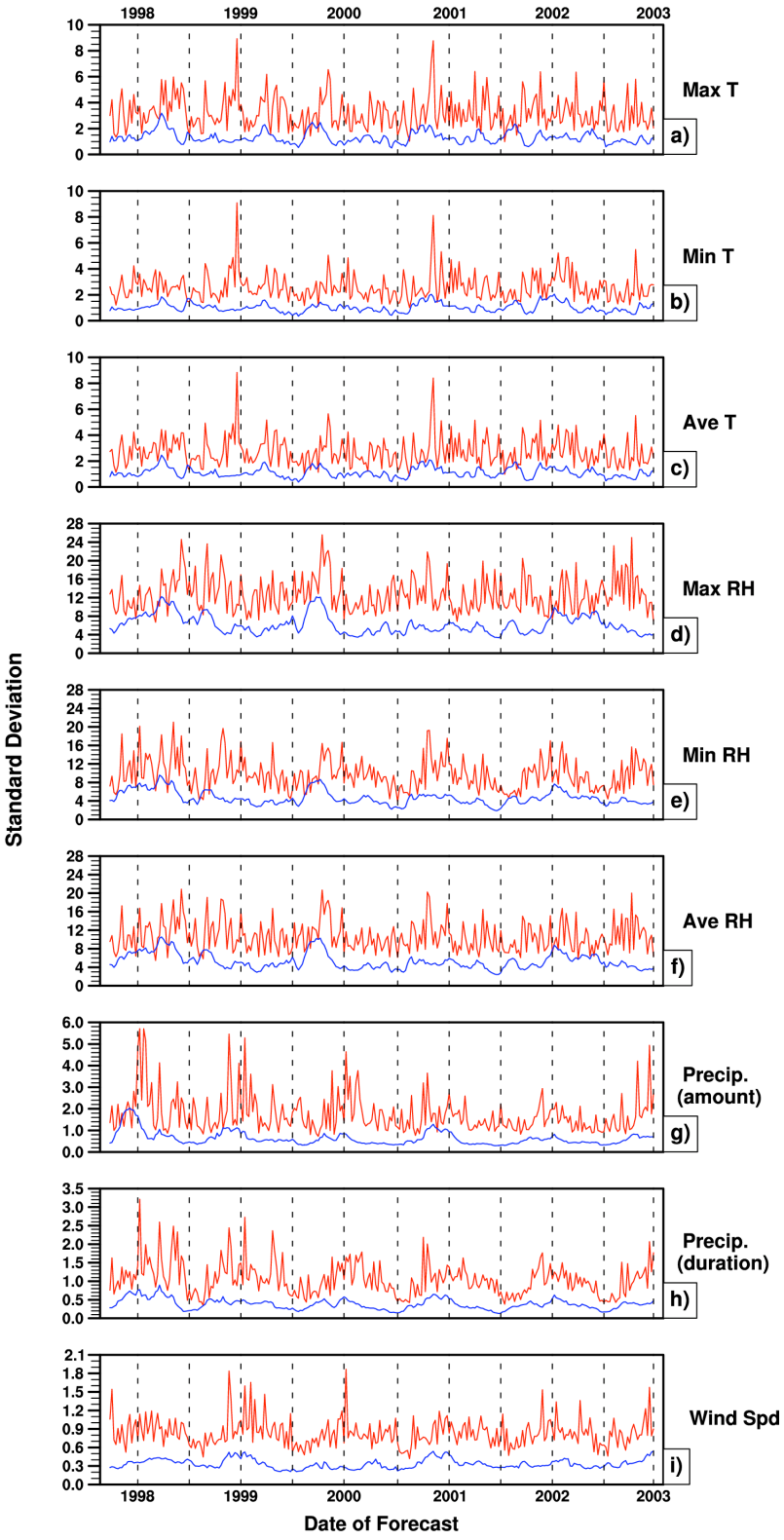

Figure 5-7 RAWS seasonal (blue line) and weekly (red line) standard deviations (SD) for (a) Max T (K); (b) Min T (K); (c) Ave T (K); (d) Max RH (%); (e) Min RH (%); (f) Ave RH (%); (g) Precip Amt (mm); (h) Precip Dur (hrs); (i) Wind Spd (m/s).

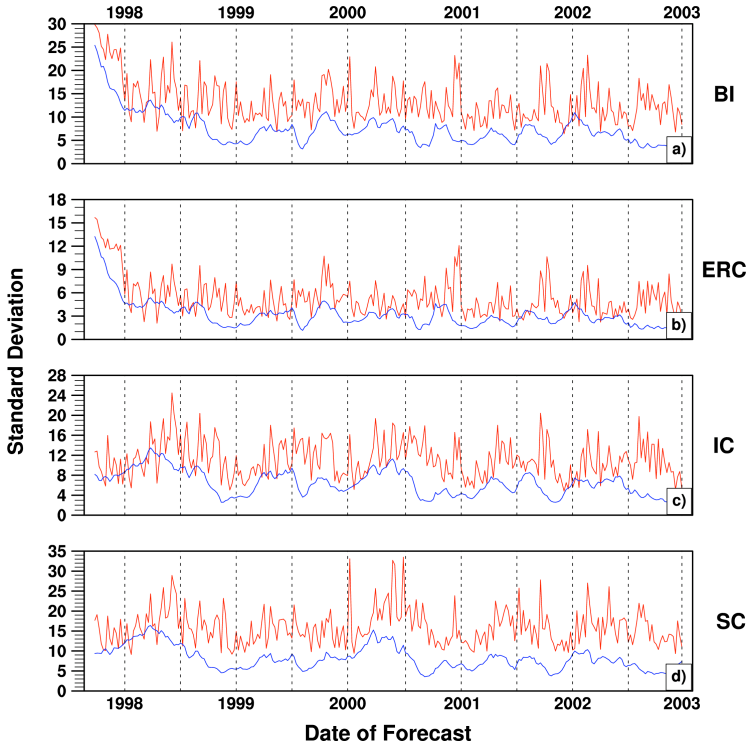

Figure 5-8 RAWS seasonal (blue line) and weekly (red line) standard deviations (SD) for (a) BI; (b) ERC; (c) IC; (d) SC.

The SD for the atmospheric validating observations (Figure 5-9) has a seasonal pattern very similar to that of the RAWS observations. The only notable differences lie in the magnitude of the SD for the maximum RH and precipitation duration. The RAWS maximum RH variation is approximately 6% greater than validation maximum RH variation most of the time. The variation in RAWS precipitation duration can be longer than the variation in the same validation element by an hour. The SD of all NFDRS indices (Figure 5-10) show a much more distinct seasonality, peaking for all of them in the latter half of summer. The forecast time series of variability (Figures 5-11 and 5-12) are very similar in magnitude and pattern to the validation SD.

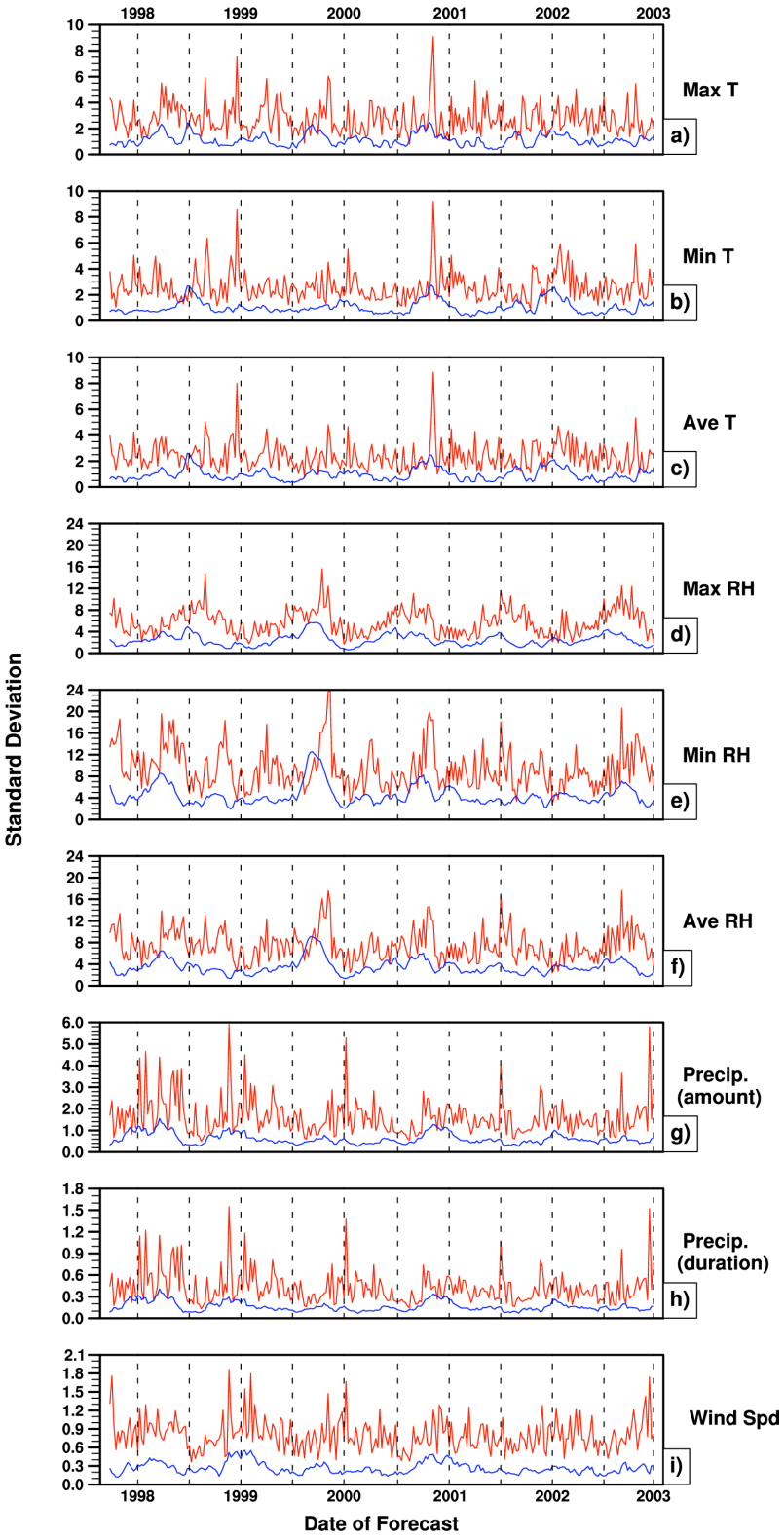

Figure 5-9 RSM validation seasonal (blue line) and weekly (red line) standard deviations (SD) for (a) Max T (K); (b) Min T (K); (c) Ave T (K); (d) Max RH (%); (e) Min RH (%); (f) Ave RH (%); (g) Precip Amt (mm); (h) Precip Dur (hrs); (i) Wind Spd (m/s).

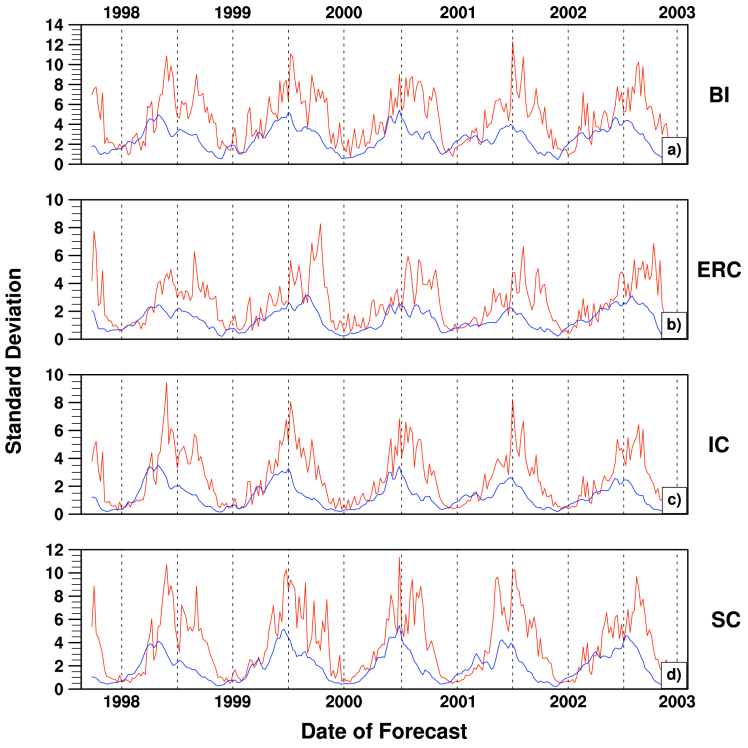

Figure 5-10 RSM validation seasonal (blue line) and weekly (red line) standard deviations (SD) for (a) BI; (b) ERC; (c) IC; (d) SC.

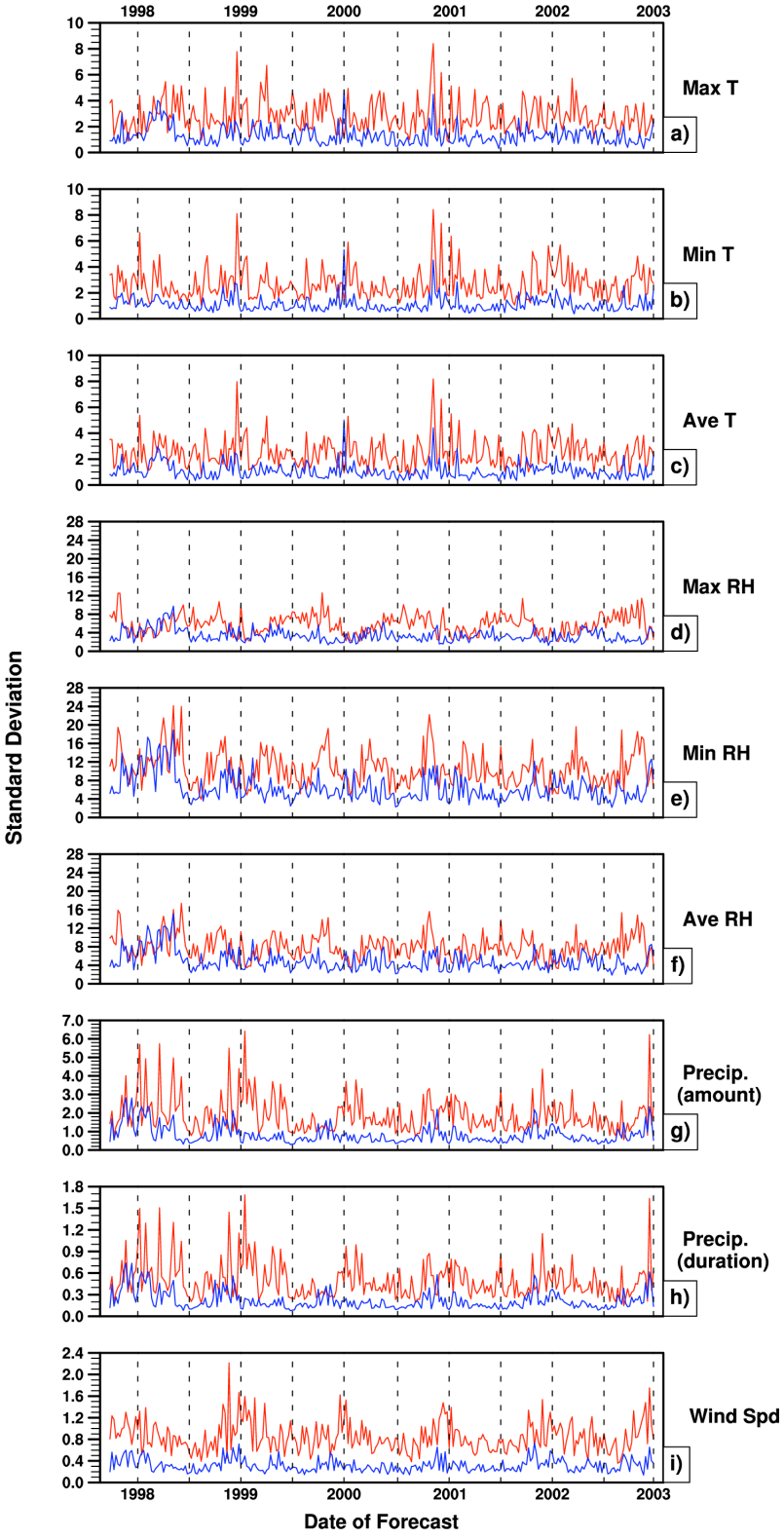

Figure 5-11 RSM forecast seasonal (blue line) and week 1 (red line) standard deviations (SD) for (a) Max T (K); (b) Min T (K); (c) Ave T (K); (d) Max RH (%); (e) Min RH (%); (f) Ave RH (%); (g) Precip Amt (mm); (h) Precip Dur (hrs); (i) Wind Spd (m/s).

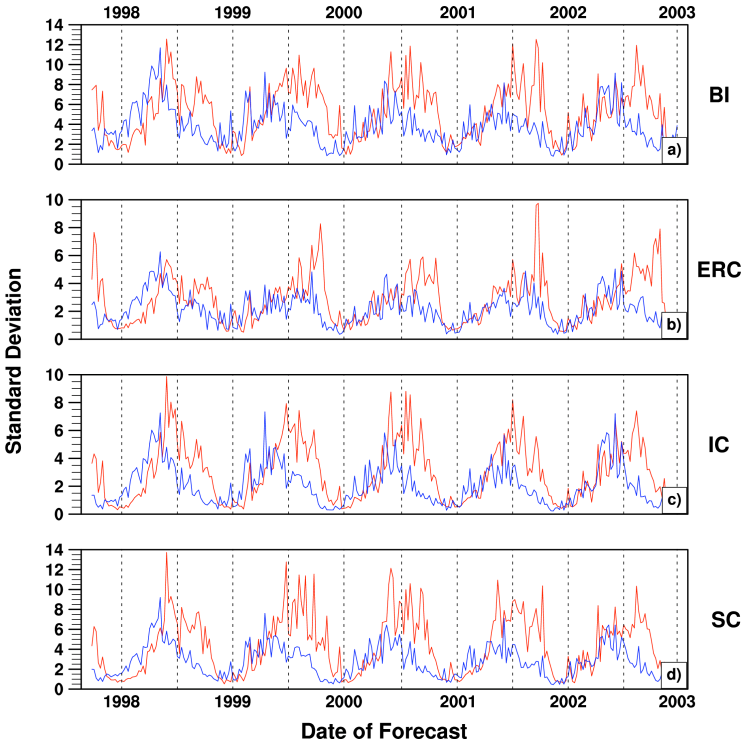

Figure 5-12 RSM forecast seasonal (blue line) and week 1 (red line) standard deviations (SD) for (a) BI; (b) ERC; (c) IC; (d) SC.

All three datasets show similar variability in the temperature values for the one-week and seasonal means. Maximum RH shows seasonal variability in all three datasets (although it is a little more difficult to detect in the RAWS series), with lower variability in winter and higher variability in summer. The variability of maximum RH is generally higher for RAWS than it is for validation or forecast data. Minimum RH shows a seasonal variability of similar magnitude in all three datasets. The RAWS data has a greater magnitude of variation than the other datasets for mean RH, but also has a less detectable seasonal variation, at least in the week one forecasts. The precipitation (both amount and duration) and wind speed standard deviations are also similar in both magnitude and seasonal variation for all three datasets (except for RAWS precipitation duration which has a higher magnitude of variability than the other two datasets).

Seasonal variation in all three datasets is most noticeable in the seasonal means. Seasonal variations in the RAWS fire danger indices are much less noticeable than the distinct seasonal variations in the other two datasets. In addition, the magnitude of RAWS variation is much greater than the other two datasets.

Bias

Bias is useful in determining the correspondence between the average forecast and the average observation. RAWS versus the ECPC forecasts (RF; Figure 5-13) shows a negative bias of about 3 K for both week one and seasonal means in the maximum daily temperature. The negative bias for both week one and seasonal means is smaller for minimum and average temperature at approximately –1 K and –2 K, respectively. Seasonal variations in the RF bias of the temperature values are difficult to detect. Maximum daily relative humidity shows a consistent positive bias of about 15% decreasing to around 10% in winter (seasonal variability is difficult to see in the first two years). Minimum and average RH have a strong positive bias of approximately 30% and 25%, respectively. There is clear seasonality in the relative humidity RF bias, with the largest values during winter (40% minimum, 30% average), and lowest values in the summer (5% minimum, 10% average). Precipitation amount has a positive RF bias with a magnitude of 1-2 mm in summer but much smaller values in winter. Conversely, precipitation duration has a negative bias of one quarter to one half hour. Precipitation amount exhibits a seasonal cycle, but none is detected in the duration. There is a seasonal variation for wind speed bias with a positive value of 1.5 m/s in winter and almost no bias in summer. Because there is little differentiation in the magnitude and seasonality of the

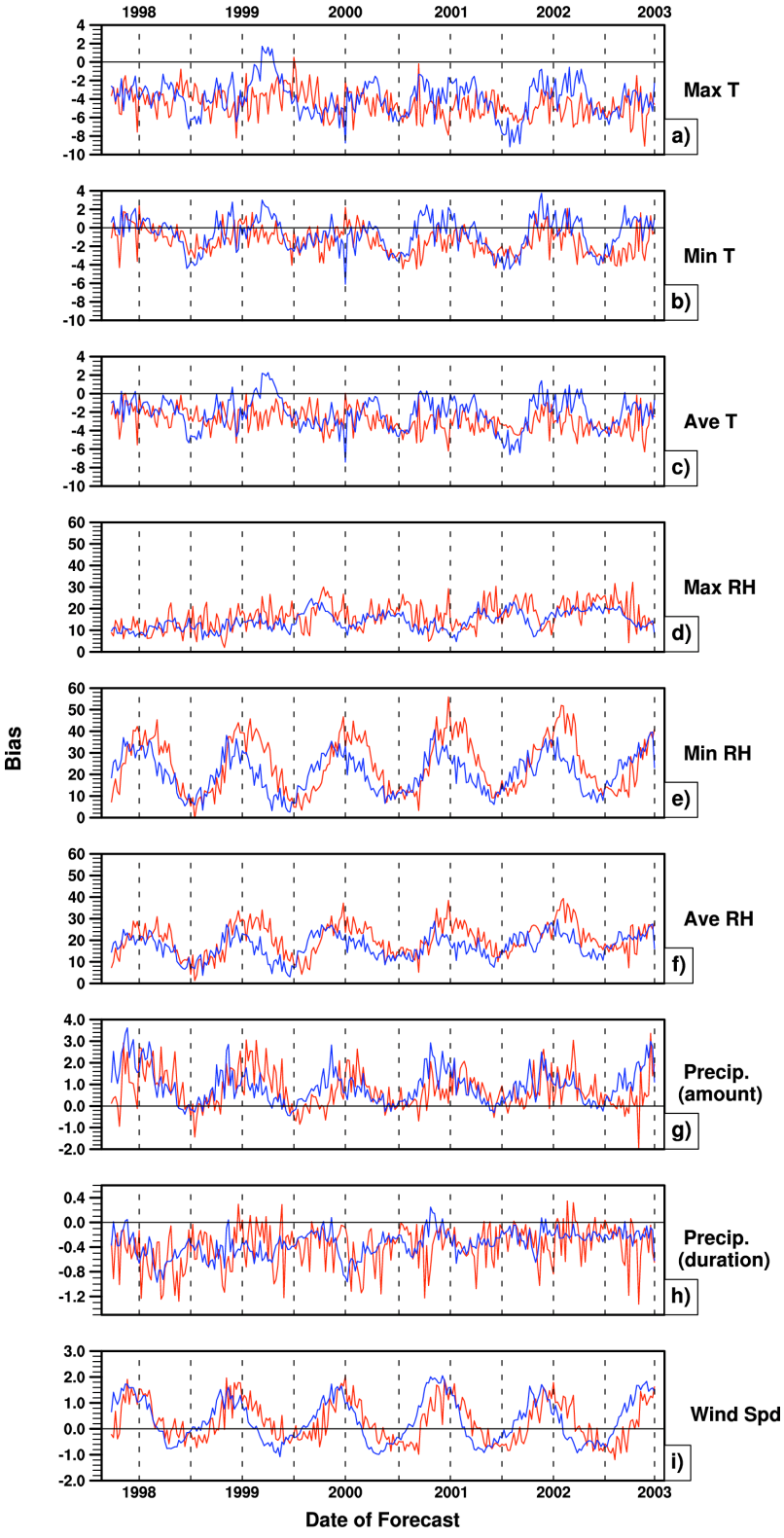

Figure 5-13 RAWS vs RSM forecast seasonal (blue line) and week 1 (red line) bias for (a) Max T (K); (b) Min T (K); (c) Ave T (K); (d) Max RH (%); (e) Min RH (%); (f) Ave RH (%); (g) Precip Amt (mm); (h) Precip Dur (hrs); (i) Wind Spd (m/s).

RF bias for the week one and seasonal means, the bias values mentioned above apply to both the week one and seasonal means.

The NFDRS indices (Figure 5-14) all have a negative RF bias (Figures 5-10 and 5-11). ERC has the smallest bias with values around –6. Seasonally, the ERC bias is less negative in fall (-2) than in spring (-9). BI has a less noticeable seasonal bias than any of the other indices, with an average negative value of –25. IC and SC have a similar pattern of negative bias, which varies from about –12 to –38. It should be noted that the bias for all fire danger indices is less negative for 1998.

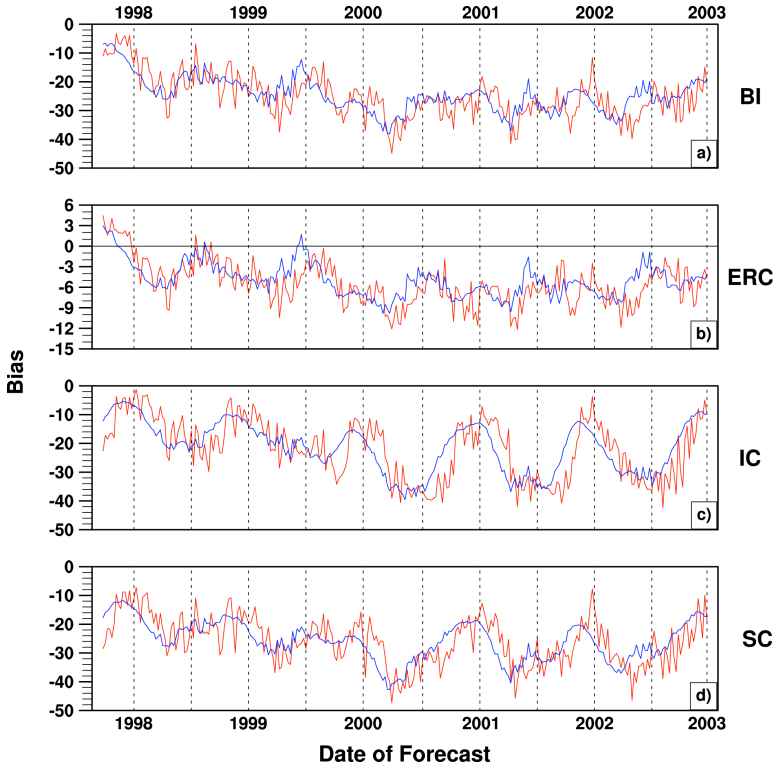

Figure 5-14 RAWS versus RSM forecast seasonal (blue line) and week 1 (red line) bias for (a) BI; (b) ERC; (c) IC; (d) SC.

The bias values for weekly means of RAWS versus ECPC validating observations are remarkably similar (RV; Figures 5-15 and 5-16) to the RF biases (comprised of week

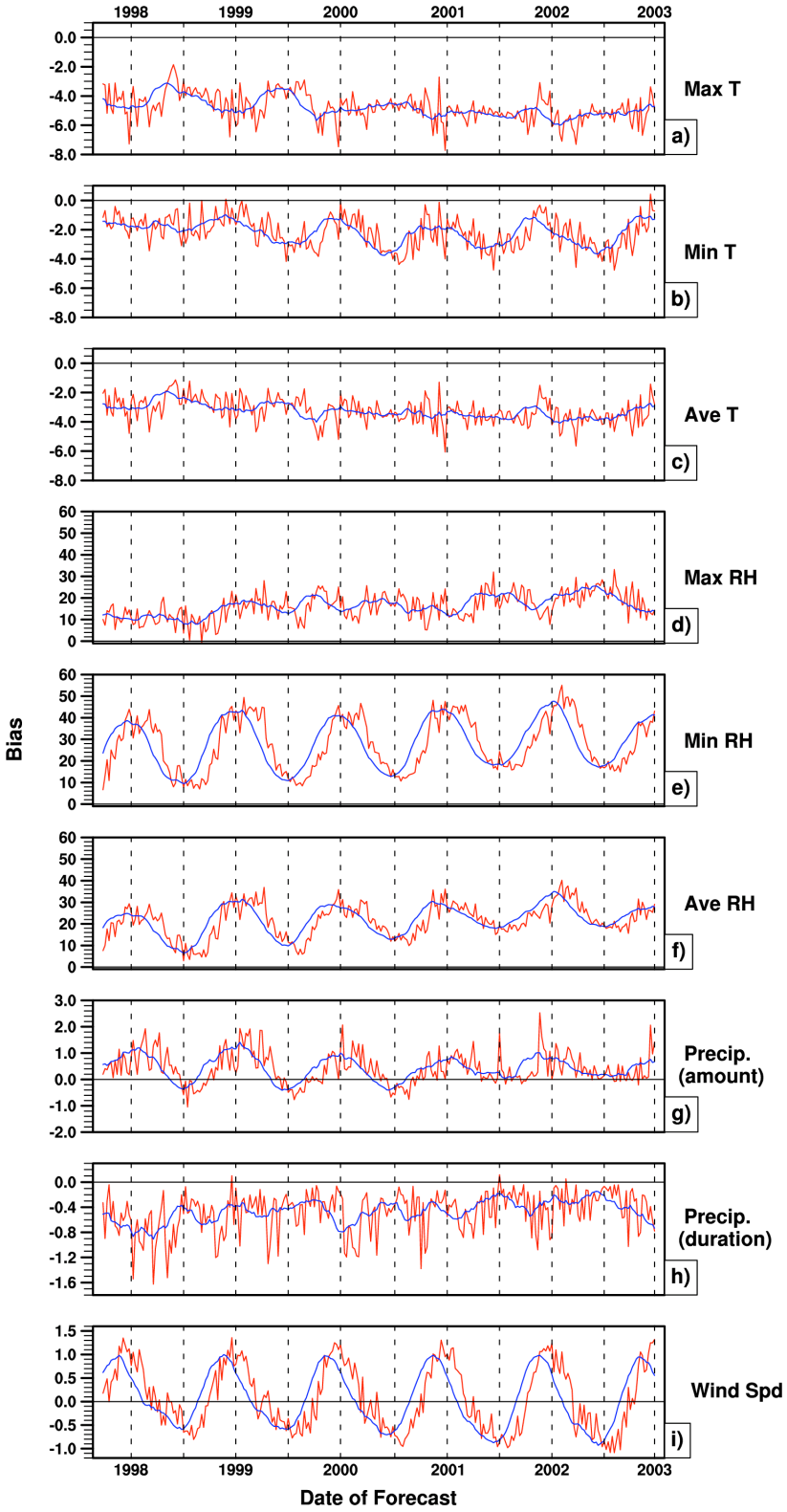

Figure 5-15 RAWS versus RSM validation seasonal (blue line) and week 1 (red line) bias for (a) Max T (K); (b) Min T (K); (c) Ave T (K); (d) Max RH (%); (e) Min RH (%); (f) Ave RH (%); (g) Precip Amt (mm); (h) Precip Dur (hrs); (i) Wind Spd (m/s).

one means). The seasonal variations in the RV biases match the RF biases very well for all atmospheric elements and NFDRS indices.

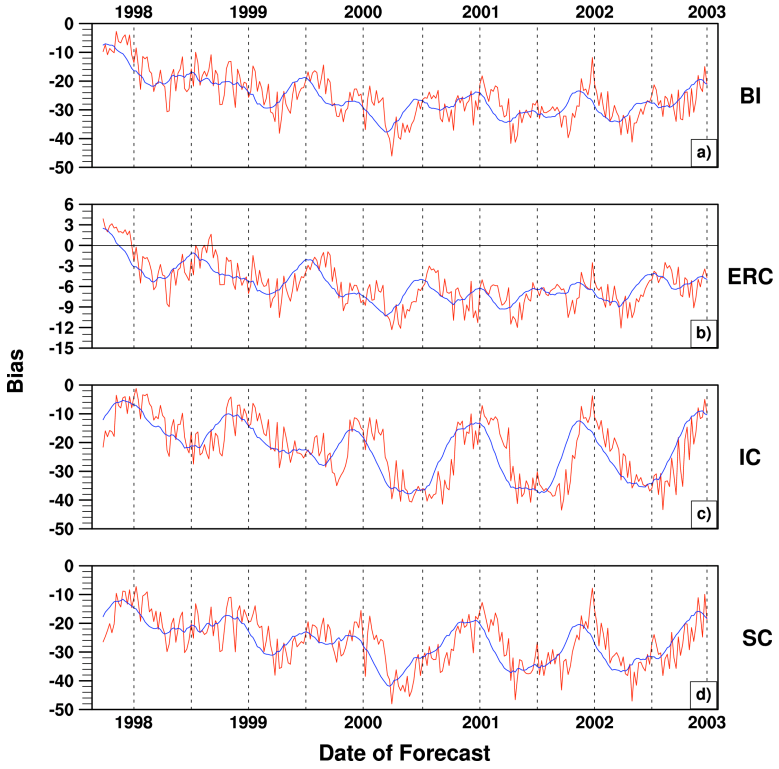

Figure 5-16 RAWS versus RSM validation seasonal (blue line) and week 1 (red line) bias for (a) BI; (b) ERC; (c) IC; (d) SC.

In contrast, the ECPC validating observations versus the ECPC forecasts (VF; Figure 5-17) show much smaller biases in all elements. The temperature values all show a small positive bias close to 1 K for week one means and 2 K for seasonal means. The VF maximum RH bias is much smaller than for RF and RV (-2% for week one, -4% for seasonal). The bias for minimum and average RH is more negative with –5% for week one means and –10% for seasonal. Precipitation amount has a positive bias of about 0.8 mm for both week one and seasonal means. The bias for precipitation duration is positive, with a value of one-quarter to half an hour. The VF NFDRS indices (Figure 5-

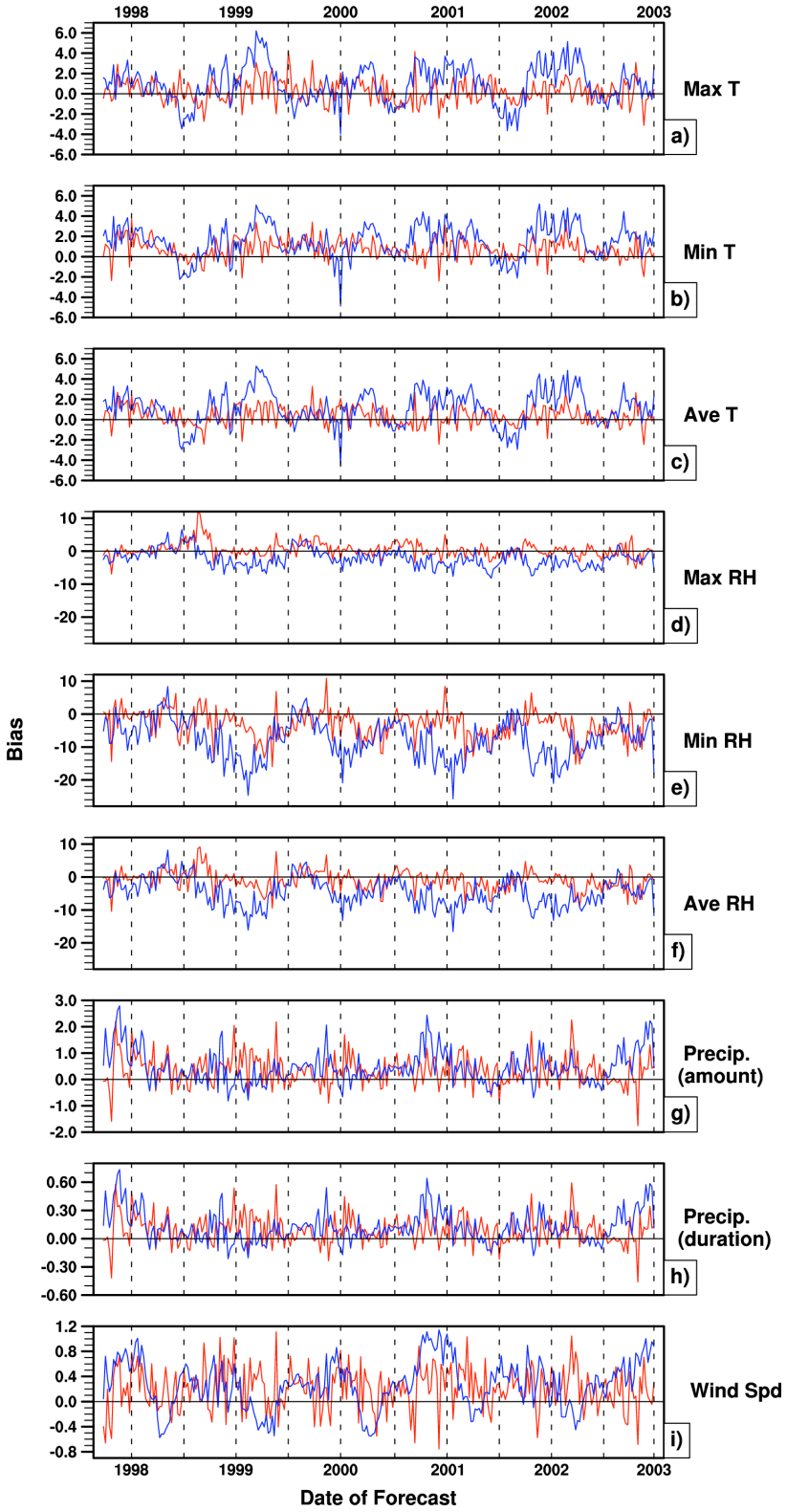

Figure 5-17 RSM validation versus RSM forecast seasonal (blue line) and week 1 (red line) bias for (a) Max T (K); (b) Min T (K); (c) Ave T (K); (d) Max RH (%); (e) Min RH (%); (f) Ave RH (%); (g) Precip Amt (mm); (h) Precip Dur (hrs); (i) Wind Spd (m/s).

18) have a much smaller bias than for RF and RV. For instance, BI only has a positive bias of 2 for week one means and 4 for seasonal means during the spring and summer. In winter, BI bias is very closer to 0.5. The other three NFDRS indices have a similar seasonal variation pattern, with approximate spring and summer values of ERC, IC and SC at 1.5, 3, and 2 for respective seasonal (12-week) means and 0.5, 1, and 1.0 for the respective week 1 means.

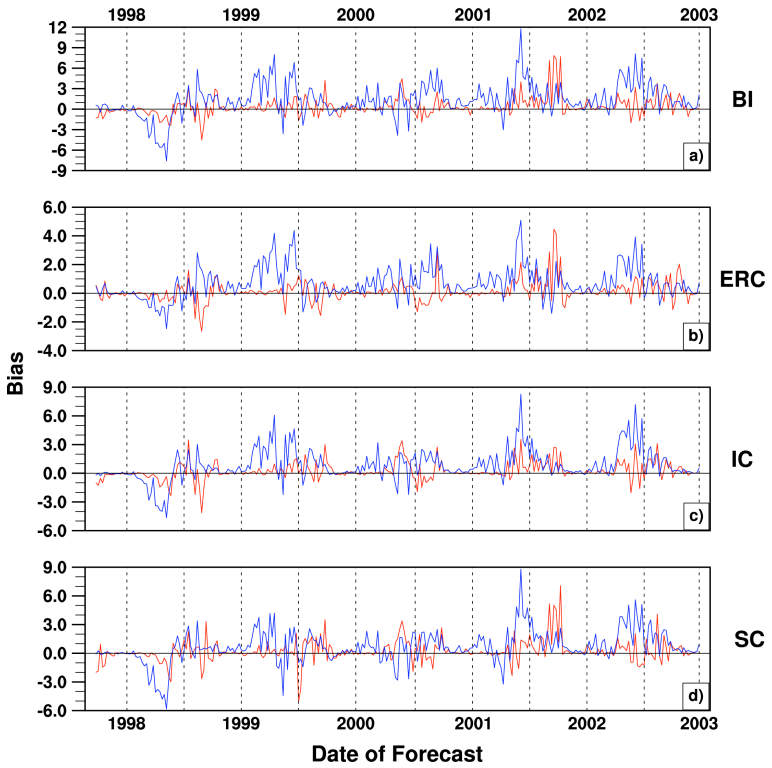

Figure 5-18 RSM validation versus RSM forecast seasonal (blue line) and week 1 (red line) bias for (a) BI; (b) ERC; (c) IC; (d) SC.

The strong similarity between the biases of the RF and RV elements indicates that the strong RF biases are most attributable to substantial differences between RAWS and the observations used to initialize the model (as approximated by the validating observations). The magnitude for most RF and RV bias is comparable or less than the

RAWS SD (Figure 5-7). However, the magnitude of the RF and RV bias for the relative humidity and NFDRS indices exceeds that of the SD in many places, giving the bias for those indices more significance. These biases do not imply that the model is not skillful, but they may adversely affect other verification statistics used to measure skill, such as correlations. As mentioned in Chapter 4, anomaly correlation minimizes these biases because the correlations generated reflect the accuracy of the forecast pattern more than the accuracy of the forecast element magnitudes.

Root-mean square error

Figures 5-19 and 5-20 show the performance of the weekly, monthly and seasonal forecast means for all three comparisons in terms of the root mean square error (RMSE), which is essentially a measure of the magnitude of the forecast errors for each type of forecast. These figures show the magnitude of forecast error on a year-round basis, for each type of forecast mean for RF, RV, and VF. The red line represents the RMSE for forecast weeks 1-12 from the RF comparison. The green line is the same but for VF. The average RF (✳) and VF (△) month 1-3 means are listed on weeks 2, 6, and 10 (the midpoint of each monthly mean). The average RF seasonal mean (square) is listed on week 6. The RMSE of the RV weekly (✡), monthly (▽) and seasonal (o) means are all plotted on week 5 to keep the overlap of symbols to a minimum. The RMSE for the VF seasonal mean (⊗) is plotted on week 7 for the same reason.

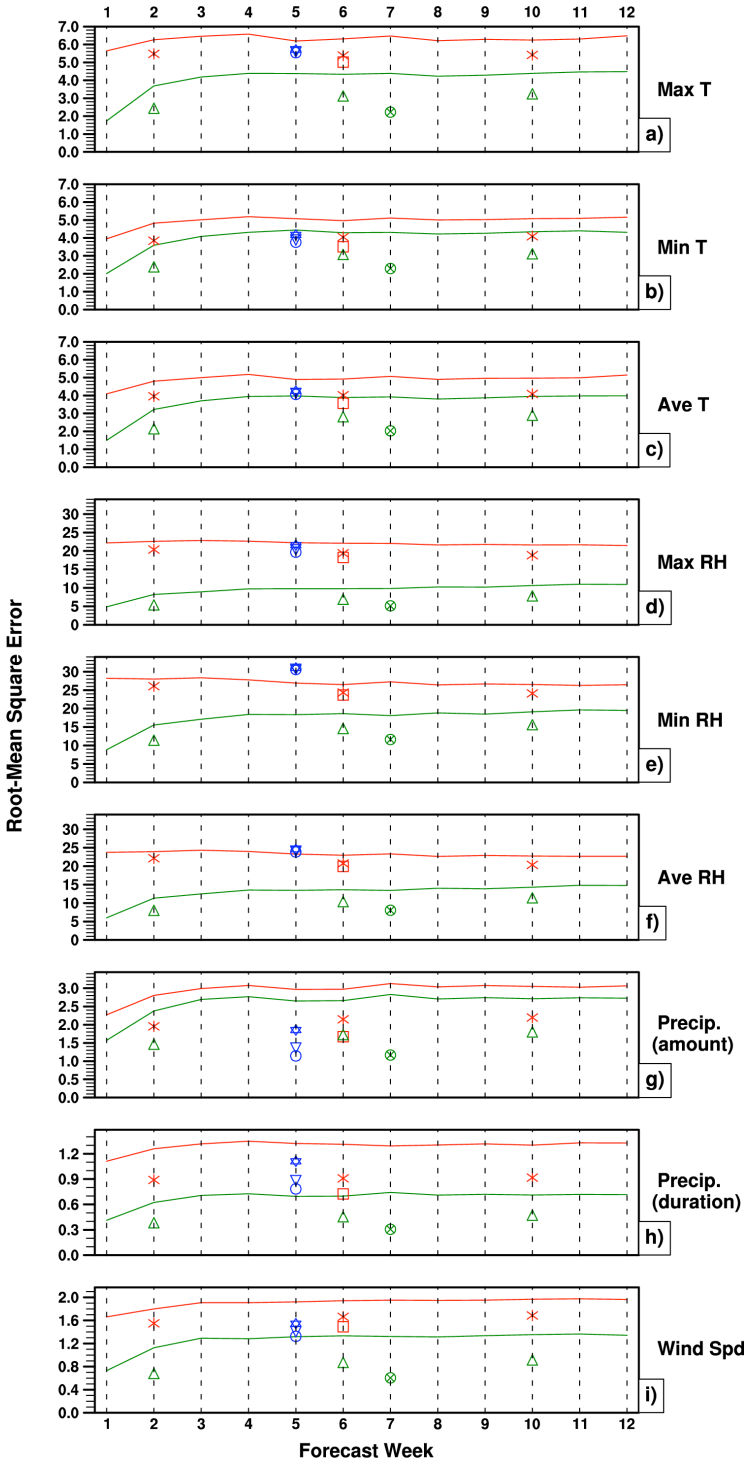

Figure 5-19 RF weekly (red line), monthly (✳), seasonal (square), VF weekly (green line), monthly (△), seasonal (⊗), and RV weekly (✡), monthly (▽), and seasonal (o) RMSE. Monthly and seasonal values are plotted at the center points (i.e. week 2 for month 1, week 6 for RF seasonal, week 5 for RV values and week 7 for VF seasonal). Atmospheric elements are (a) Max T (K); (b) Min T (K); (c) Ave T (K); (d) Max RH (%); (e) Min RH (%); (f) Ave RH (%); (g) Precip Amt (mm); (h) Precip Dur (hrs); (i) Wind Spd (m/s).

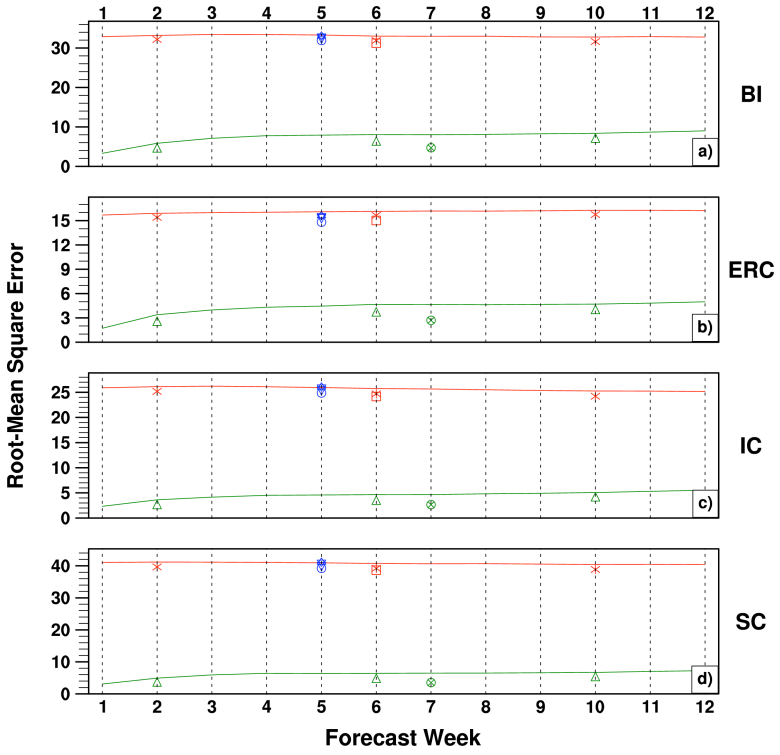

Figure 5-20 RF weekly (red line), monthly (✳), seasonal (square), VF weekly (green line), monthly (△), seasonal (⊗), and RV weekly (✡), monthly (▽), and seasonal (o) RMSE. Monthly and seasonal values are plotted at the center points (i.e. week 2 for month 1, week 6 for RF seasonal, week 5 for RV values and week 7 for VF seasonal). Fire danger indices are (a) BI; (b) ERC; (c) IC; (d) SC.

From these two graphs, one can see the magnitude of the differences between the three comparisons. The RMSE (for most RF and all VF elements) is lowest for week one, but reaches a higher plateau by week 3 or 4. The RF relative humidity and NFDRS indices have relatively level RMSE through all twelve weeks. If there is weekly pattern in the RH and NFDRS indices similar to the other RF indices, it is most likely obscured by the large bias values for these indices. In all cases, VF has lower RMSE than RF and RV because the inherent biases are much smaller than the other two comparisons. The weekly RV results are comparable in magnitude to the RF week one and month one (✳) results. The seasonal (o) and monthly (▽) RV means have a smaller RMSE than RF or VF for precipitation amount. The fire danger indices show a clear difference in

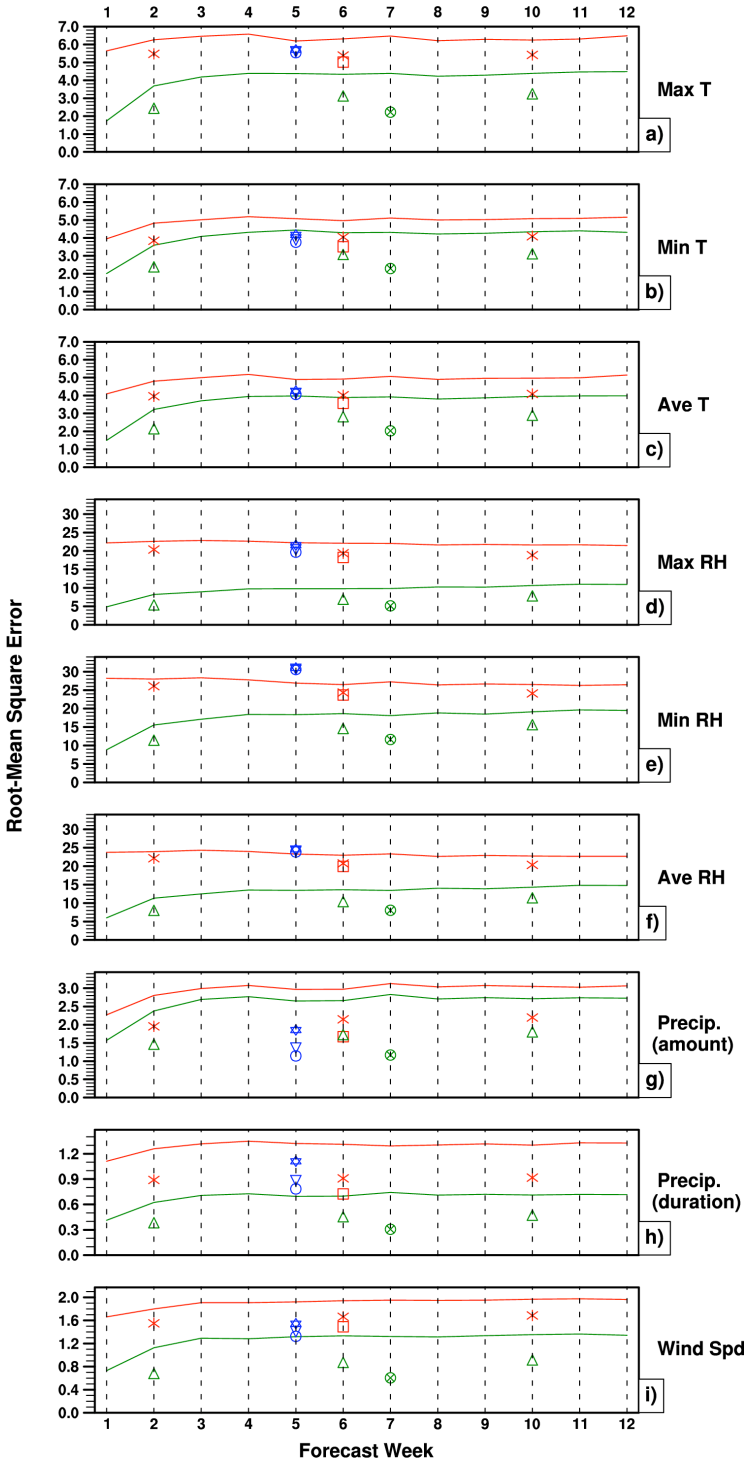

Figure 5-21 Summer RF weekly (red line), monthly (✳), seasonal (square), VF weekly (green line), monthly (△), seasonal (⊗), and RV weekly (✡), monthly (▽), and seasonal (o) RMSE. Monthly and seasonal values are plotted at the center points (i.e. week 2 for month 1, week 6 for RF seasonal, week 5 for RV values and week 7 for VF seasonal). Atmospheric elements are (a) Max T (K); (b) Min T (K); (c) Ave T (K); (d) Max RH (%); (e) Min RH (%); (f) Ave RH (%); (g) Precip Amt (mm); (h) Precip Dur (hrs); (i) Wind Spd (m/s).

magnitude between VF and RF and RV. The RMSE for the fire danger indices are, in general, higher for RF than for VF (by a factor of 10), with ERC again showing the smallest RMSE.

Summer means (Figures 5-21 and 5-22) reveal higher RMSE for maximum RH, minimum temperature and the NFDRS indices, at least for the first forecast week. All other RF elements have lower RMSE in summer, especially RMSE which drops by 13% for the week 1 means. Most of the summer atmospheric elements have slightly lower RMSE for VF and RV, while the fire danger indices have a slightly higher RMSE.

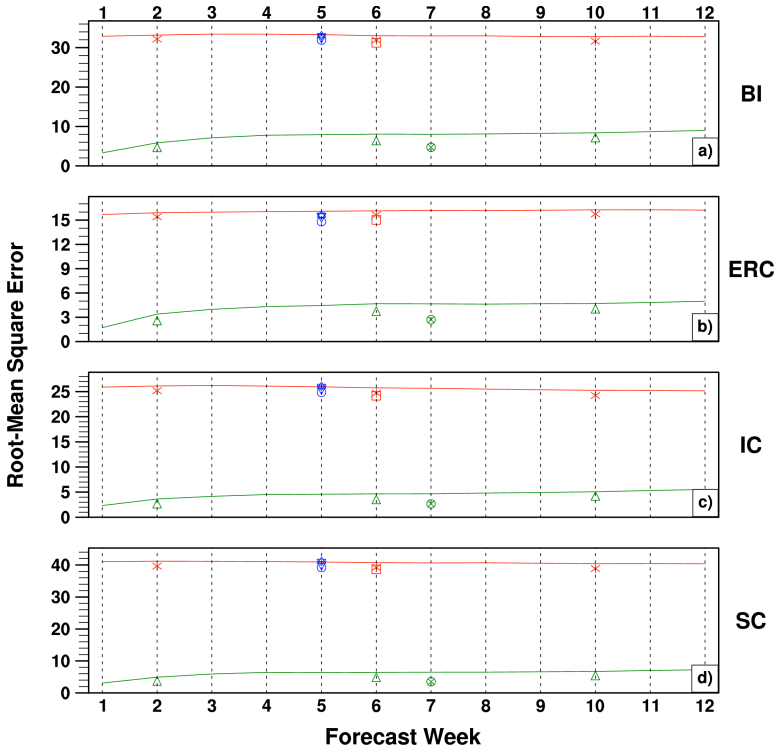

Figure 5-22: Summer RF weekly (red line), monthly (✳), seasonal (square), VF weekly (green line), monthly (△), seasonal (⊗), and RV weekly (✡), monthly (▽), and seasonal (o) RMSE. Monthly and seasonal values are plotted at the center points (i.e. week 2 for month 1, week 6 for RF seasonal, week 5 for RV values and week 7 for VF seasonal). Fire danger indices are (a) BI; (b) ERC; (c) IC; (d) SC.

Anomaly Correlation

Anomaly correlation is the primary measure of accuracy or skill in this study. This type of correlation utilizes anomalies rather than actual values and reduces the influence of bias by focusing on the accuracy in the pattern of the forecast. Positive values of 1 indicate the highest positive correlation in departures from normal (climatology), and values of -1 indicate the highest negative correlation. Values near zero indicate weak correlation.

For RF (Figure 5-23), the one week forecasts show a very high correlation, as might be expected, especially for the temperature and relative humidity indices. There are occasional negative correlations for all six temperature and relative humidity anomalies, but for the most part they have an approximate correlation of 0.6. The precipitation anomalies have a lower but consistently positive correlation of approximately 0.4. The correlation for week one wind speed is not as impressive (approximately 0.25), as it is effectively the most difficult element to forecast, but is consistently positive. Seasonal means for all atmospheric anomalies are lower than the one-week means (typically by 0.4 to 0.2) with the temperature anomalies showing the most dramatic difference. However, all seasonal means remain, on average, positive (most at about 0.2, except for wind speed which correlates at 0.05). In contrast with the atmospheric anomalies (especially temperature and relative humidity), the fire danger anomalies (Figure 5-24) show much less, though still positive, correlation (approximately 0.2 for week one and 0.1 for seasonal). However, while given a very low correlation, these anomalies do show a slight seasonal variation, where the correlation tends to improve in late summer and early fall.

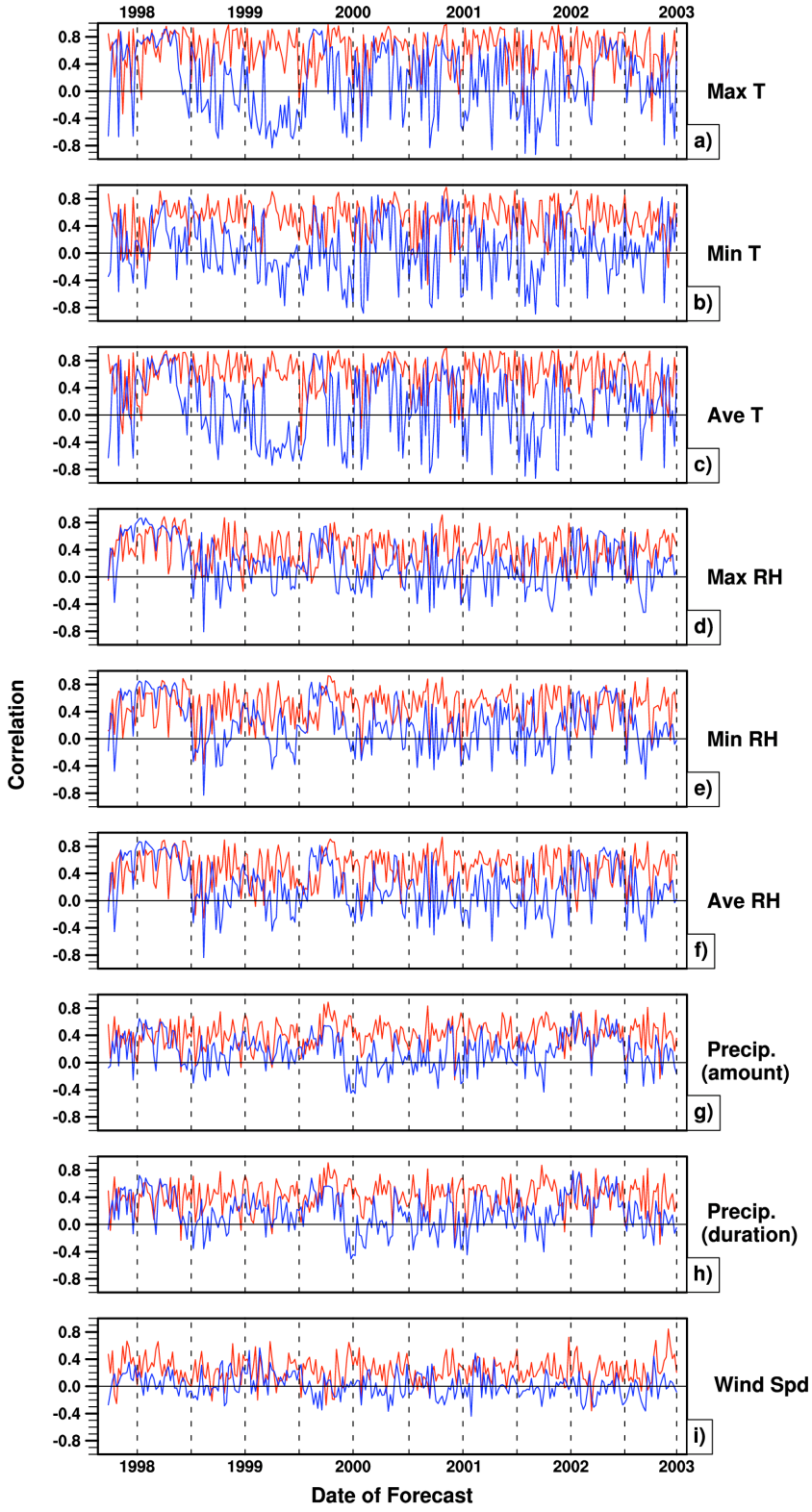

Figure 5-23 RF seasonal (blue line) and week 1 (red line) anomaly correlations for (a) Max T; (b) Min T; (c) Ave T; (d) Max RH; (e) Min RH; (f) Ave RH; (g) Precip Amt; (h) Precip Dur; (i) Wind Spd.

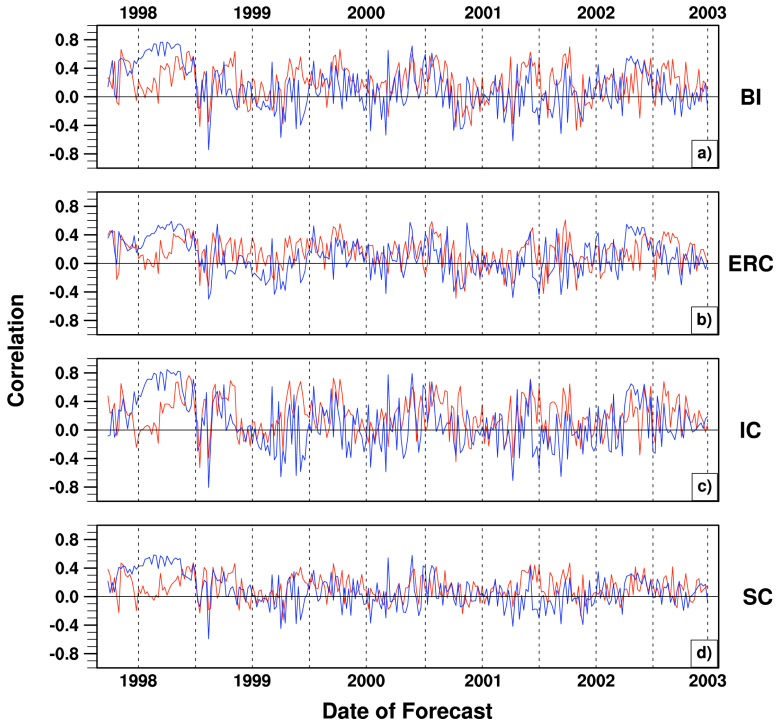

Figure 5-24 RF seasonal (blue line) and week 1 (red line) anomaly correlations for (a) BI; (b) ERC; (c) IC; (d) SC.

RV (Figure 5-25) shows a good correlation between both weekly and seasonal means. For all anomalies, the RV results seem to show a slight improvement compared to RF. Also, the RV seasonal means are much closer to the week one means than for the RF forecasts. These results were expected to show a level of positive correlation, as the RV is basically a comparison of two different observational networks. The RV fire danger anomalies (Figure 5-26) are a different story. While these correlations are higher than for RF, they still average out to very low correlations for both the week one and seasonal means. This comparison also shows the slight seasonal variation lending to better correlations in the summer.

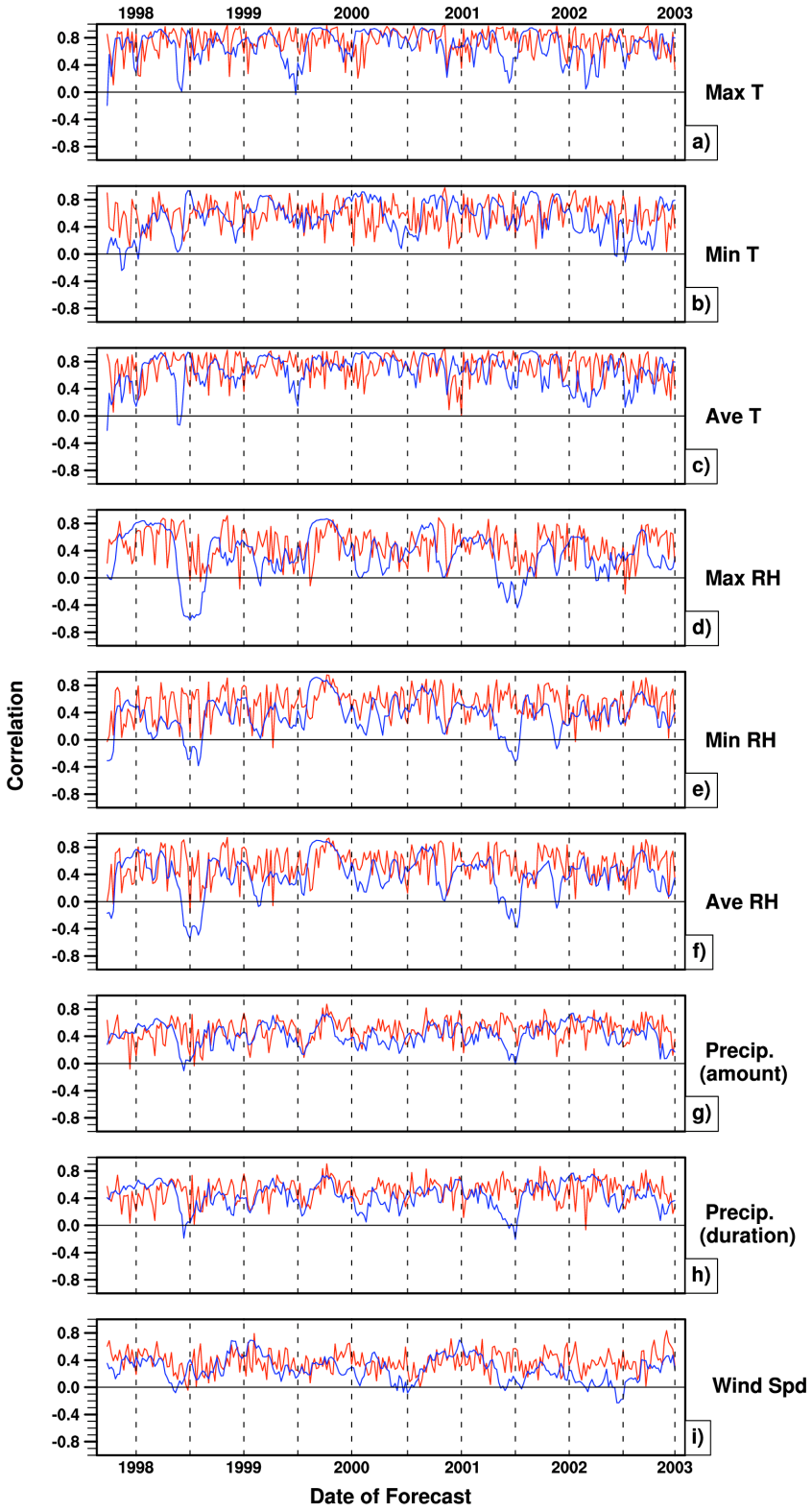

Figure 5-25 RV seasonal (blue line) and week 1 (red line) anomaly correlations for (a) Max T; (b) Min T; (c) Ave T; (d) Max RH; (e) Min RH; (f) Ave RH; (g) Precip Amt; (h) Precip Dur; (i) Wind Spd.

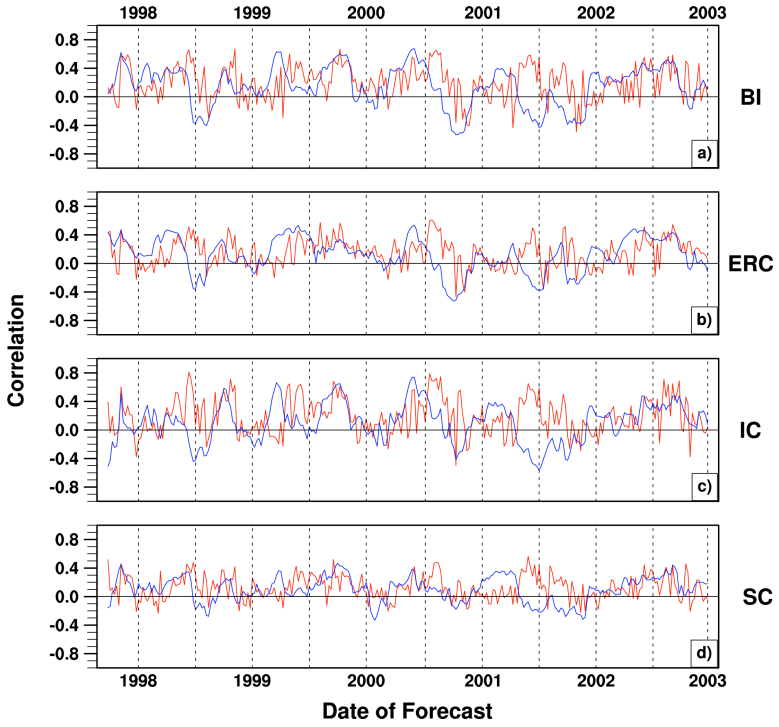

Figure 5-26 RV seasonal (blue line) and week 1 (red line) anomaly correlations for (a) BI; (b) ERC; (c) IC; (d) SC.

The week one forecast means (Figure 5-27) for the VF comparison are very high for all atmospheric anomalies, notably precipitation (0.6 in both amount and duration) and wind speed (0.5). However, the correlations for seasonal anomaly means drop to approximately 0.2. The fire danger anomalies (Figure 5-28) also show much higher correlation values (0.7 for BI and ERC, and 0.6 for IC and SC) when compared to RF and RV, especially for the week one means. The seasonal means are understandably lower (approximately 0.3), but are still higher than the week one means in the other two analyses.

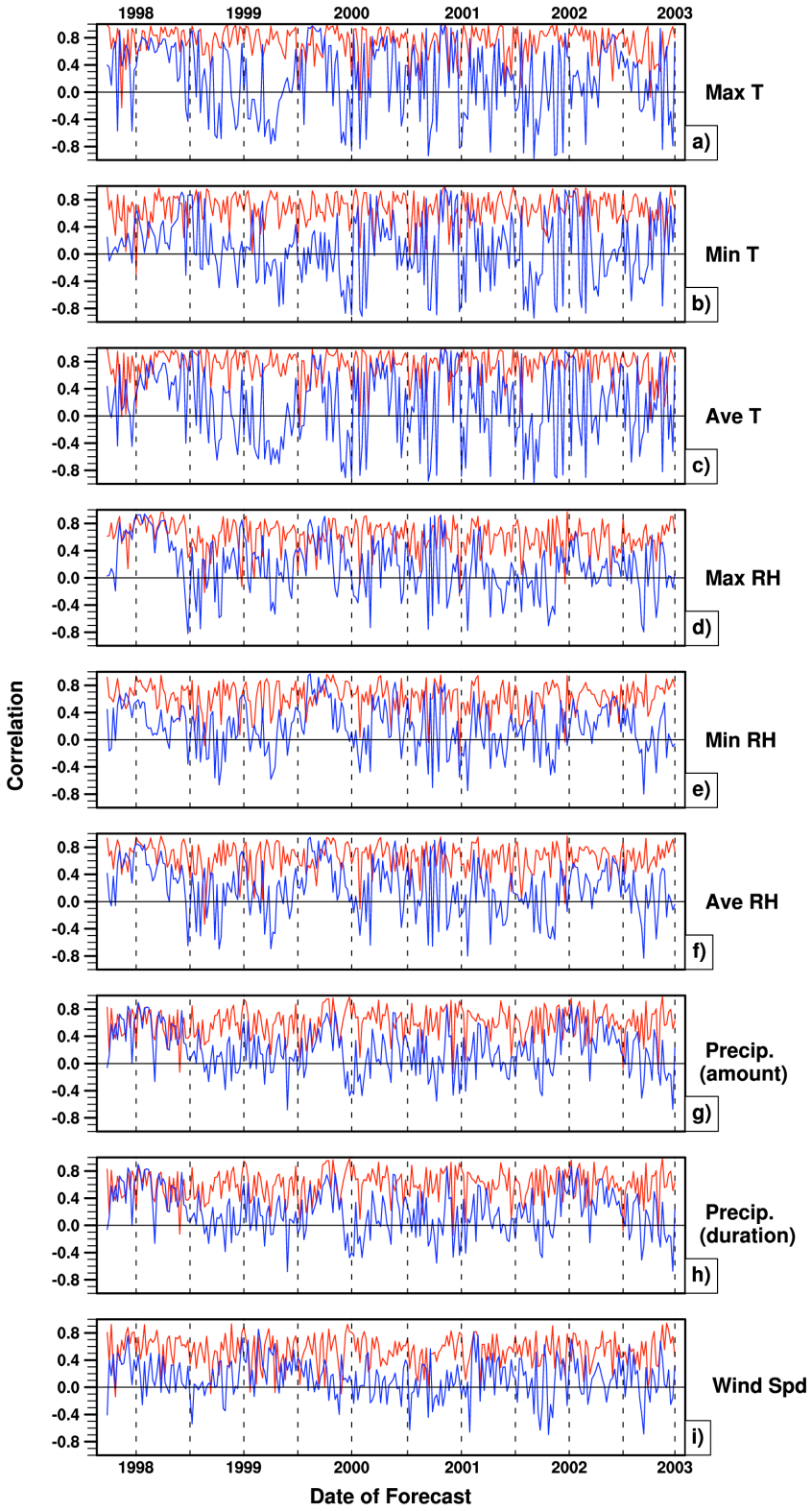

Figure 5-27 VF seasonal (blue line) and week 1 (red line) anomaly correlations for (a) Max T; (b) Min T; (c) Ave T; (d) Max RH; (e) Min RH; (f) Ave RH; (g) Precip Amt; (h) Precip Dur; (i) Wind Spd.

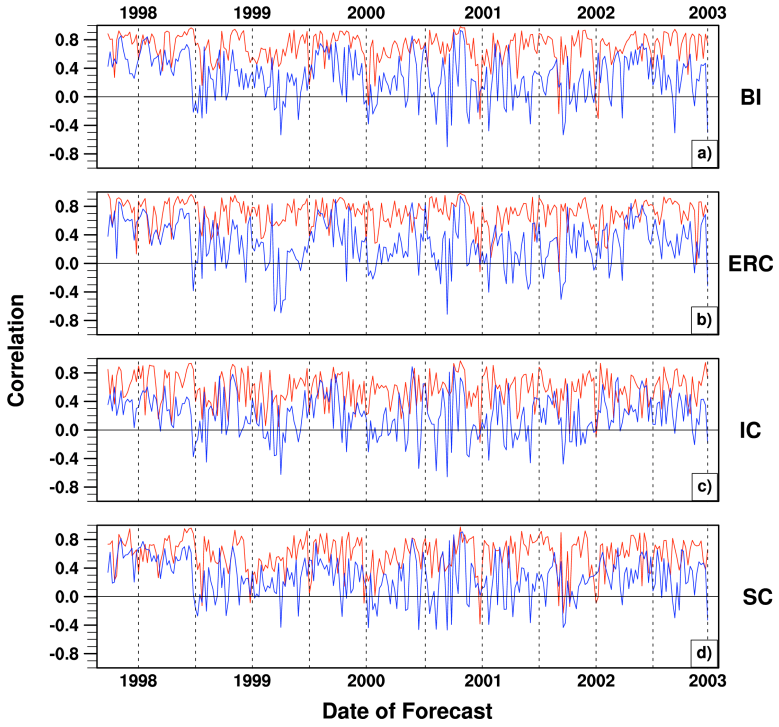

Figure 5-28 VF seasonal (blue line) and week 1 (red line) anomaly correlations for (a) BI; (b) ERC; (c) IC; (d) SC.

Figures 5-29 and 5-30 show the performance of each weekly, monthly and seasonal mean of all three comparisons in terms of the anomaly correlation (AC). The plotting scheme is similar to that of Figures 5-19 through 5-22.

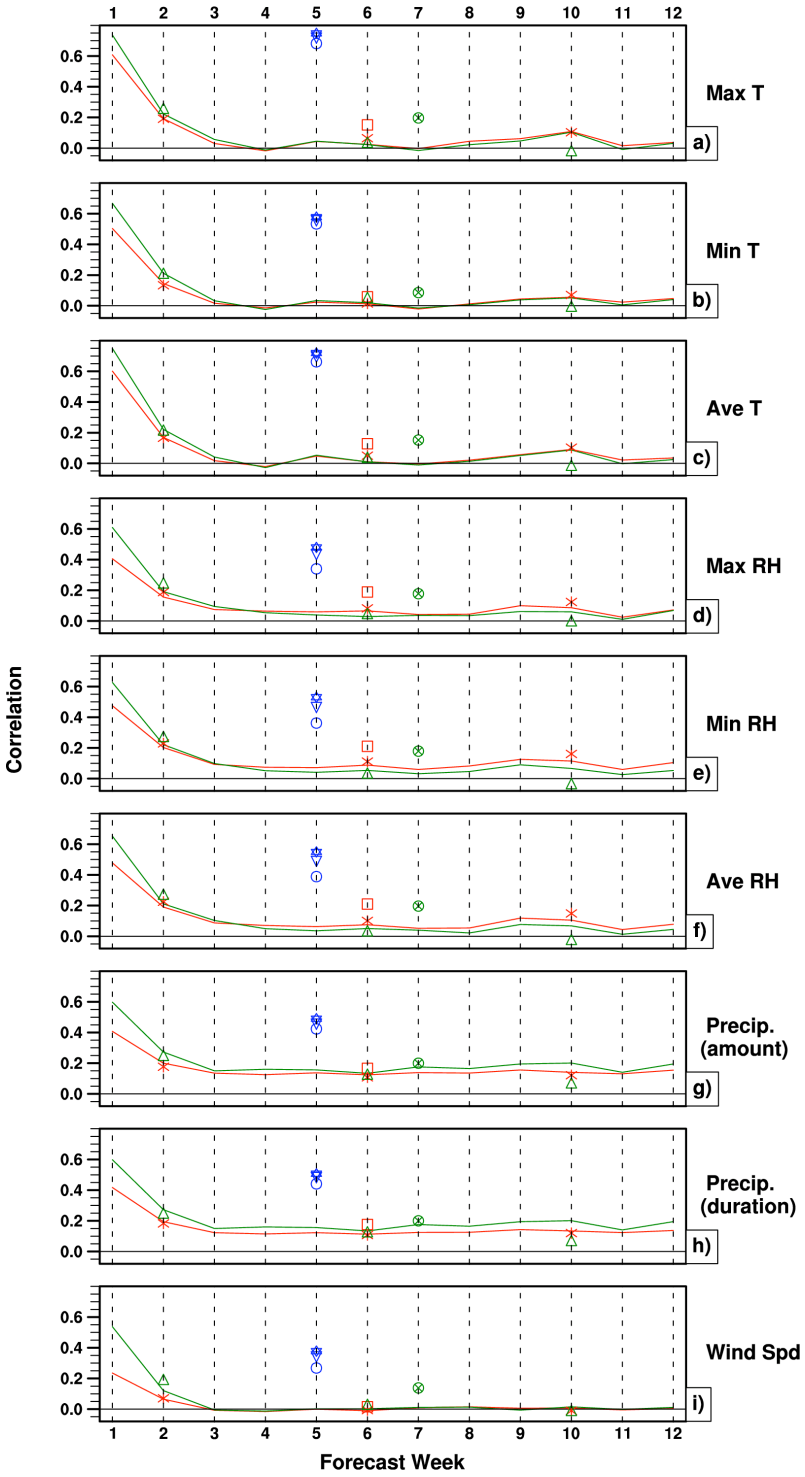

Figure 5-29: RF weekly (red line), monthly (✳), seasonal (square), VF weekly (green line), monthly (△), seasonal (⊗), and RV weekly (✡), monthly (▽), and seasonal (o) anomaly correlations. Monthly and seasonal values are plotted at the center points (i.e. week 2 for month 1, week 6 for RF seasonal, week 5 for RV values and week 7 for VF seasonal). Atmospheric elements are (a) Max T; (b) Min T; (c) Ave T; (d) Max RH; (e) Min RH; (f) Ave RH; (g) Precip Amt; (h) Precip Dur; (i) Wind Spd.

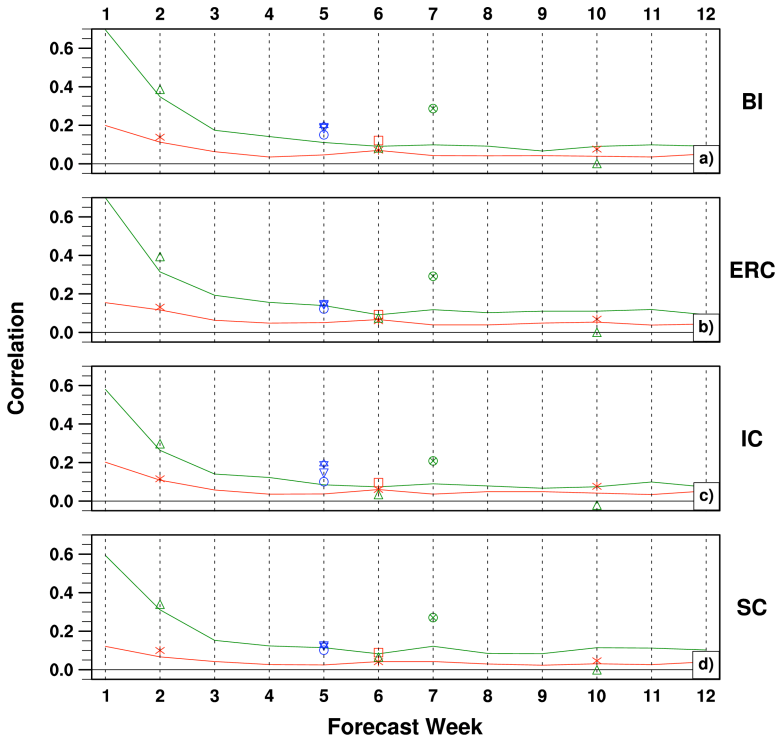

Figure 5-30 RF weekly (red line), monthly (✳), seasonal (square), VF weekly (green line), monthly (△), seasonal (⊗), and RV weekly (✡), monthly (▽), and seasonal (o) anomaly correlations. Monthly and seasonal values are plotted at the center points (i.e. week 2 for month 1, week 6 for RF seasonal, week 5 for RV values and week 7 for VF seasonal). Fire danger indices are (a) BI; (b) ERC; (c) IC; (d) SC.

The weekly means, somewhat predictably, start off with high correlation in week one, drop significantly by week two, and level off to a lower, but still positive correlation from weeks 3 through 12. VF atmospheric anomalies show high week one correlation values usually around 0.6 (0.7 or greater for temperature). The fire danger anomalies also maintain an approximate 0.6 correlation for week one. In contrast, RF shows a correlation of 0.6 only for the maximum and average temperature. Minimum temperature, minimum relative humidity and average relative humidity all have values near 0.5, with maximum relative humidity, precipitation amount and precipitation duration all closer to 0.4. Wind speed and the fire danger anomalies show the lowest RF correlation with values of 0.2 or less. Beyond week 3, both RF and VF level out at about

the same correlation value for all variables (typically between 0.1 and 0, although the precipitation indices level out closer to 0.15). The weekly mean for RV (✡) is usually below the VF and above the RF week one correlations.

In most cases the RF (✳) and VF (△) monthly means could probably be approximated by the week 2, week 6 and week 10 weekly means, although month 3 correlations tend to fall below these values. The RV (▽) monthly correlation is typically much higher than the other monthly means, and just below the VF weekly correlation.

RF (square) and VF (⊗) correlations for the seasonal forecast means tend to be lower than the week one means, on the order of about 0.2, although the RF seasonal correlations for minimum temperature and wind speed are less than 0.1. The VF seasonal mean correlations are consistently higher than the corresponding RF correlations (by about 0.5), especially for the fire danger anomalies, but with the exception of the relative humidity anomalies. For the fire danger anomalies, the VF seasonal mean correlations are higher compared to the VF atmospheric means (approaching 0.4) while the RF correlations drop to 0.1 or 0.15. RV seasonal mean (o) correlations are very high for the atmospheric anomalies, but drop to the level of the RF seasonal mean correlations for the fire danger anomalies.

Looking at mean anomaly correlations for summer forecasts (Figures 5-31 and 5-32), there are a few differences when compared to the year-round averages shown in Figures 5-29 and 5-30. There is little difference in the summer RF, VF and RV (✡) week one mean atmospheric anomaly correlations, which are all about 0.05 lower than the values for the corresponding elements in Figure 5-29, with the exception of minimum and daily temperature. The summer monthly means show little difference as well, except for

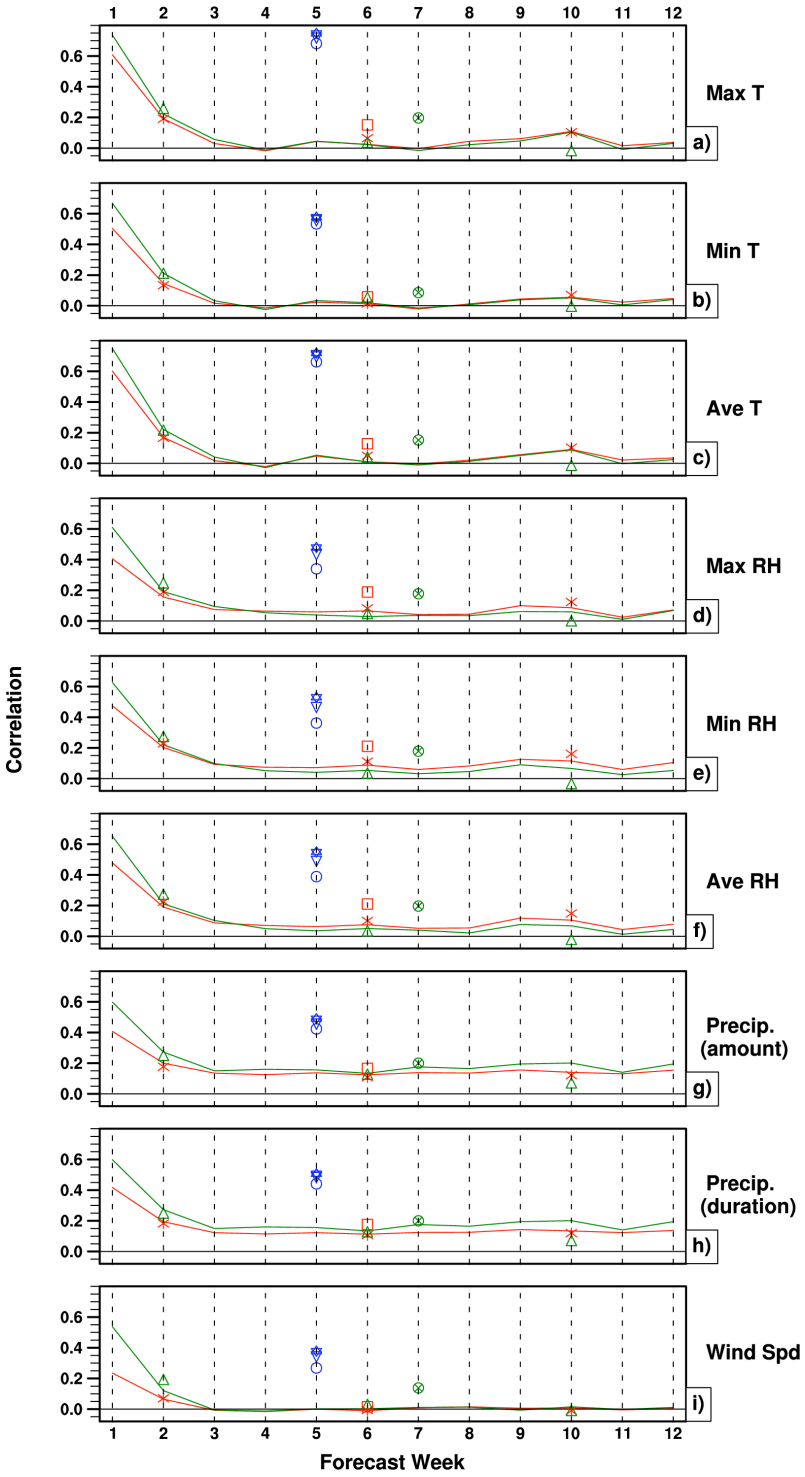

Figure 5-31 Summer RF weekly (solid line), monthly (✳), seasonal (square), VF weekly (green line), monthly (△), seasonal (⊗), and RV weekly (✡), monthly (▽), and seasonal (o) anomaly correlations. Monthly and seasonal values are plotted at the center points (i.e. week 2 for month 1, week 6 for RF seasonal, week 5 for RV values and week 7 for VF seasonal). Atmospheric elements are (a) Max T; (b) Min T; (c) Ave T; (d) Max RH; (e) Min RH; (f) Ave RH; (g) Precip Amt; (h) Precip Dur; (i) Wind Spd.

noticeable drops in RF (✳), VF (△), and RV (▽) monthly means of precipitation duration and amount. Surprisingly, the VF (⊗) seasonal means improve during summer, with the exception of maximum relative humidity. The change in RF (square) seasonal means is not the same for every element. When compared to Figure 5-29, the correlations of RF seasonal means in Figure 5-31 are greater for maximum relative humidity (by about 0.1) and wind speed (by 0.05), but remain about the same for the rest of the elements. The RV (o) seasonal correlation means decrease for every atmospheric element in summer, especially maximum temperature, maximum humidity and wind speed (by about 0.3 for all three).

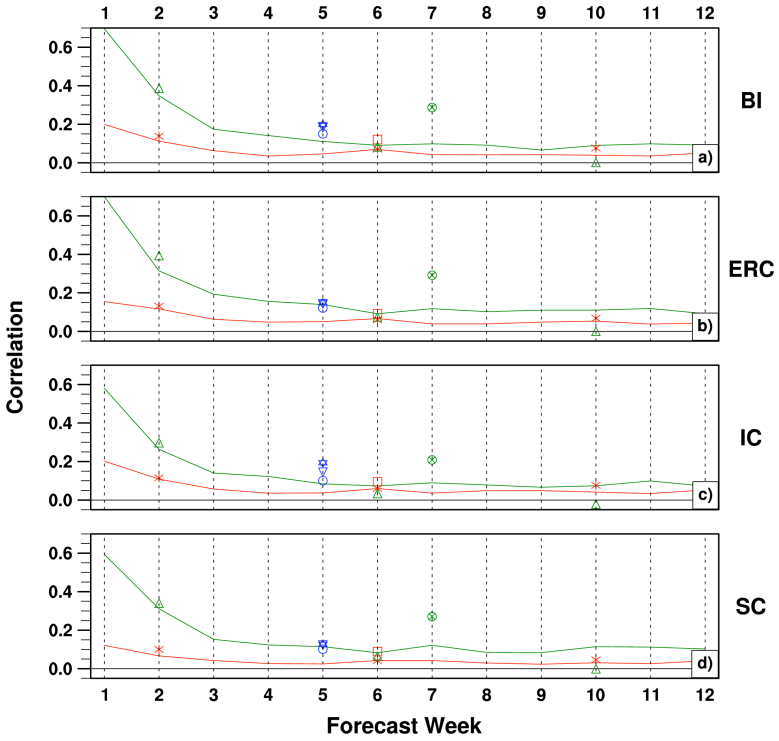

Figure 5-32 Summer RF weekly (red line), monthly (✳), seasonal (square), VF weekly (green line), monthly (△), seasonal (⊗), and RV weekly (✡), monthly (▽), and seasonal (o) anomaly correlations. Monthly and seasonal values are plotted at the center points (i.e. week 2 for month 1, week 6 for RF seasonal, week 5 for RV values and week 7 for VF seasonal). Fire danger indices are (a) BI; (b) ERC; (c) IC; (d) SC.

The summer correlations of the RF and VF weekly, monthly and seasonal means (Figure 5-32) for the fire danger indices all increase slightly when compared to the same means in Figure 5-30. Most significantly, the RF summer week one means for SC and IC increase by approximately 0.1. The RV weekly correlations increase during summer as well (0.1 for BI, IC, and SC), although there is little change in the RV monthly and seasonal means.

CHAPTER 6

SPATIAL ANALYSIS

This chapter discusses the spatial variations in the RF, RV, and VF comparisons in order to determine those regions in the West where the model forecasts are (and are not) most accurate. Recall from Chapter 4 that eight regions were chosen utilizing a cluster analysis (Figure 4-1). A summary of the root mean square error and anomaly correlation for each of the eight regions is presented first. Next, spatial variation is examined by the spatial version of the anomaly correlation discussed in Chapter 4.

Figures 6-1 and 6-2 give the regional root mean square error of the RF, RV and VF week one means. The x-axis value zero represents the whole western U.S. study area for purposes of comparison with each region. The week one means for RV and RF show fairly consistent temperature and wind speed RMSE throughout the regions. All three comparisons have the highest regional RMSE for precipitation amount in the coastal northwest (region 3). The RF and RV RMSE in precipitation duration also spikes in region 3. In contrast, the RF and RV RMSE in the relative humidity indices is lower there. The southern portions of the southwestern states and California (regions 1, 7, and 8) have the lowest RMSE for precipitation amount.

The burning index (Figure 6-2) shows the greatest error in southern California (regions 7 and 8). The ERC has a relatively small error everywhere except the four corners area (region 2) and coastal southern California (region 8). The IC and SC both have their lowest error in region 3, although region 1 shows a huge jump in SC error. The VF RMSE values are relatively low and consistent through all regions, although the

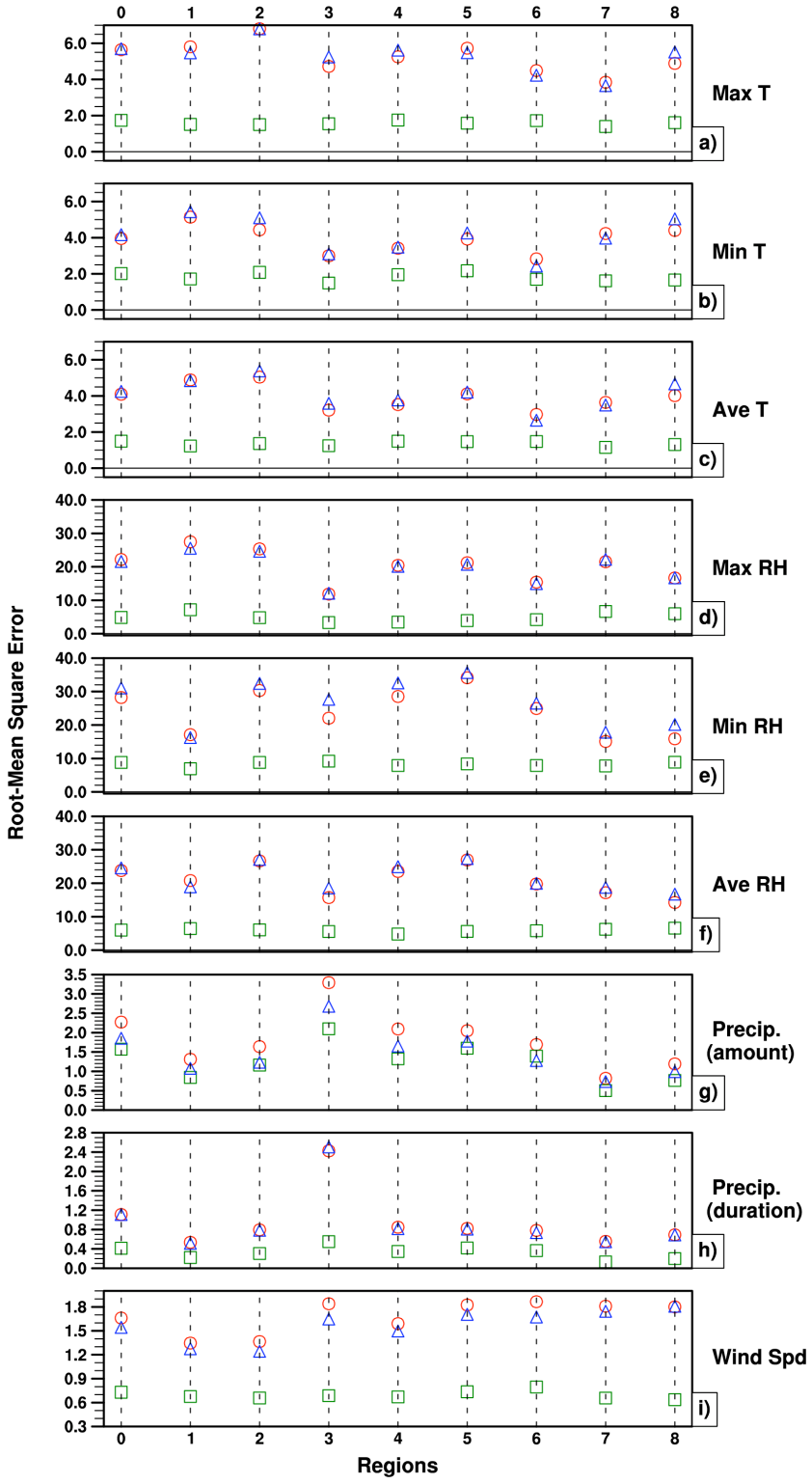

Figure 6-1 RF (circle), RV (triangle), and VF (square) Week 1 RMSE by region. The x-axis zero value represents the entire western U.S. Atmospheric elements include (a) Max T (K); (b) Min T (K); (c) Ave T (K); (d) Max RH (%); (e) Min RH (%); (f) Ave RH (%); (g) Precip Amt (mm); (h) Precip Dur (hrs); (i) Wind Spd (m/s).

visual variations between regions are minimized due to the scale difference between the VF and the RF and RV RMSE. Results for the month one and seasonal means (Figures 5-29 – 5-32) are very similar to the week one results. Neither the month one means (Figures 6-3 and 6-4) nor the seasonal means (Figures 6-5 and 6-6) change significantly in overall or regional RMSE. This is consistent with the results from Figures 5-19 and 5-20.

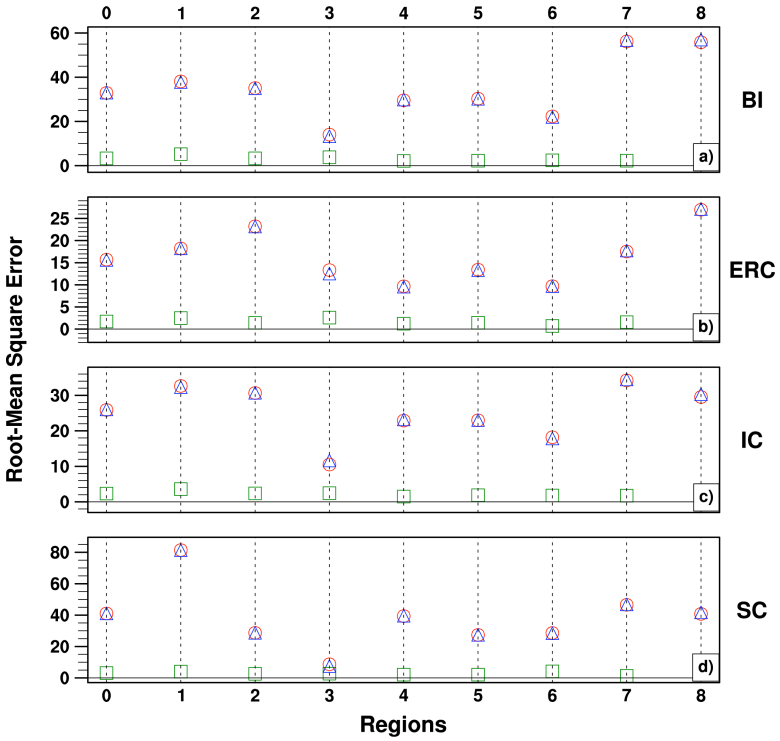

Figure 6-2 RF (circle), RV (triangle), and VF (square) Week 1 RMSE by region. The x-axis zero value represents the entire western U.S. Fire danger indices include (a) BI; (b) ERC; (c) IC; (d) SC.

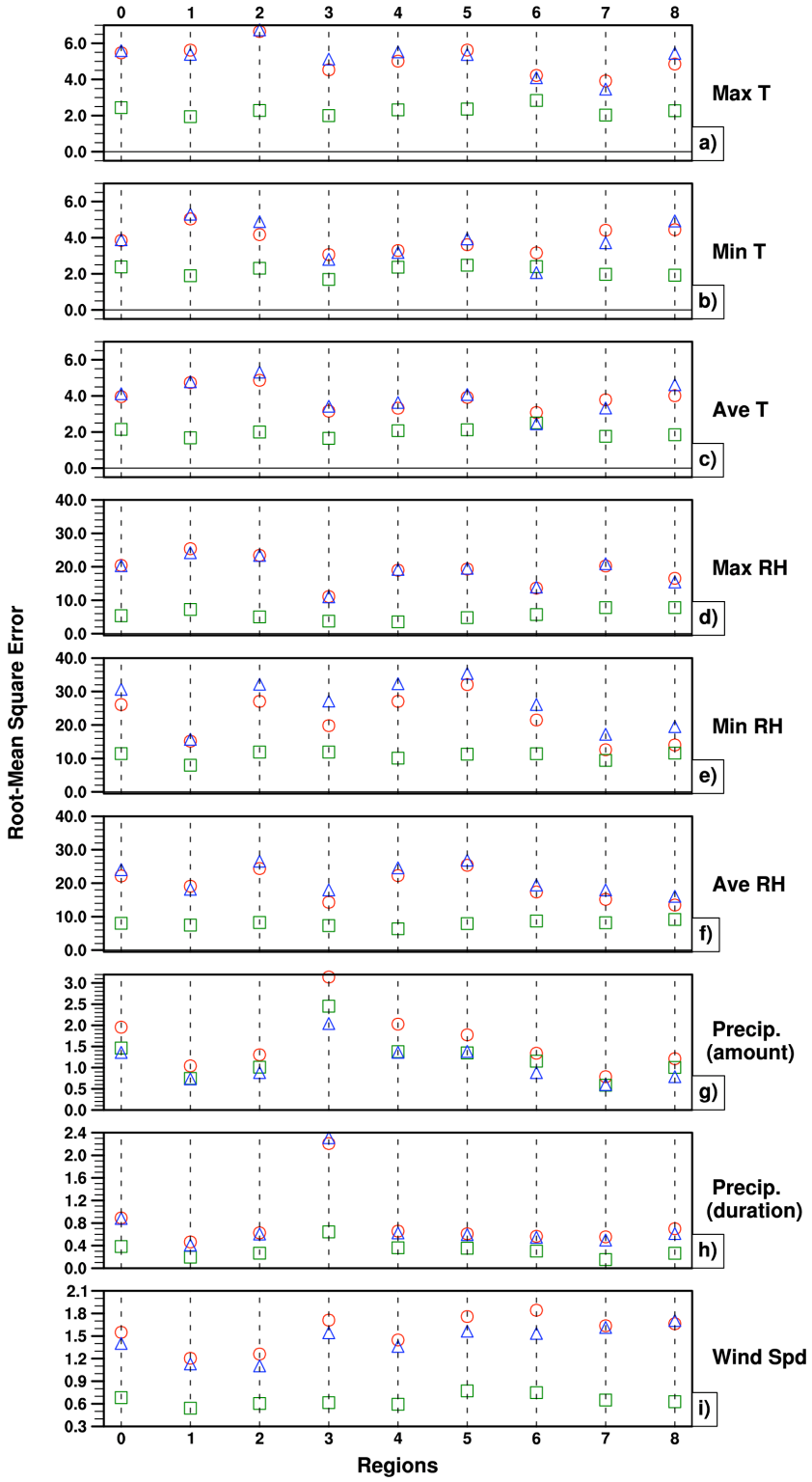

Figure 6-3 RF (circle), RV (triangle), and VF (square) Month 1 RMSE by region. The x-axis zero value represents the entire western U.S. Atmospheric elements include (a) Max T (K); (b) Min T (K); (c) Ave T (K); (d) Max RH (%); (e) Min RH (%); (f) Ave RH (%); (g) Precip Amt (mm); (h) Precip Dur (hrs); (i) Wind Spd (m/s).

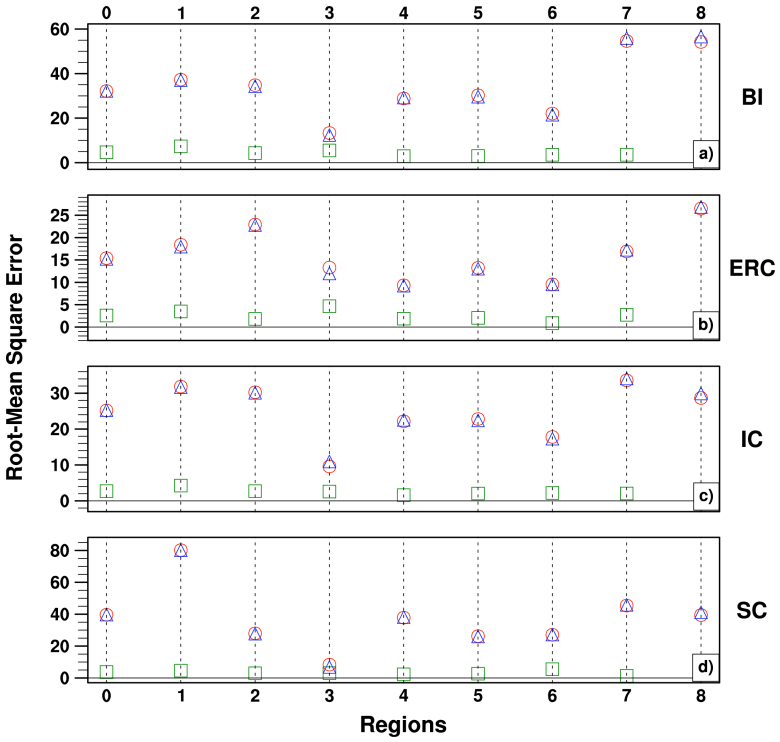

Figure 6-4 RF (circle), RV (triangle), and VF (square) Month 1 RMSE by region. The x-axis zero value represents the entire western U.S. Fire danger indices include (a) BI; (b) ERC; (c) IC; (d) SC.

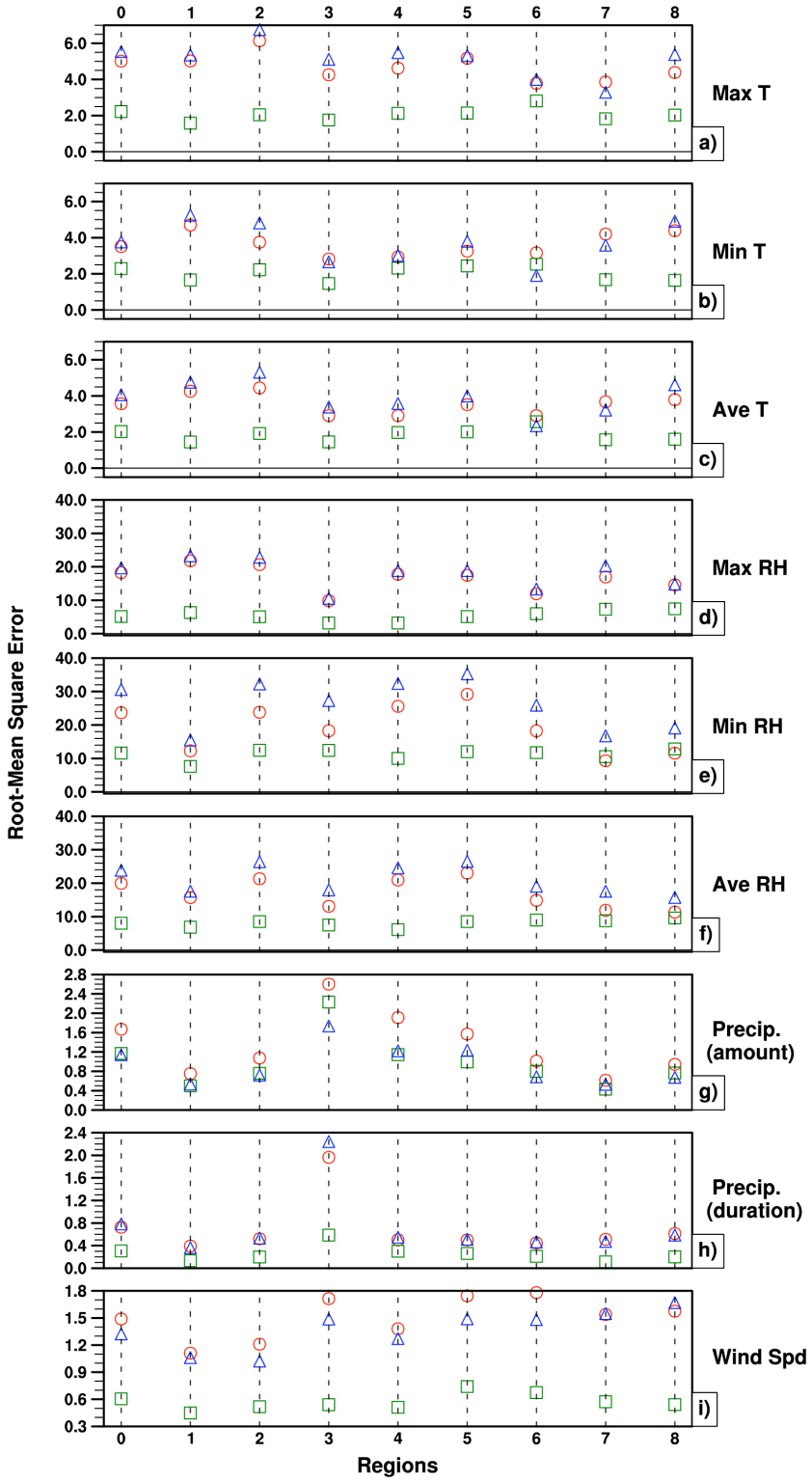

Figure 6-5 RF (circle), RV (triangle), and VF (square) Seasonal RMSE by region. The x-axis zero value represents the entire western U.S. Atmospheric elements include (a) Max T (K); (b) Min T (K); (c) Ave T (K); (d) Max RH (%); (e) Min RH (%); (f) Ave RH (%); (g) Precip Amt (mm); (h) Precip Dur (hrs); (i) Wind Spd (m/s).

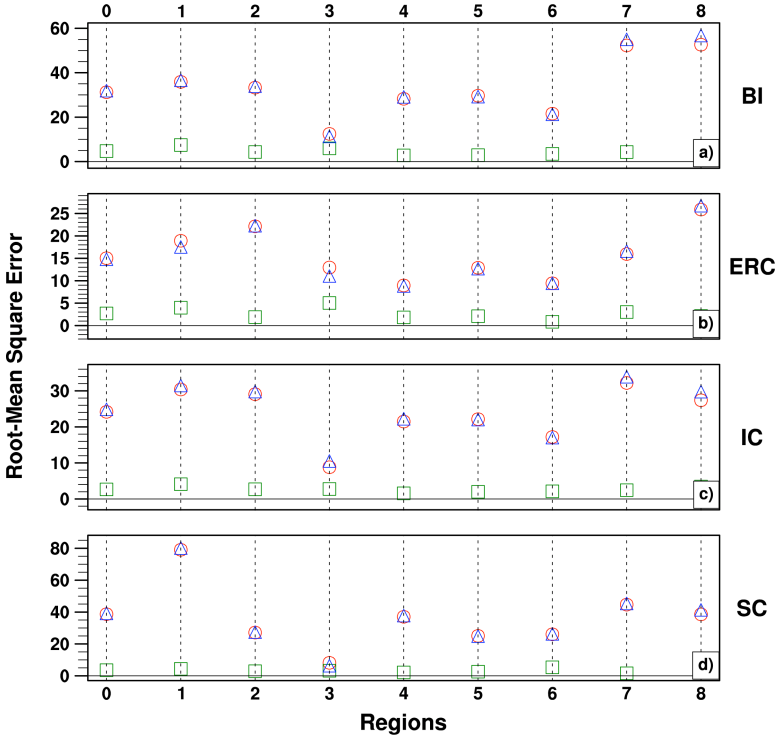

Figure 6-6 RF (circle), RV (triangle), and VF (square) Seasonal RMSE by region. The x-axis zero value represents the entire western U.S. Fire danger indices include (a) BI; (b) ERC; (c) IC; (d) SC.

Anomaly correlation values by region for RF, RV and VF week one means are shown in Figure 6-7. The week one correlations for temperature and relative humidity anomalies remain relatively constant across all of the regions. The VF indices have consistently higher correlation (0.7 for temperature and 0.6 for RH), followed by RV correlations of 0.7 (max T and ave T), 0.6 (min T and min RH), and 0.5 (max RH and ave RH), and with RF correlations of 0.6 (max T and ave T), 0.5 (min T, min RH and ave RH) and 0.4 (max RH) typically the lowest. The precipitation anomalies show that the RF and VF correlations in regions 7 and 8 are greater than the other regions by 0.2. The RV precipitation indices are also higher in regions 7 and 8, but only by 0.1. Conversely, the RV and RF wind speed correlation in regions 7 and 8 are approximately 0.2 lower than the other regions.

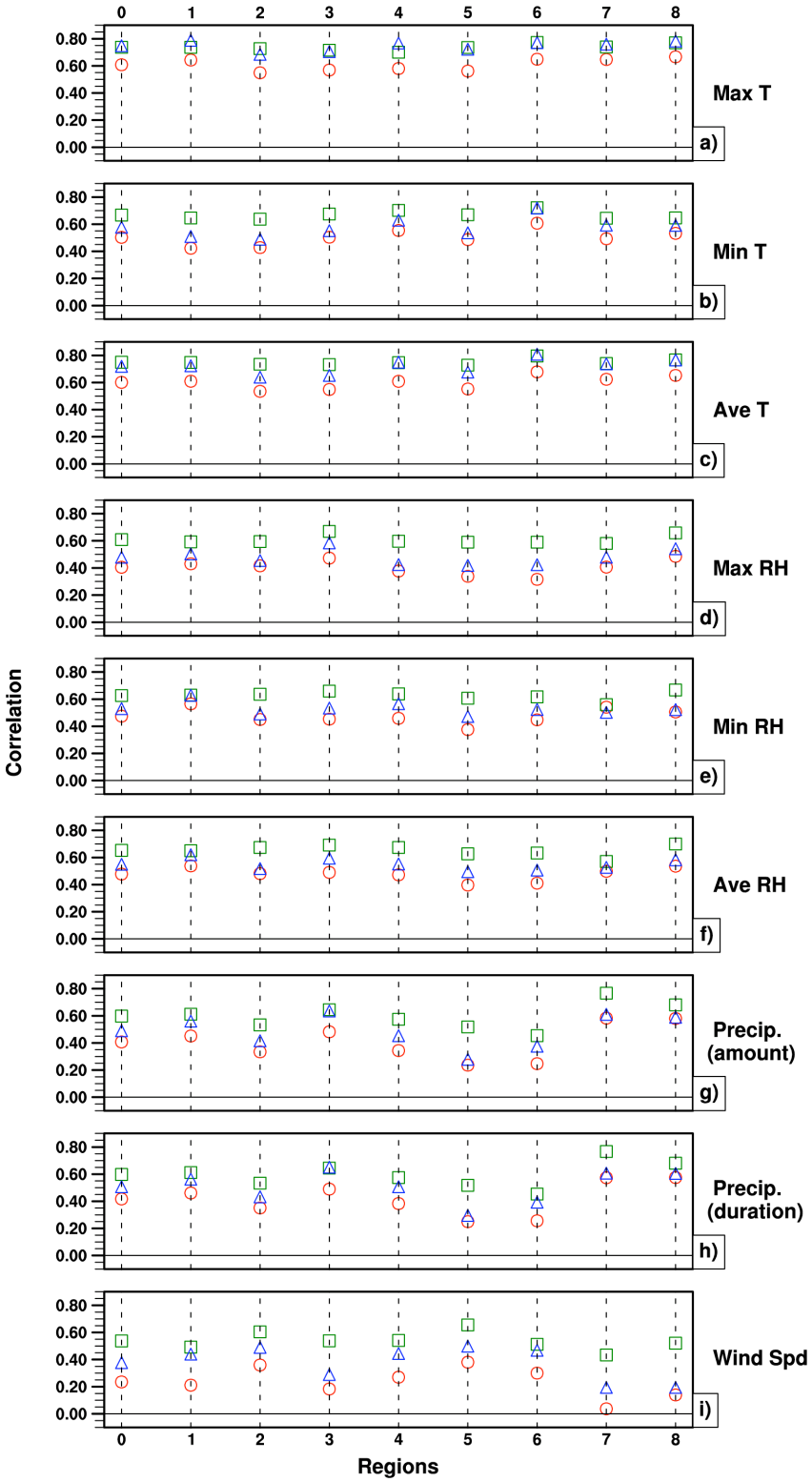

Figure 6-7 RF (circle), RV (triangle), and VF (square) Week 1 AC by region. The x-axis zero value represents the entire western U.S. Atmospheric elements include (a) Max T; (b) Max RH; (c) Min T; (d) Min RH; (e) Ave T; (f) Ave RH; (g) Precip Amt; (h) Precip Dur; (i) Wind Spd.

The regional correlations for the fire danger week one means are shown in Figure 6-8. Regions 1, 7, and 8 correlate a little better than the others for ERC. While region 8 has high RV and VF correlation for BI and IC, region 1 has noticeably higher RV and VF correlation in all fire danger indices. The VF correlations (typically 0.6) remain consistently higher than the RF and RV correlations (typically 0.2).

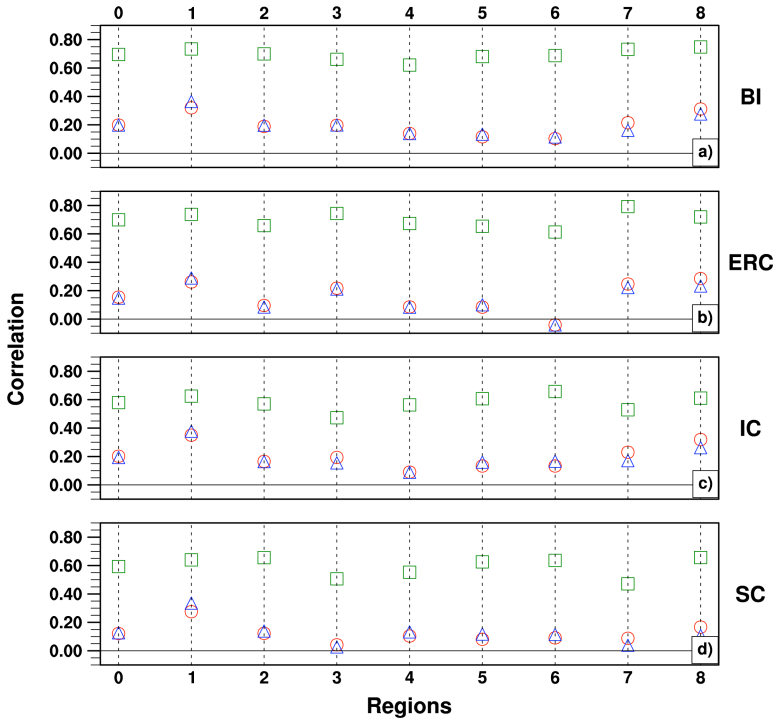

Figure 6-8 RF (circle), RV (triangle), and VF (square) Week 1 AC by region. The x-axis zero value represents the entire western U.S. Fire danger indices include (a) BI; (b) ERC; (c) IC; (d) SC.

The temperature anomalies for the month one means (Figure 6-9) are again relatively steady for RF, RV and VF, although the RF and VF correlations have dropped to values closer to 0.2 (compared to 0.6 for week one means). The relative humidity correlations are not quite as consistent regionally, with RF correlations dipping to 0.1 for regions 5 and 6. The precipitation correlations peak again in regions 7 and 8 with 0.55 for RV, 0.4 for VF and 0.25 for RF, although the RV correlation for region 3 (0.58) is

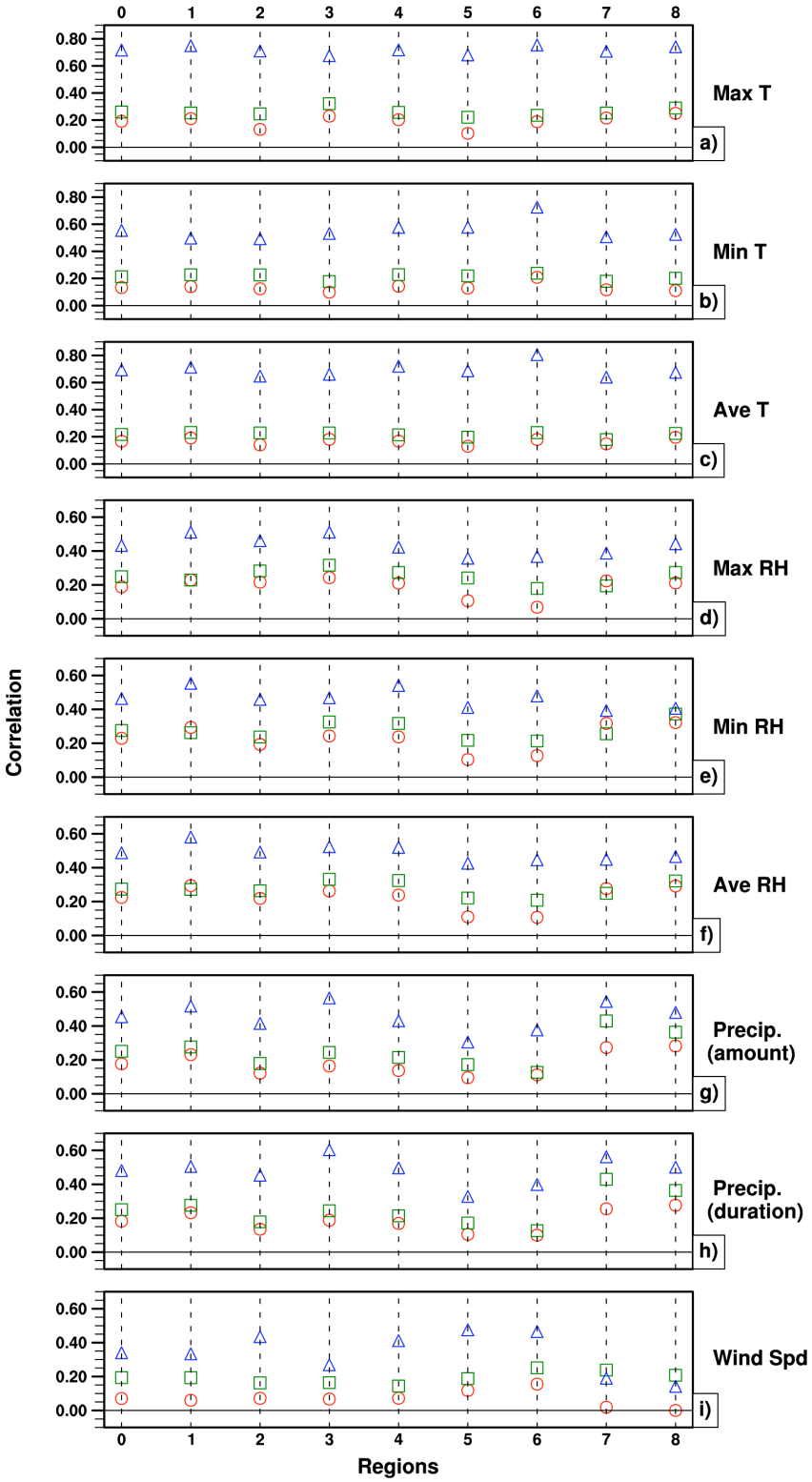

Figure 6-9 RF (circle), RV (triangle), and VF (square) Month 1 AC by region. The x-axis zero value represents the entire western U.S. Atmospheric elements include (a) Max T; (b) Min T; (c) Ave T; (d) Max RH; (e) Min RH; (f) Ave RH; (g) Precip Amt; (h) Precip Dur; (i) Wind Spd.

also a peak. The RV wind speed correlation is lowest for region 3 (0.26) and with similar correlation decreases in region 7 and 8 for RV (0.2 and 0.15, respectively) and RF (0.05 and 0, respectively).

The regional correlations of monthly means (Figure 6-10) for the RF, RV and VF fire danger indices have highest correlation again in regions 1, 7 and 8. The RF fire danger indices are typically higher than the same VF indices for region 7. It is worth noting that the VF and RF correlations for the month one means, while still not high (around 0.2) are not much lower than the week one correlations.

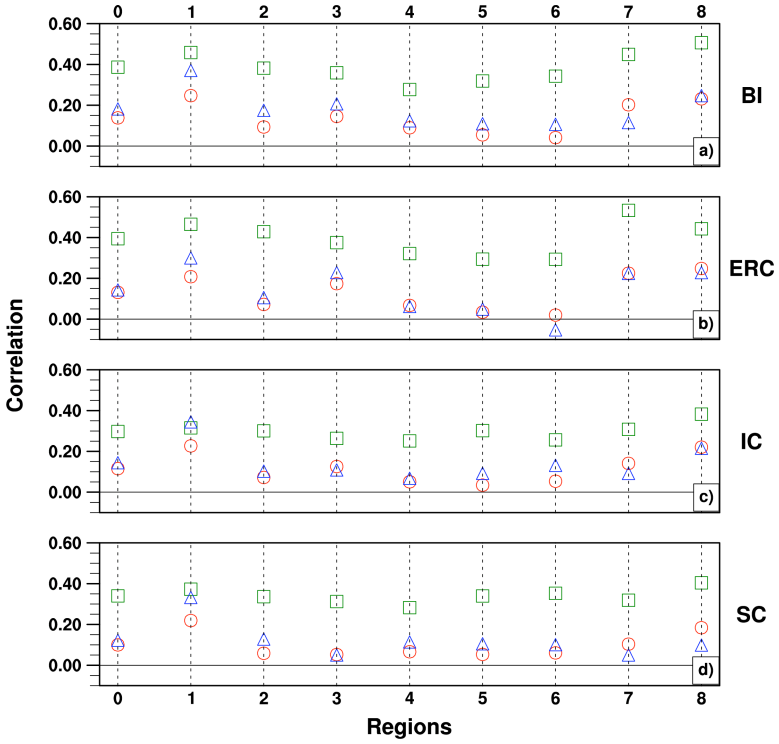

Figure 6-10 RF (circle), RV (triangle), and VF (square) Month 1 AC by region. The x-axis zero value represents the entire western U.S. Fire danger indices include (a) BI; (b) ERC; (c) IC; (d) SC.

The atmospheric RV correlations for seasonal means (Figure 6-11) show much the same pattern as the month one means, though with slightly lower correlation values.

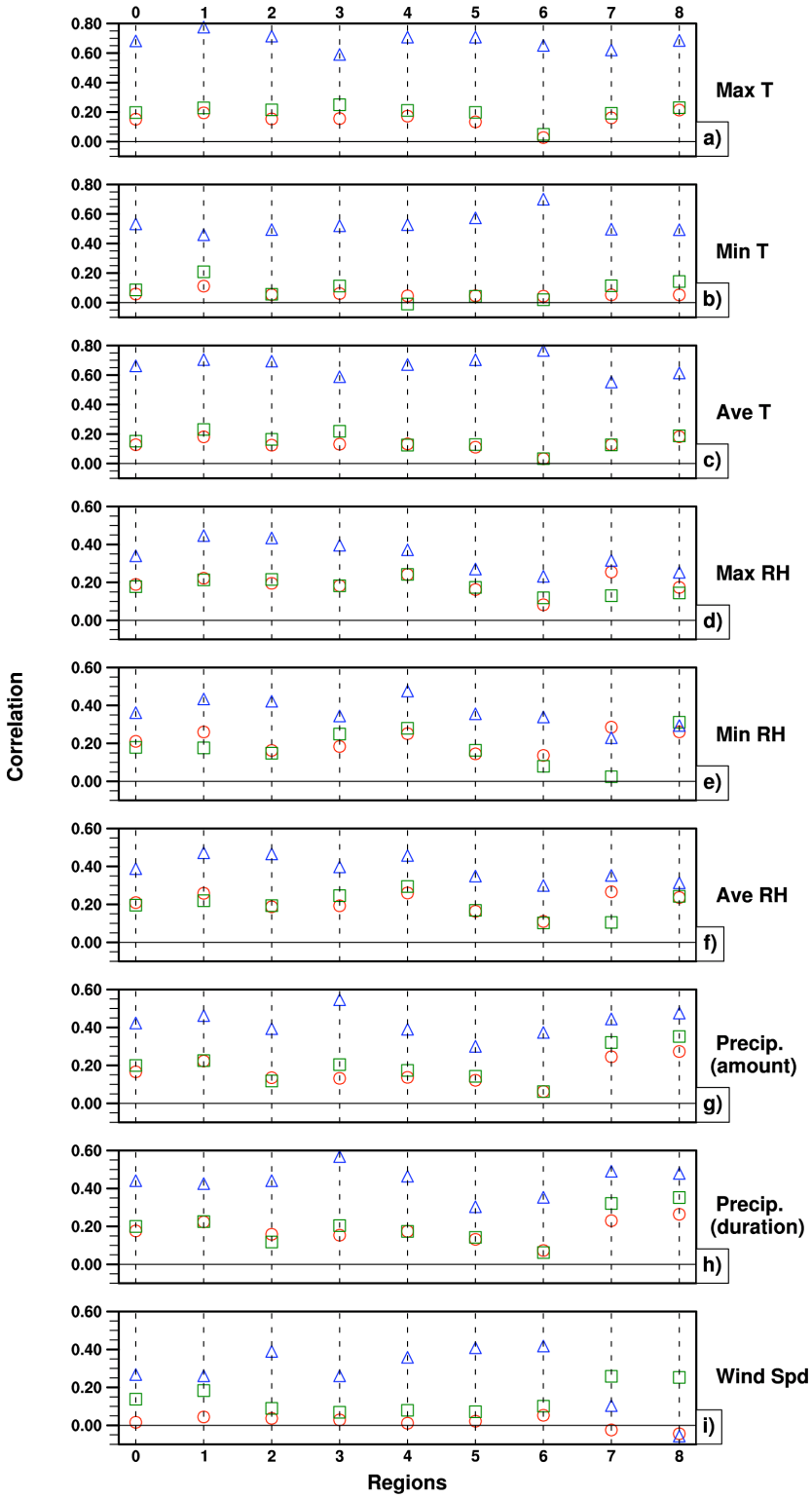

Figure 6-11 RF (circle), RV (triangle), and VF (square) seasonal AC by region. The x-axis zero value represents the entire western U.S. Atmospheric elements include (a) Max T; (b) Min T; (c) Ave T; (d) Max RH; (e) Min RH; (f) Ave RH; (g) Precip Amt; (h) Precip Dur; (i) Wind Spd.

The VF and RF correlations for maximum and average temperature and maximum and average relative humidity remain steady in most regions (approximately 0.2 for all), but tend to be lowest in region 6 (between 0.05 and 0.1). In contrast, the RV minimum temperature correlation (0.7) peaks in the same region. The RF minimum relative humidity correlation is actually higher than the RV and VF correlations in Southern California (region 7). The results for the precipitation and wind speed indices are similar to the month 1 results, except in this case the VF wind speed correlation does noticeably better in regions 7 and 8 than the other regions.

For the seasonal means of the fire danger indices (Figure 6-12), region 1 is still has the highest correlation for all RV anomalies. The magnitude of all correlations has

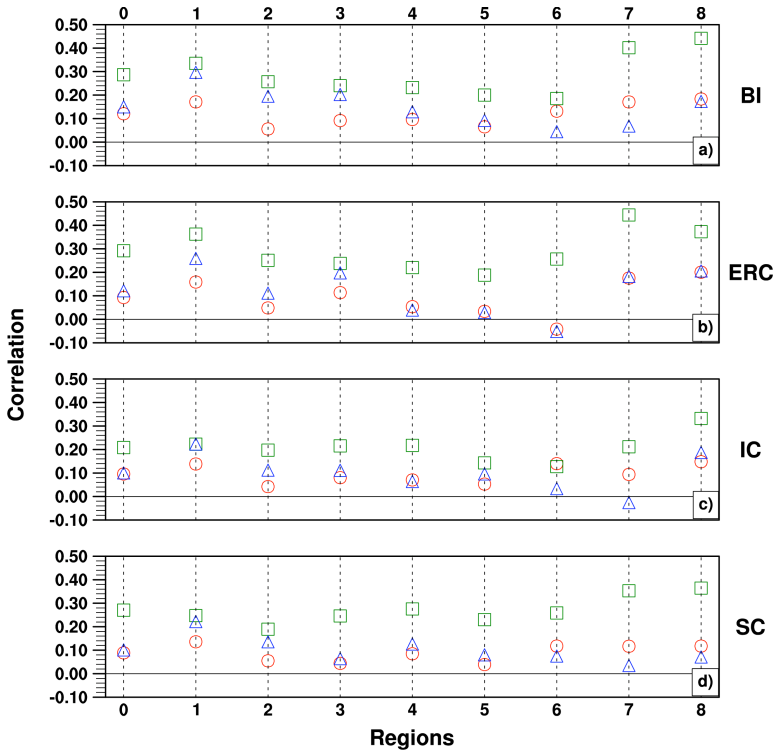

Figure 6-12 RF (circle), RV (triangle), and VF (square) seasonal AC by region. The x-axis zero value represents the entire western U.S. Fire danger indices include (a) BI; (b) ERC; (c) IC; (d) SC.

decreased to about 0.1 for RF and RV, and 0.2 or 0.3 for VF anomalies. Regions 7 and 8 show the highest correlation for the VF anomalies with correlations as high as 0.4 or 0.3.

The focus for this next section will be the spatial anomaly correlation of the seasonal forecasts, both year round and for summer (JJA) and winter (DJF) separately. First, Figures 6-13 through 6-18 give the standard deviation of the RAWS dataset contoured over the western U.S. These values seem to be indicative of the general climate for each region. Figure 6-13 shows the SD for the RAWS seasonal means for all forecasts. The temperature and minimum relative humidity indices have relatively uniform variability over the West. Maximum and average relative humidity both show higher variability in Arizona and Nevada, possibly due to contributions from summer precipitation. The precipitation indices have their highest variability on the West Coast, probably due to frequent winter precipitation. The areas of higher wind speed variability are not as easily defined, but tend to be found in the northern half of the West.

The contributions of summer and winter variability can be seen in Figures 6-14 and 6-15, respectively. For instance, the precipitation SD on the west coast is higher than the rest of the west in winter, but shifts to southern Arizona and New Mexico during the summer. This pattern is representative of the west coast winter storms and the Southwest Monsoon precipitation in the summer. The relative humidity indices have their highest variability in southern Arizona and New Mexico during the winter, which shifts north to Utah and Nevada (at least for maximum and average RH) during the summer (although variability in Arizona and New Mexico remains relatively high). Additionally, temperature variability during the winter is highest in the northeastern portion of the

West, and in Utah, Colorado, and Wyoming (to a lesser degree) during the summer.

Wind speed varies most during the winter, especially further north.

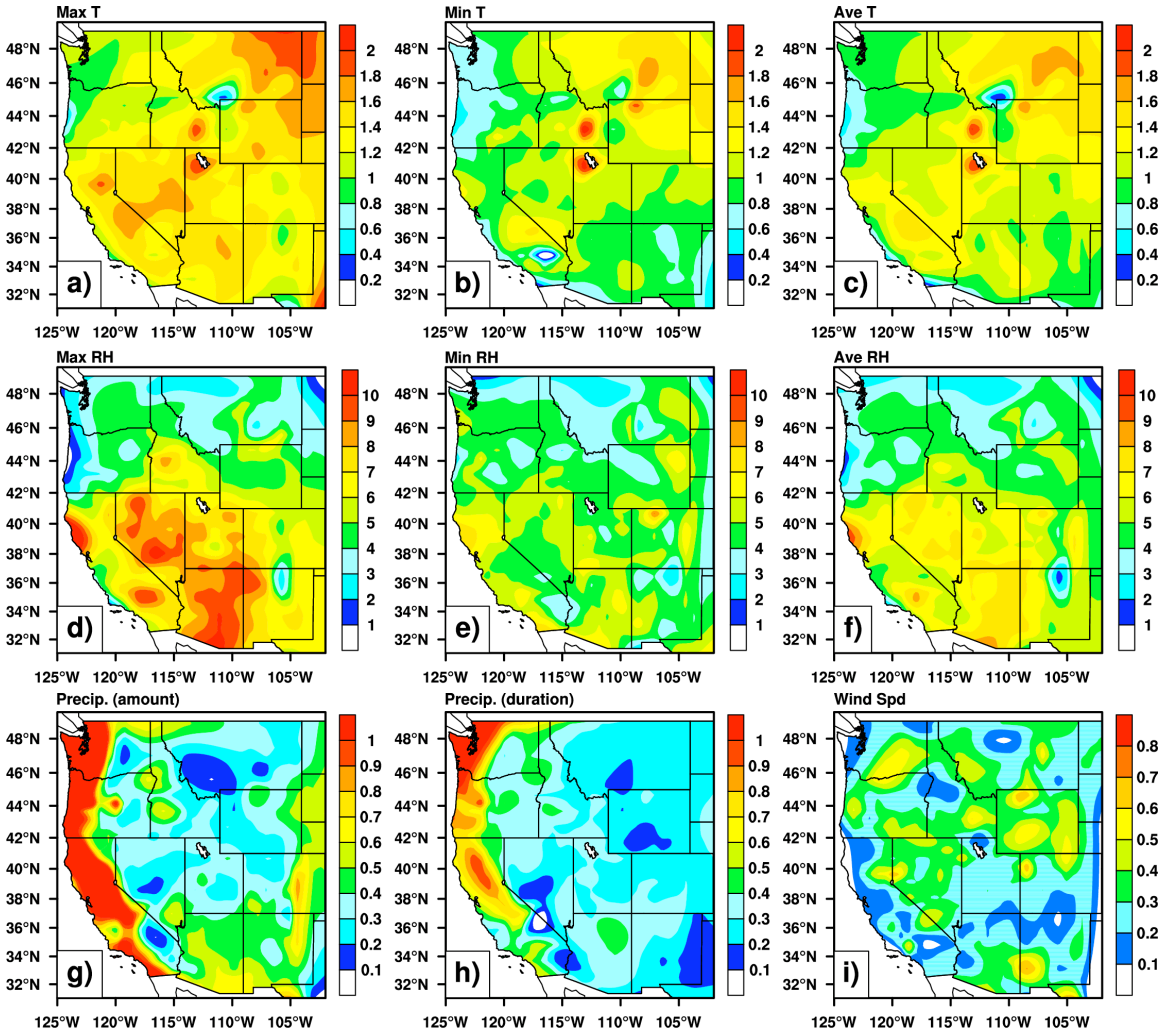

Figure 6-13 RAWS Seasonal SD (a) Max T (K); (b) Min T (K); (c) Ave T (K); (d) Max RH (%); (e) Min RH (%); (f) Ave RH (%); (g) Precip Amt (mm); (h) Precip Dur (hrs); (i) Wind Spd (m/s).

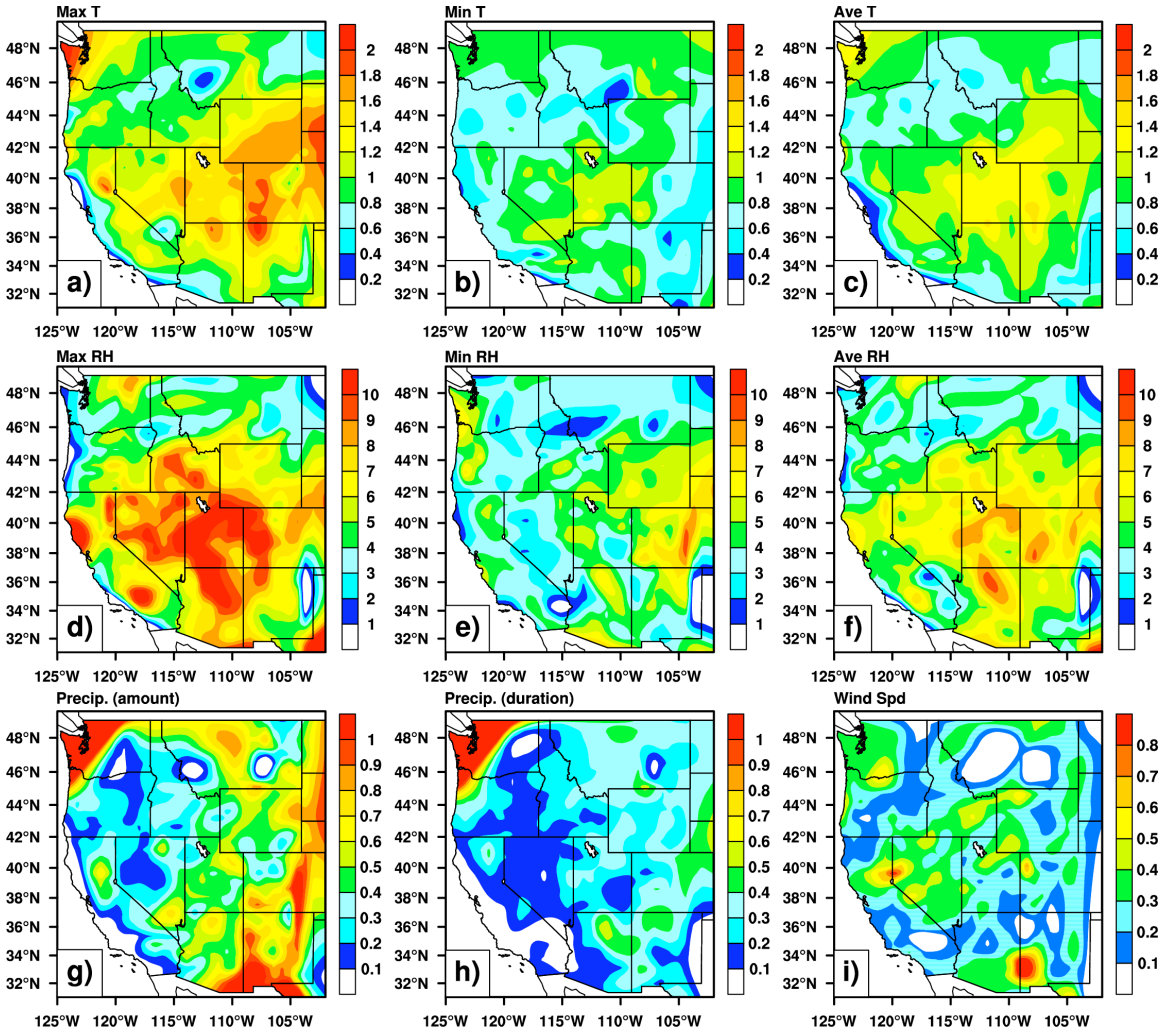

Figure 6-14 RAWS summer (JJA) season SD for (a) Max T (K); (b) Max RH (%); (c) Min T (K); (d) Min RH (%); (e) Ave T (K); (f) Ave RH (%); (g) Precip Amt (mm); (h) Precip Dur (hrs); (i) Wind Spd (m/s).

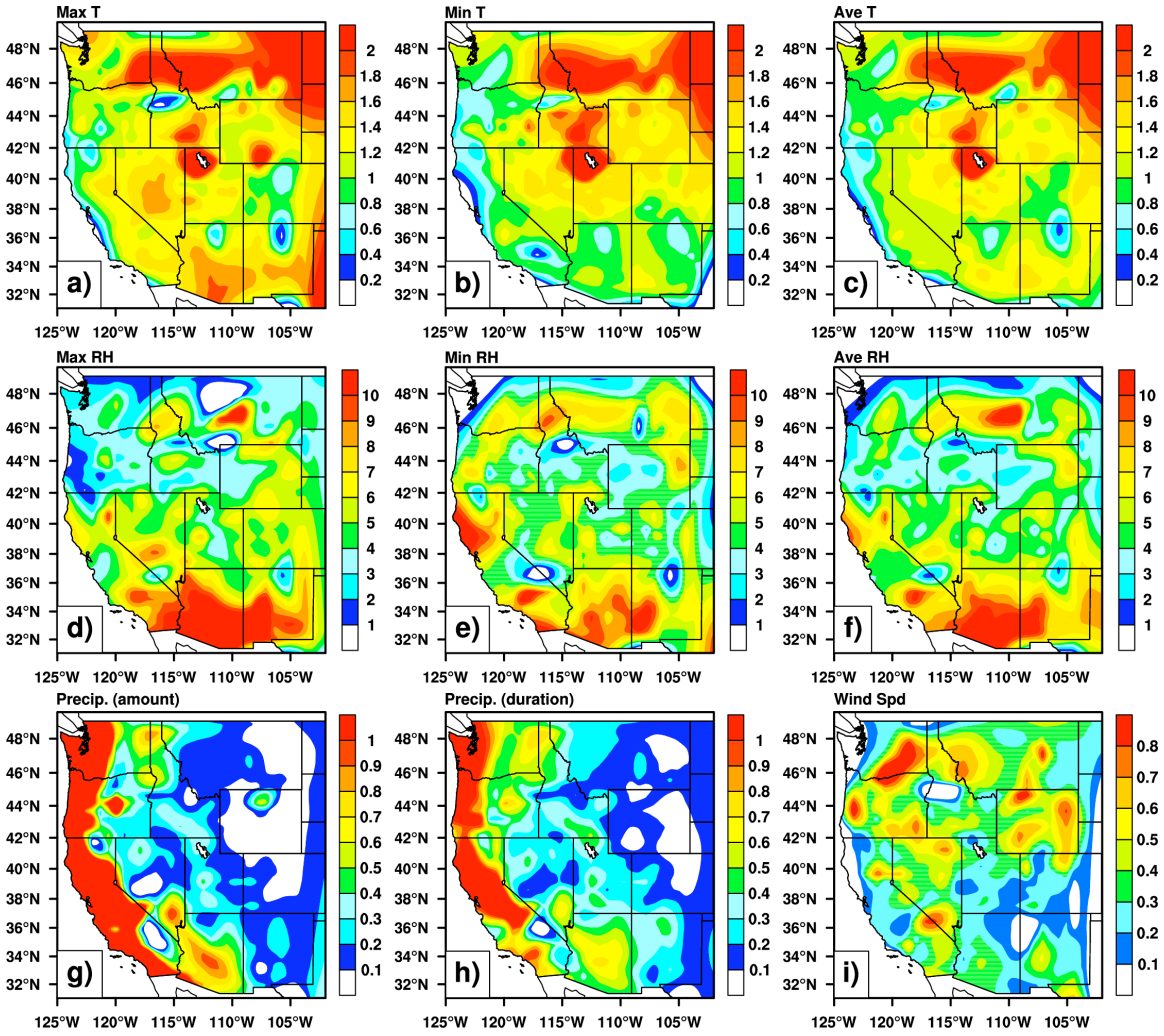

Figure 6-15 RAWS Winter (DJF) season SD (a) Max T (K); (b) Min T (K); (c) Ave T (K); (d) Max RH (%); (e) Min RH (%); (f) Ave RH (%); (g) Precip Amt (mm); (h) Precip Dur (hrs); (i) Wind Spd (m/s).

Similarly, SD for the fire danger indices also shows seasonality (Figure 6-16). SC, regardless of season, has the greatest SD in the great basin and the southern portions of Arizona and New Mexico, with a corresponding low SD in northern California, Oregon, Colorado, and Montana. ERC, again regardless of summer (Figure 6-17) or winter (Figure 6-18), has low SD everywhere except the four-corners area and southern California. Variability in IC is relatively low in the Northwest during the winter. Greater

SD for IC typically occurs in the southern portion of the West, with the highest summer SD positioned around the intersection of Utah, Colorado, and Wyoming. BI deviation is high in southern California and Utah, regardless of season. As a cautionary note, when examining the contours, keep in mind RAWS locations (see Figures 3-1 and 4-1). Some plots, such as ERC SD for example, show high values in areas where there are no RAWS, in this case northeastern Arizona and central California. This may be a contouring software artifact, and may not represent realistic values.

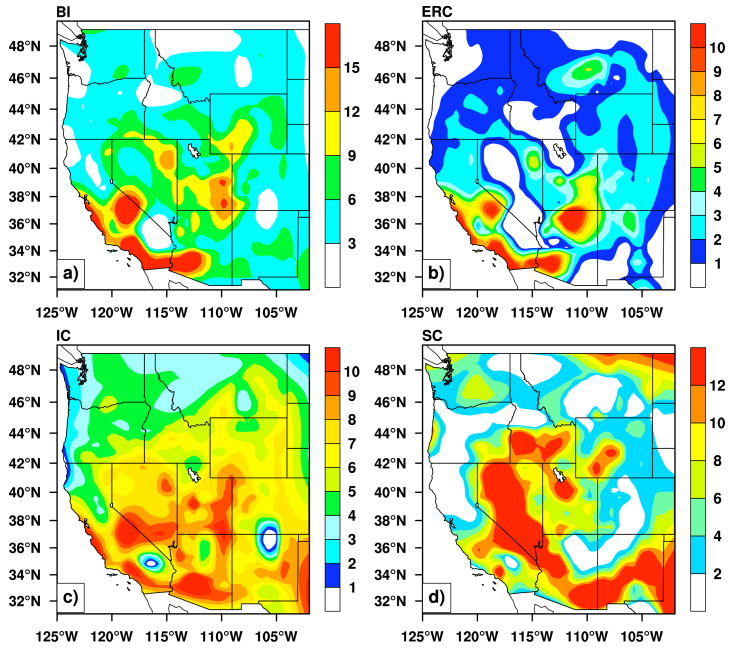

Figure 6-16 RAWS Seasonal SD for (a) BI; (b) ERC; (c) IC; (d) SC.

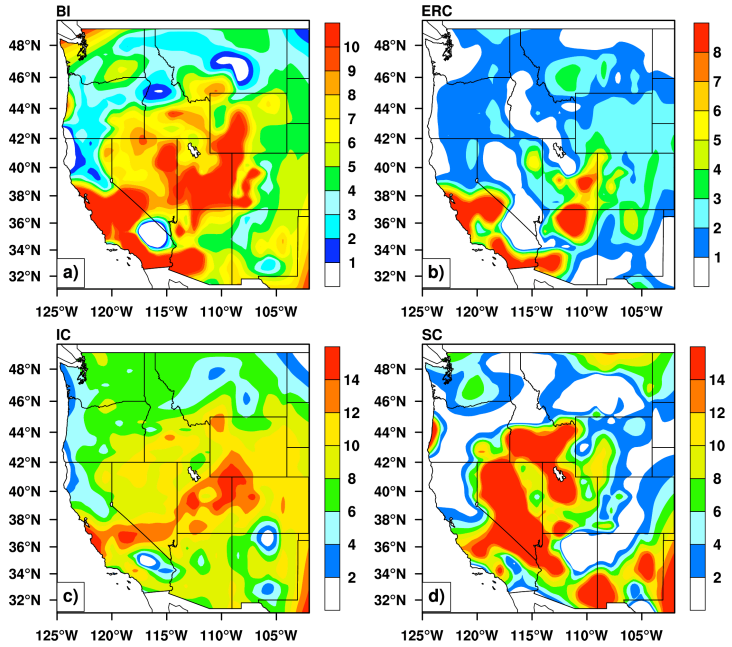

Figure 6-17 RAWS summer (JJA) season SD for (a) BI; (b) ERC; (c) IC; (d) SC.

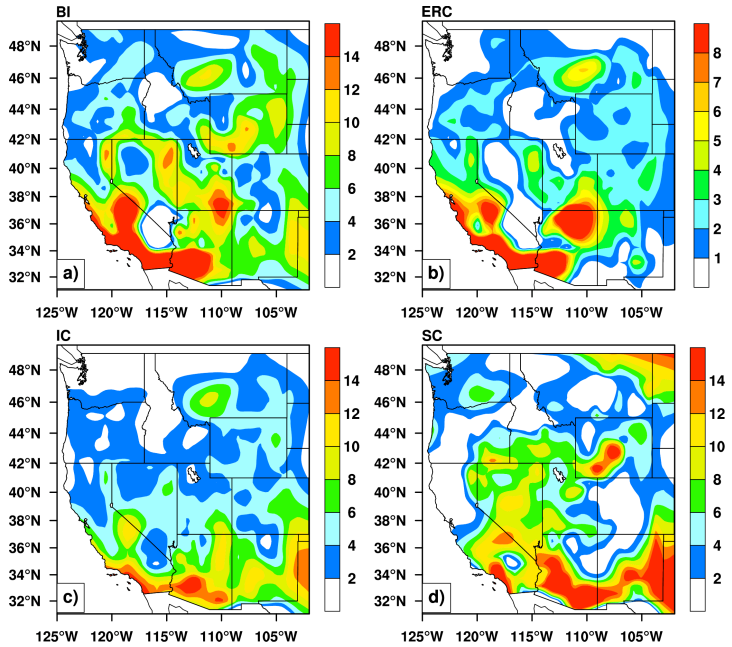

Figure 6-18 RAWS Winter (DJF) season SD for (a) BI; (b) ERC; (c) IC; (d) SC.

The RF anomaly correlations of seasonal means are shown in Figures 6-19 through 6-24. For the atmospheric elements, the year-round seasonal means (Figure 6-19) generally have lower peak correlations compared to summer (Figure 6-20) and winter

(figure 6-21) means. Winter anomalies usually have higher correlations over wider areas than summertime anomalies for those same elements (specific area coverage varies with each atmospheric element). The relative humidity anomalies seem to have the highest correlation in the southwestern portion of the map (large parts of Arizona, Nevada and California) regardless of the season. The lowest RH correlation occurs in Wyoming, Colorado, and New Mexico. Temperature anomalies have the strongest correlations in the Southwest for the year as a whole, although the minimum temperature correlation is highest only in Arizona and parts of Washington. In winter, maximum, minimum and average temperature all have higher correlations in the northeastern area close to and including Montana. Maximum temperature also has a high correlation in the Southwest (Arizona and California). New Mexico always has poor temperature anomaly correlations. Precipitation indices have their highest correlation in the Southwest (California and Nevada), including both summer and winter. Precipitation correlation is generally poor in Washington, Wyoming, Colorado, and New Mexico. Wind speed has the lowest correlation of all of the atmospheric elements, with virtually no strong correlation over the full year. The correlations of wind speed are best for Washington, Oregon, Colorado and New Mexico during the summer. In the winter, wind speed seems to correlate best in the Southwest.

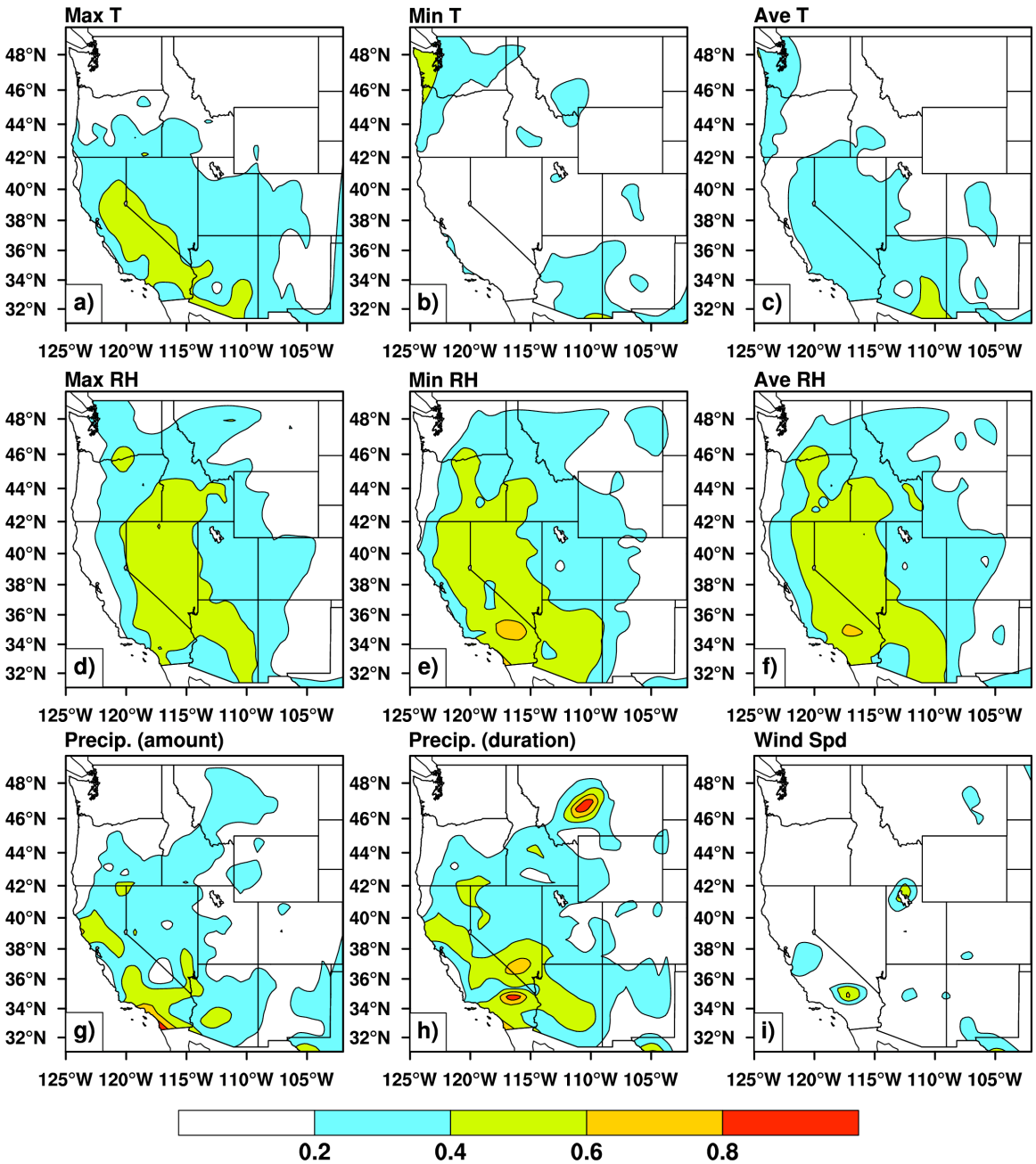

Figure 6-19 RF seasonal mean correlations for (a) Max T; (b) Min T; (c) Ave T; (d) Max RH; (e) Min RH; (f) Ave RH; (g) Precip Amt; (h) Precip Dur; (i) Wind Spd.

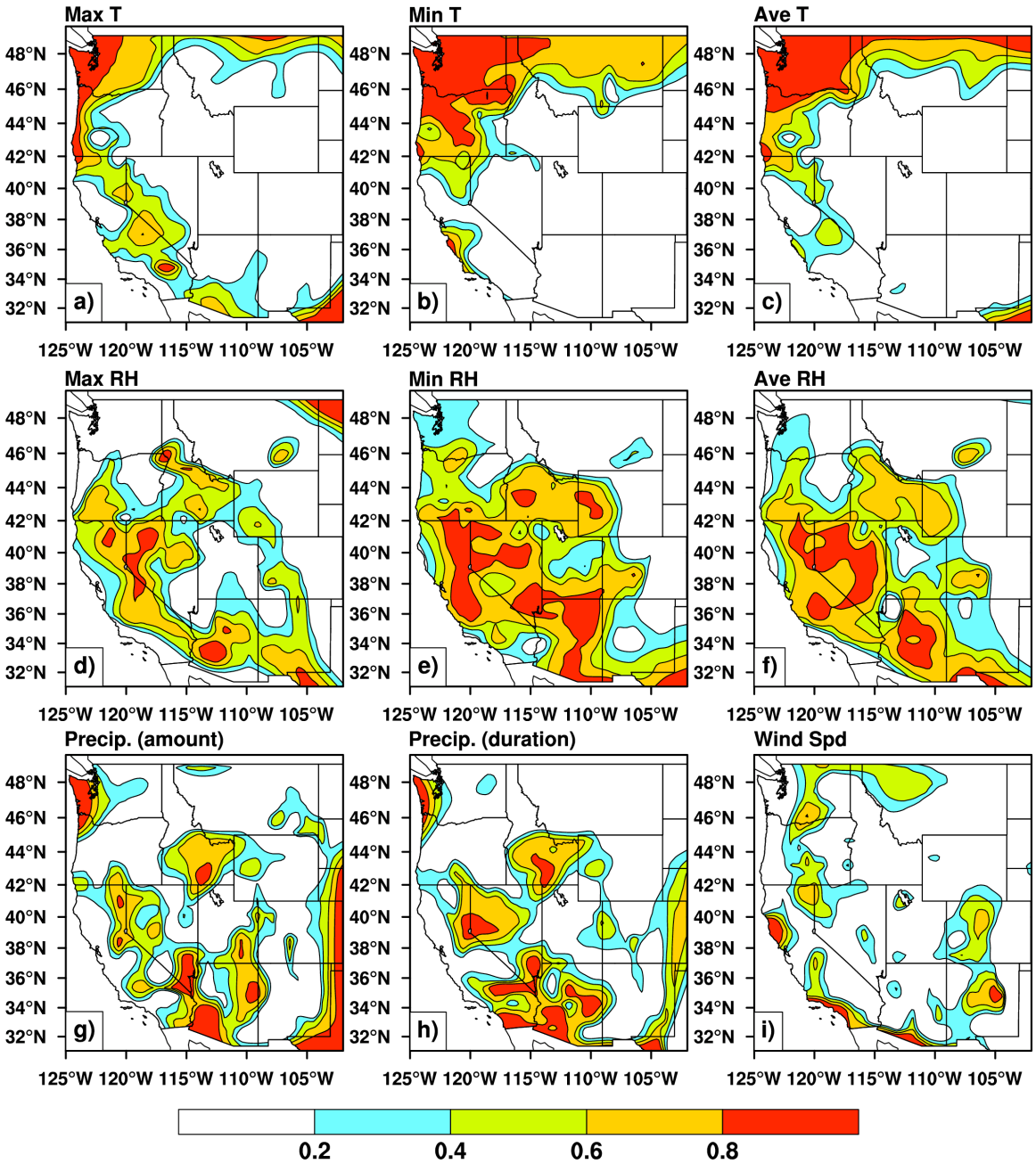

Figure 6-20 RF summer (JJA) season mean correlations for (a) Max T; (b) Min T; (c) Ave T; (d) Max RH; (e) Min RH; (f) Ave RH; (g) Precip Amt; (h) Precip Dur; (i) Wind Spd.

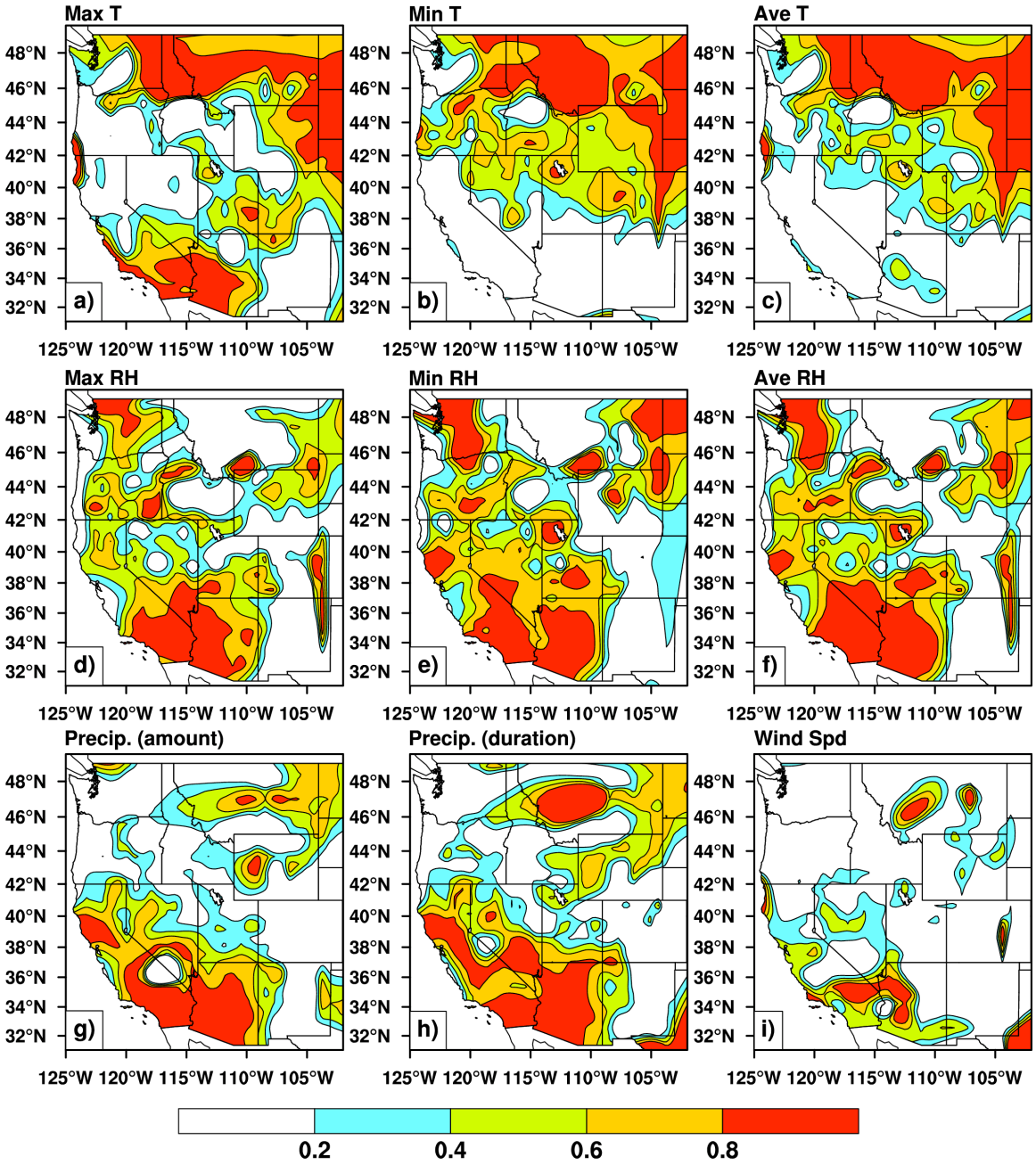

Figure 6-21 RF winter (DJF) season mean correlations for (a) Max T; (b) Min T; (c) Ave T; (d) Max RH; (e) Min RH; (f) Ave RH; (g) Precip Amt; (h) Precip Dur; (i) Wind Spd.

Throughout the year (Figure 6-22) and in summer (6-23) the fire danger anomalies have their highest correlation in Nevada and California. Additionally, the BI,

IC and SC also have an area of higher correlation in southeastern Montana during the summer and year-round. The highest winter correlation (Figure 6-24) seems mostly limited to southern California and Arizona for all of the indices. Elsewhere, the BI and IC correlate well in the Great Basin during the winter, while the ERC and SC have good correlation in parts of Montana and Wyoming. All four indices perform well in Southern California and Arizona, especially during the winter. It is interesting to note that the fire danger indices seem to have higher correlations in areas where the correlations for the relative humidity and precipitation indices are high. While the fire danger indices are less useful to practitioners outside of the fire season (i.e. winter), they are still useful for overall model assessment.

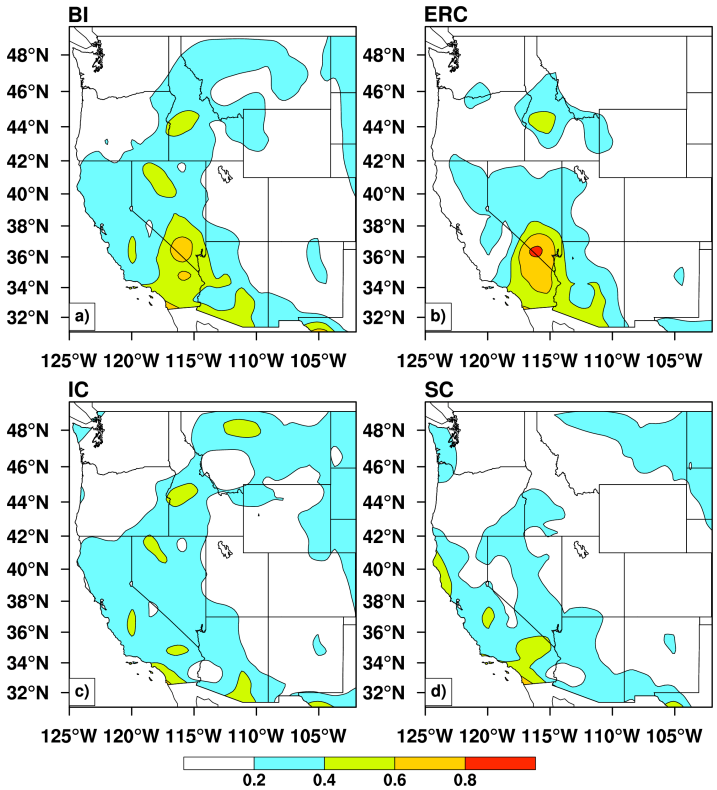

Figure 6-22 RF seasonal mean correlations for (a) BI; (b) ERC; (c) IC; (d) SC.

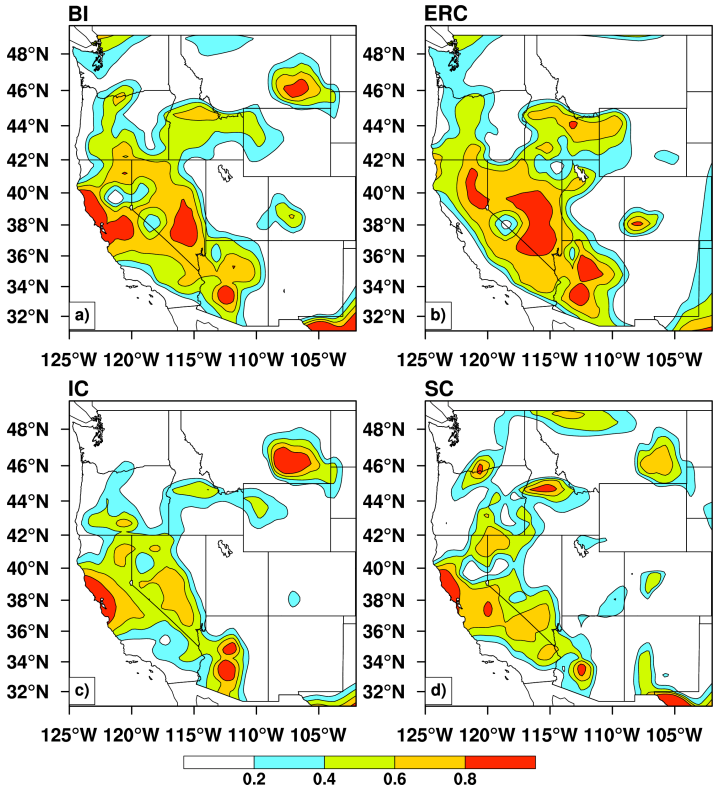

Figure 6-23 RF summer (JJA) season mean correlations for (a) BI; (b) ERC; (c) IC; (d) SC.

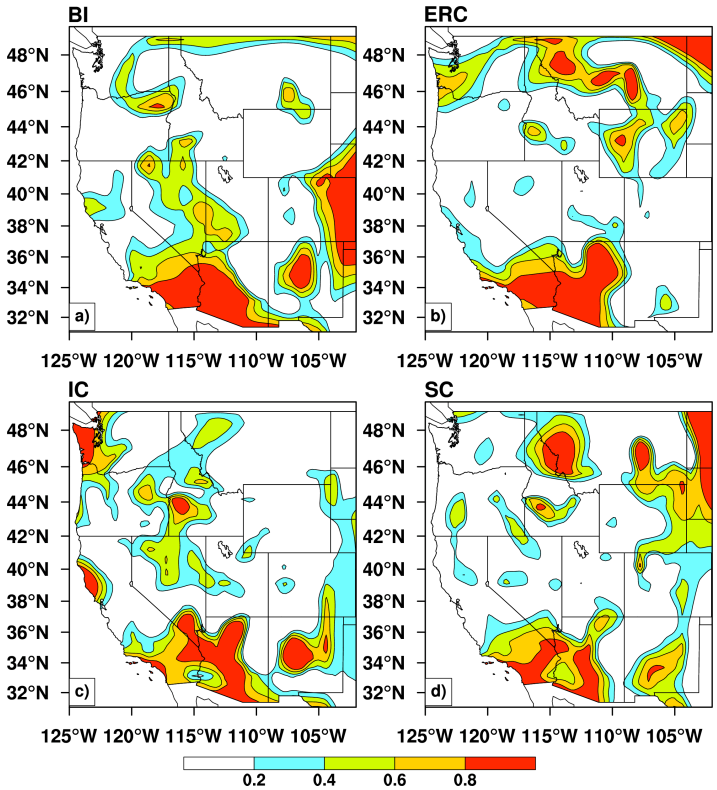

Figure 6-24 RF winter (DJF) season mean correlations for (a) BI; (b) ERC; (c) IC; (d) SC.

Figures 6-25 through 6-36 show the RV and VF spatial variation in the anomaly correlations for comparison and contrast with the RF correlations. The RV atmospheric correlations are very high over most of the regions (Figure 6-25), as might be expected

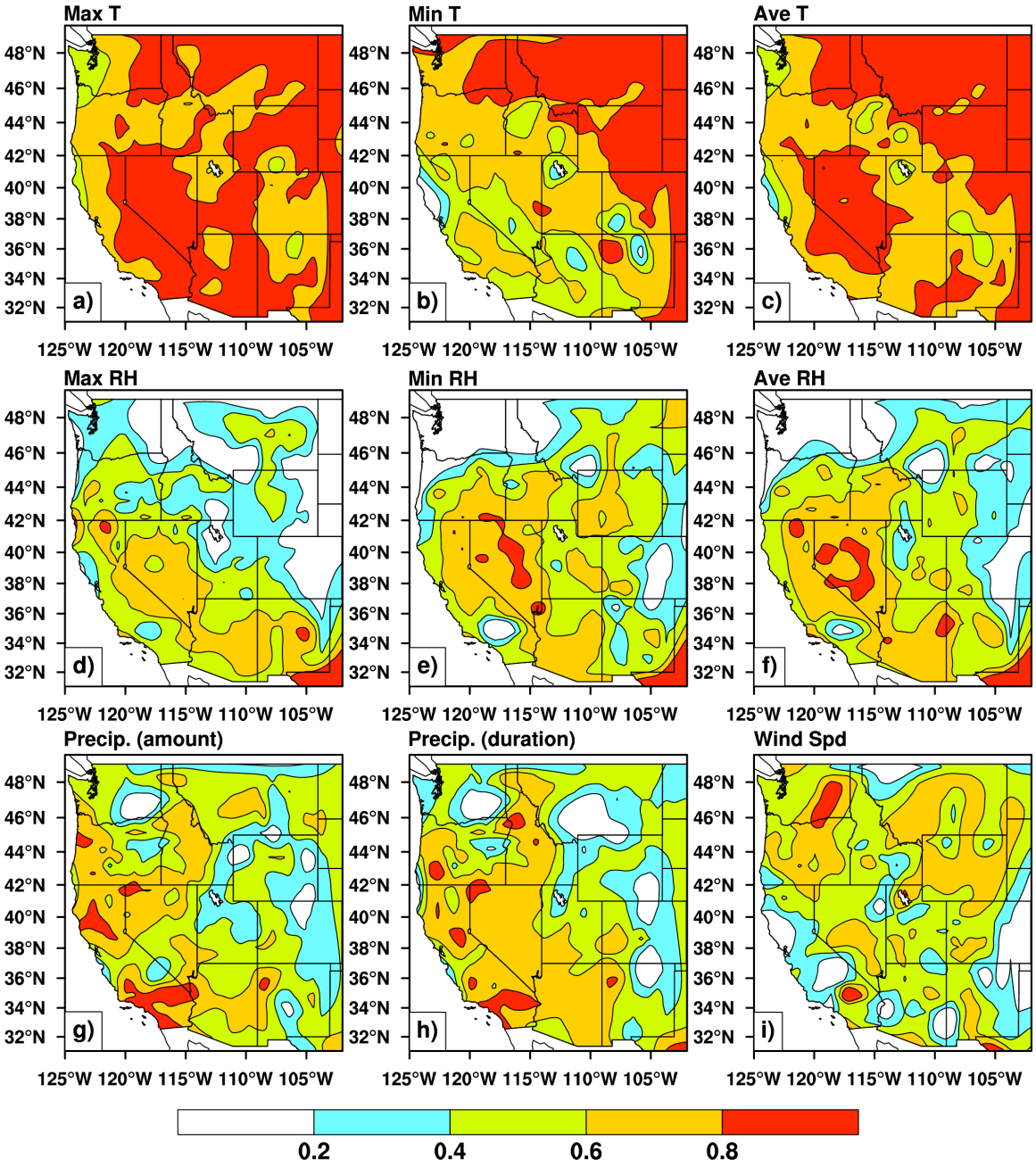

Figure 6-25 RV seasonal mean correlations for (a) Max T; (b) Min T; (c) Ave T; (d) Max RH; (e) Min RH; (f) Ave RH; (g) Precip Amt; (h) Precip Dur; (i) Wind Spd.

from Figure 6-9. The summer means (Figure 6-26) show a higher correlation in general (although covering significantly less total area than the year-round means) while the

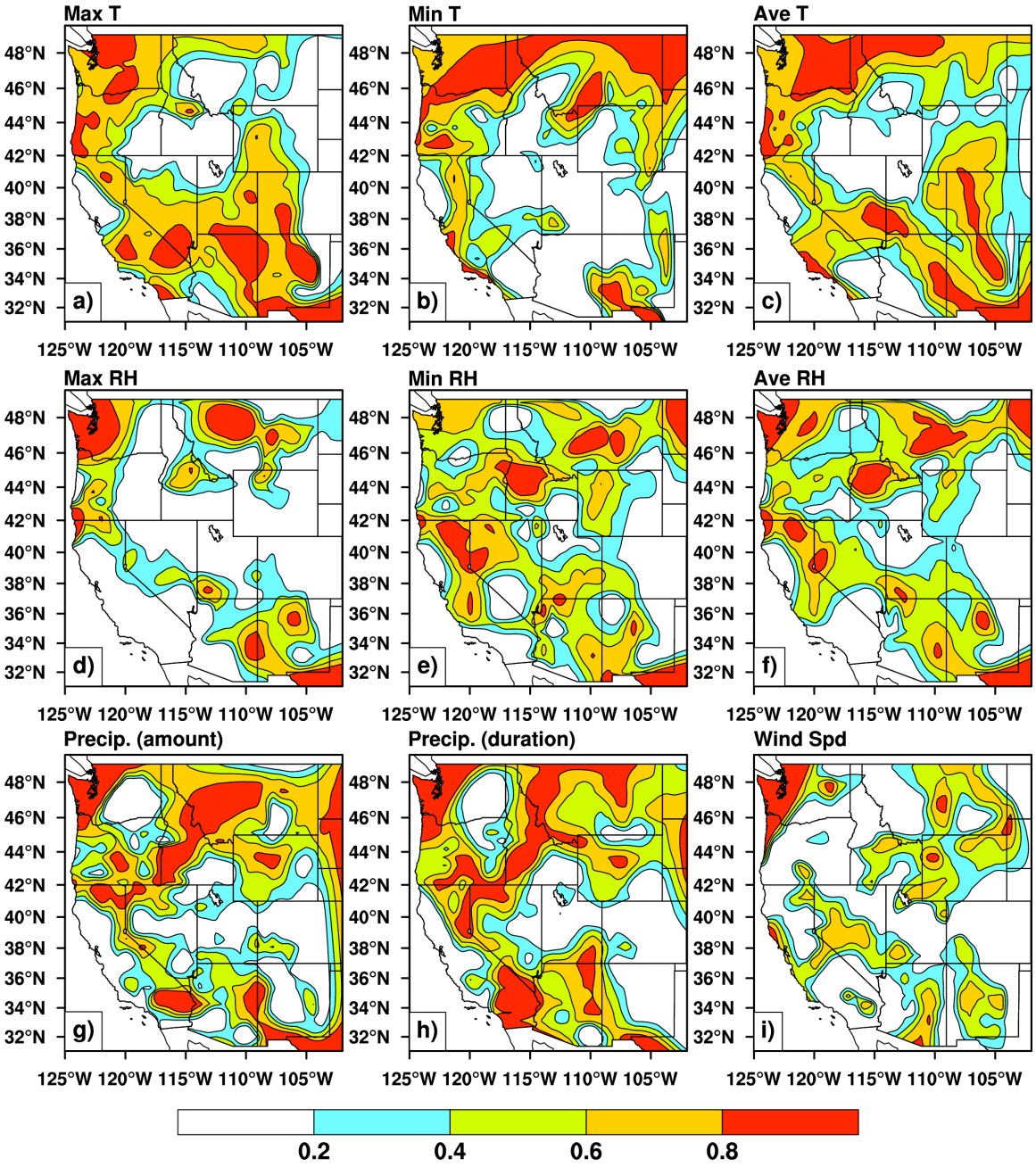

Figure 6-26 RV summer (JJA) season mean correlations for (a) Max T; (b) Min T; (c) Ave T; (d) Max RH; (e) Min RH; (f) Ave RH; (g) Precip Amt; (h) Precip Dur; (i) Wind Spd.

winter (Figure 6-27) shows similarly high correlations but covering a slightly smaller total area than the year-round means. The VF atmospheric correlations (full year, Fig. 6-28; JJA, Fig. 6-29; DJF, Fig. 6-30) are actually very similar to the RF correlations, except that the VF wind speed has a higher correlation during the summer.

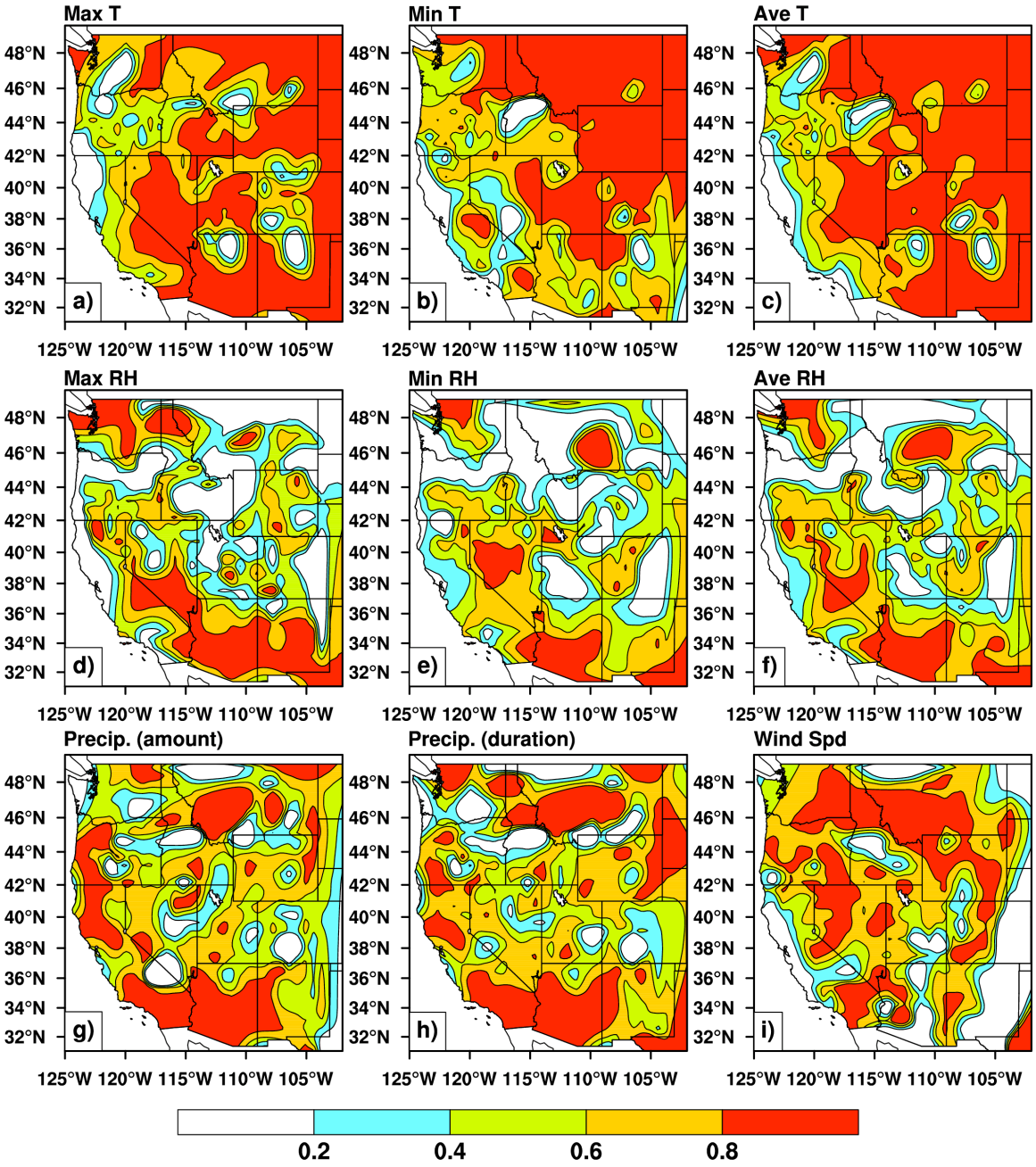

Figure 6-27 RV winter (DJF) season mean correlations for (a) Max T; (b) Min T; (c) Ave T; (d) Max RH; (e) Min RH; (f) Ave RH; (g) Precip Amt; (h) Precip Dur; (i) Wind Spd.

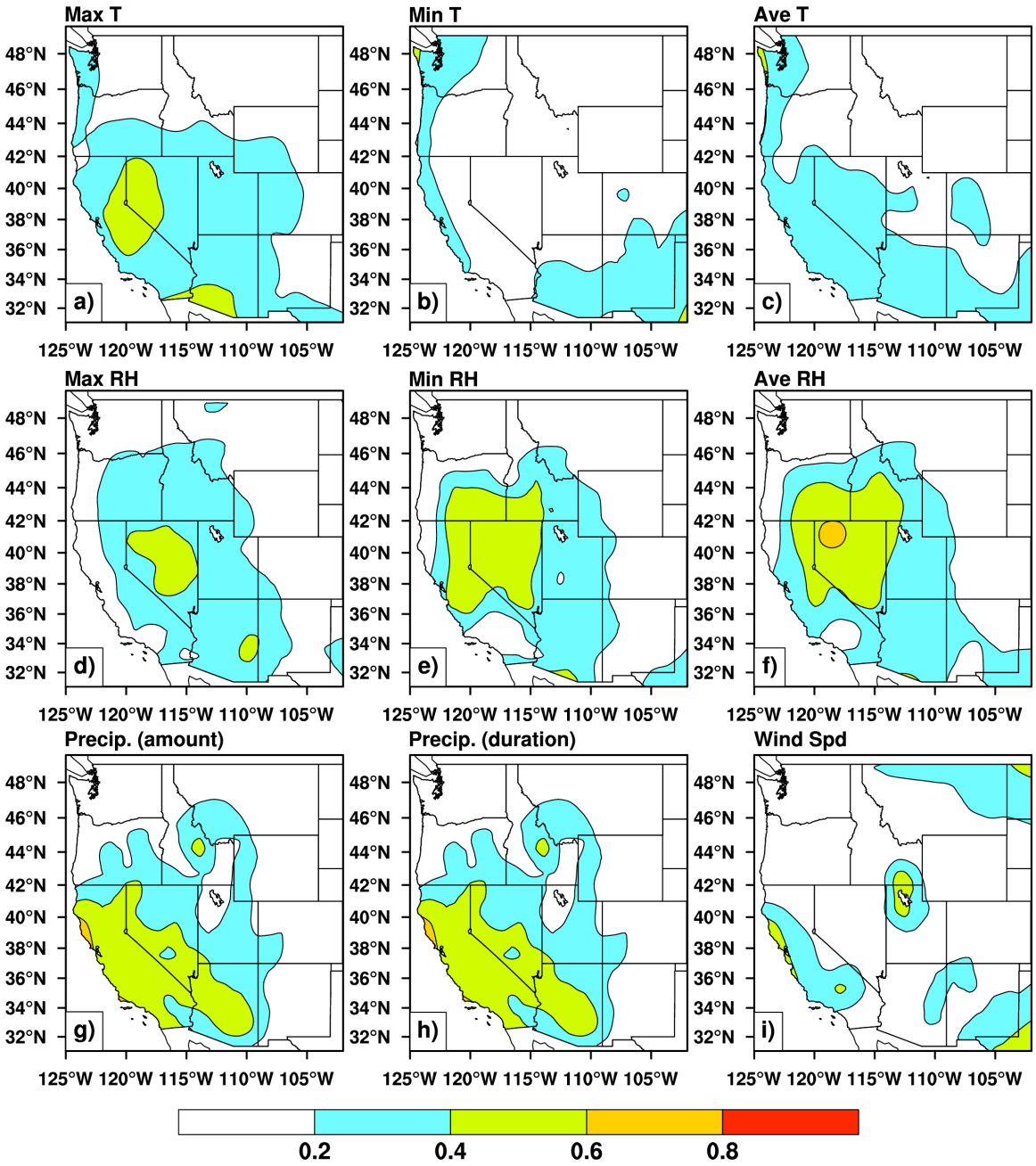

Figure 6-28 VF seasonal mean correlations for (a) Max T; (b) Min T; (c) Ave T; (d) Max RH; (e) Min RH; (f) Ave RH; (g) Precip Amt; (h) Precip Dur; (i) Wind Spd.

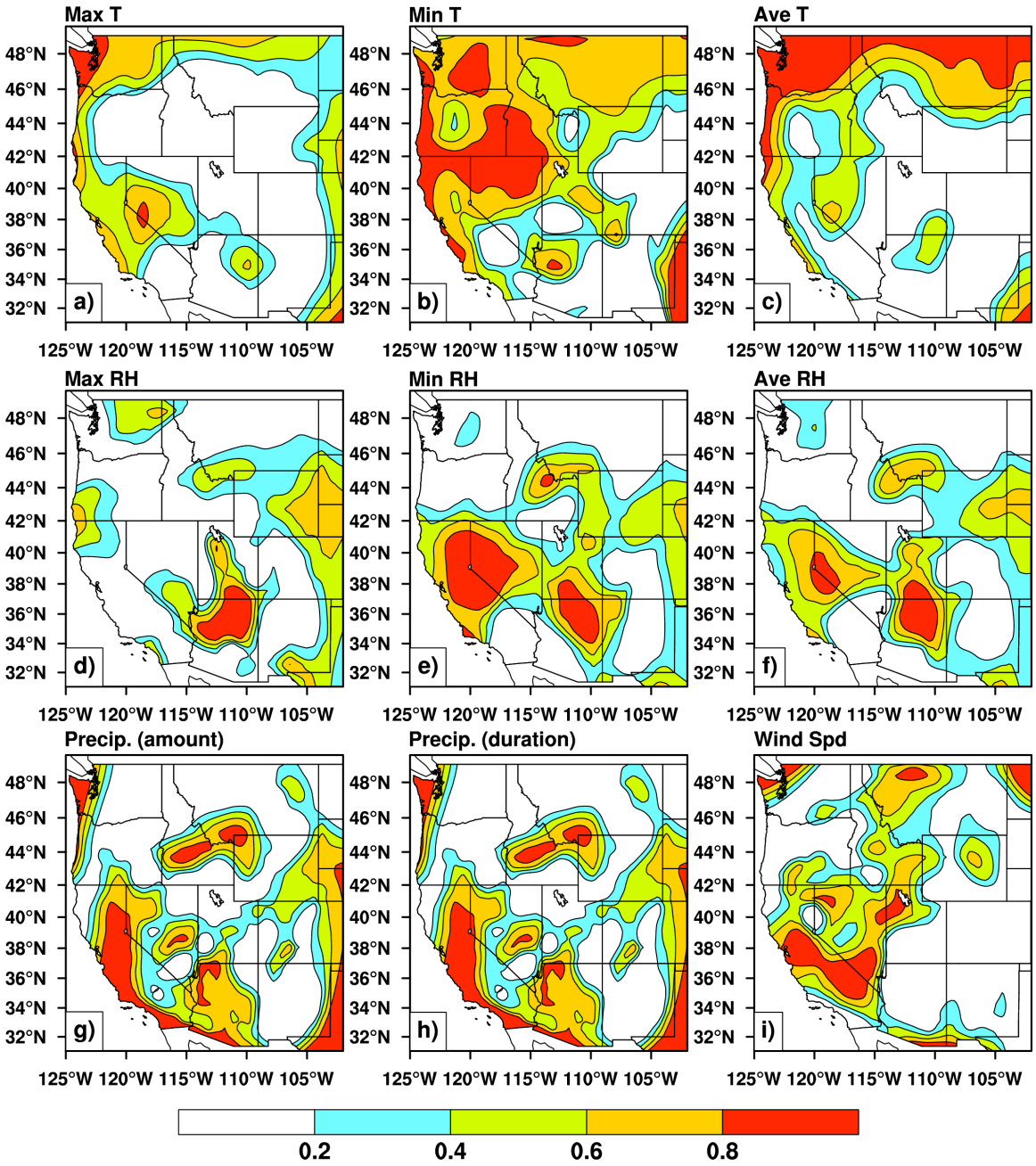

Figure 6-29 VF summer (JJA) season mean correlations for (a) Max T; (b) Min T; (c) Ave T; (d) Max RH; (e) Min RH; (f) Ave RH; (g) Precip Amt; (h) Precip Dur; (i) Wind Spd.

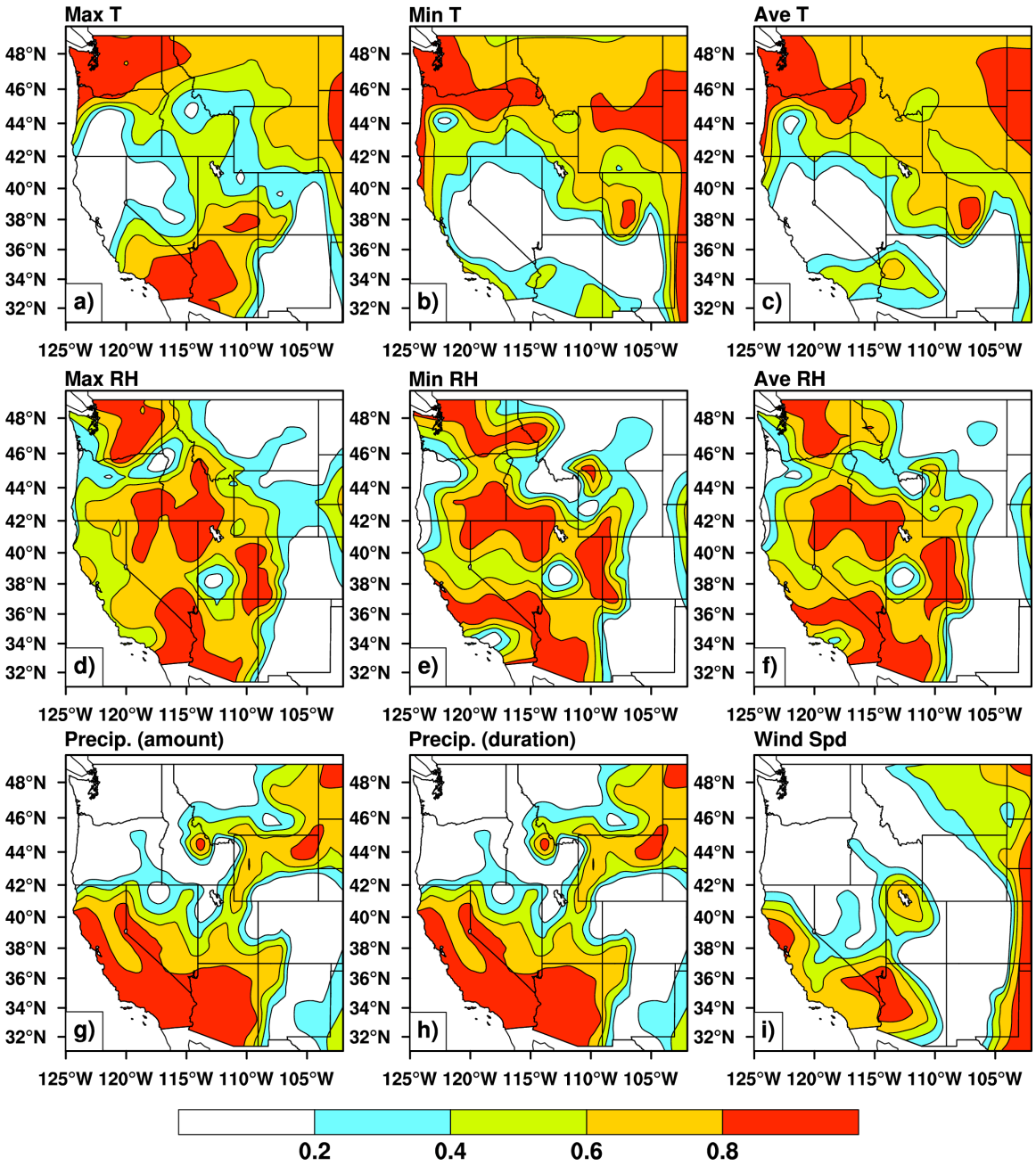

Figure 6-30 VF winter (DJF) season mean correlations for (a) Max T; (b) Min T; (c) Ave T; (d) Max RH; (e) Min RH; (f) Ave RH; (g) Precip Amt; (h) Precip Dur; (i) Wind Spd.

The RV (Figure 6-31) and VF (Figure 6-32) BI and ERC correlations are comparable to the same RF correlations for the year-round and summer analysis. The RF, RV and VF BI and ERC winter analyses compare best in southern California and Arizona. The RV (Figure 6-33) and VF (Figure 6-34) SC and IC show a bit more variation in their respective winter correlations. The year-round seasonal RV SC typically has more areas of higher correlation in the summer (Figure 6-35) than in the winter. The RV and VF IC winter correlations tend to have opposite tendencies when compared to the RV and VF summer (Figure 6-36) correlations. For instance, northern California and Nevada may have little IC correlation in winter, but relatively high correlation in summer. The correlation in Washington and Oregon behave in much the same way, except that they show better correlation in winter, not summer.

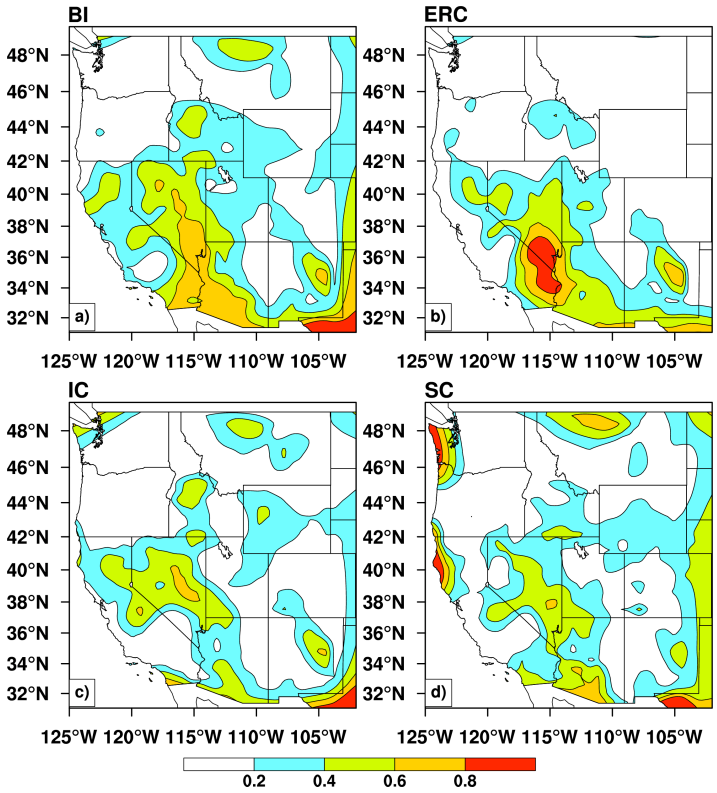

Figure 6-31 RV seasonal mean correlations for (a) BI; (b) ERC; (c) IC; (d) SC.

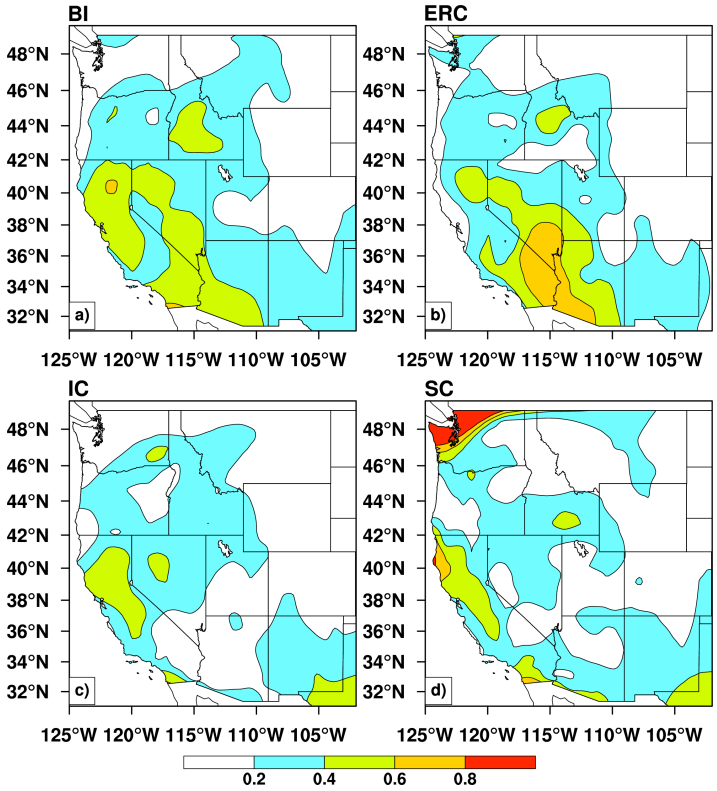

Figure 6-32 VF seasonal mean correlations for (a) BI; (b) ERC; (c) IC; (d) SC.

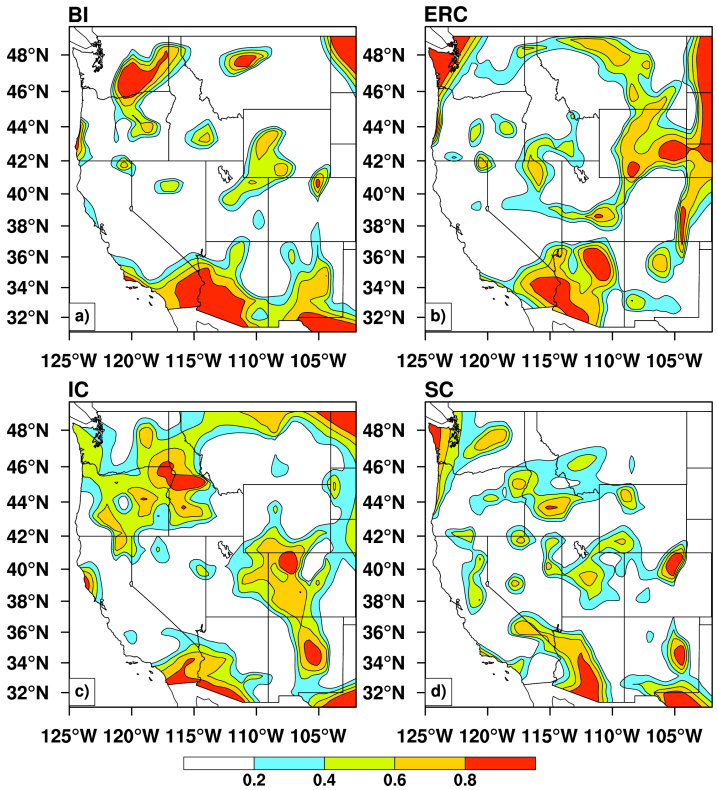

Figure 6-33 RV winter (DJF) season mean correlations for (a) BI; (b) ERC; (c) IC; (d) SC.

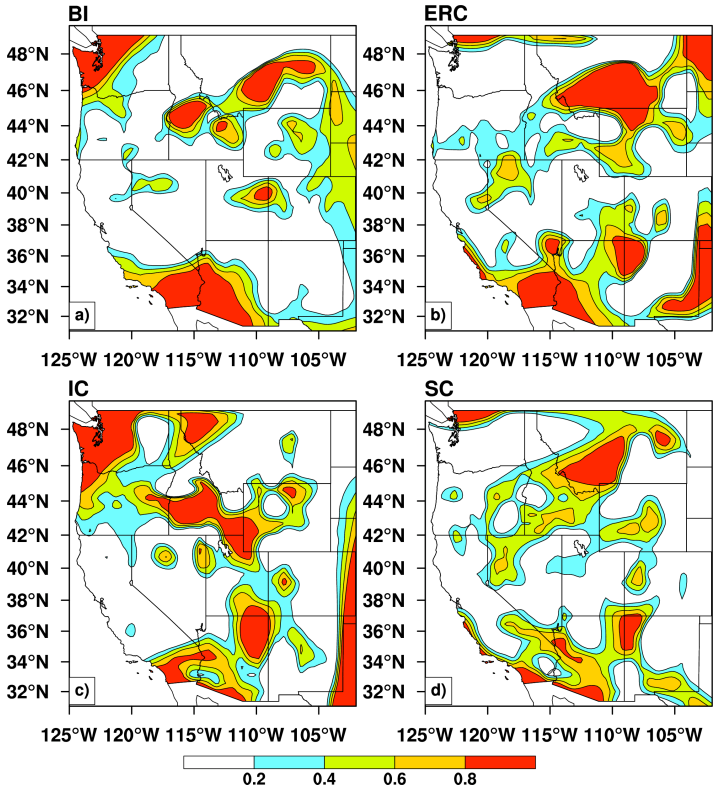

Figure 6-34 VF winter (DJF) season mean correlations for (a) BI; (b) ERC; (c) IC; (d) SC.

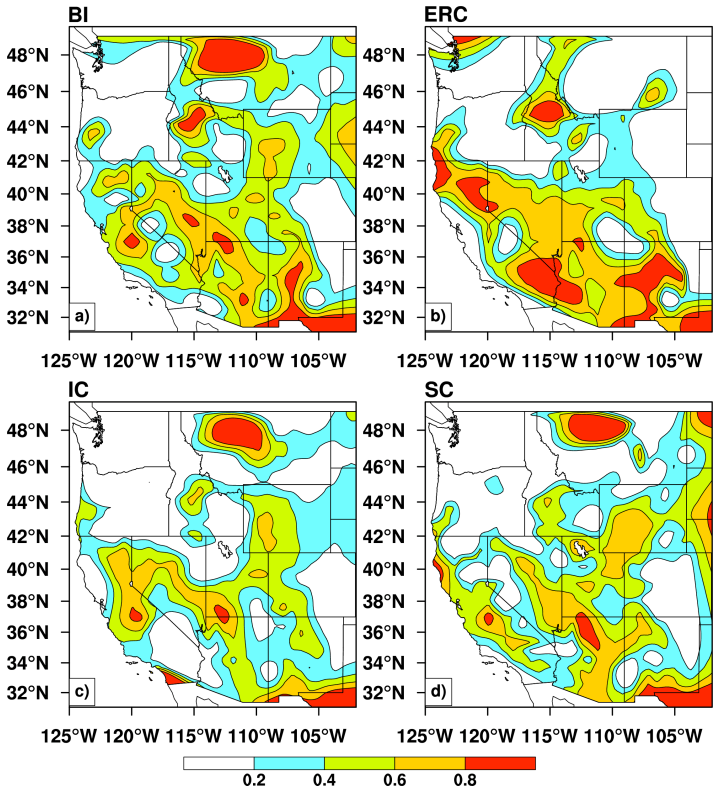

Figure 6-35 RV summer (JJA) season mean correlations for (a) BI; (b) ERC; (c) IC; (d) SC.

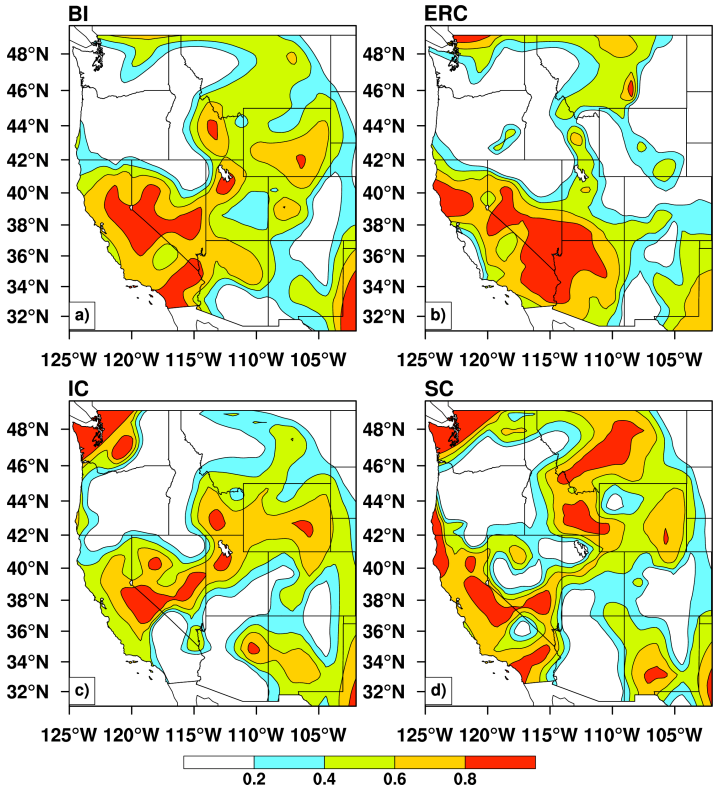

Figure 6-36 VF summer (JJA) season mean correlations for (a) BI; (b) ERC; (c) IC; (d) SC.

CHAPTER 7

DISCUSSION AND CONCLUSION

The goal of this study was to test the skill of a dynamical forecast model making seasonal forecasts of weather elements and fire danger rating indices important to fire management. Since fire danger indices rely largely on weather elements that have predictability to varying skill depending on the time scale, it seems that fire danger indices should also have a corresponding level of skill. In an effort to make these forecasts more useful in application to land managers, a set of observations from RAWS were used to determine model skill from the period September 1997 through December 31, 2002.

All biases, both atmospheric element and fire danger index, between the RAWS observations and RSM forecasts and validations have a greater magnitude than the biases between the elements of the RSM forecasts and RSM validations. Overall, the relative humidity biases are the largest. For the nine atmospheric elements assessed, this is likely due to at lease in part, to differences between RAWS observations and the NCEP data used to create the validation files (see Figure 5-15). RAWS are generally located in forest, wilderness and rangeland areas in order to help assess fire danger, while atmospheric soundings and surface data incorporated into the NCEP analysis/reanalysis grids are usually gathered from a broader range of locations. Additional sources of bias may stem from the fact that the RSM validations (which are 1-day forecasts) are themselves only close approximations of the NCEP data (Roads 2003a,b) and that the RSM surface grid is interpolated to RAWS sites for this study. Using a more advanced

interpolation algorithm, reducing output grid size or increasing the number of RAWS in the study could reduce bias due to interpolation. Bias in the fire danger indices may also be due to differences between RAWS and ECPC site descriptions (fuel model, slope) that are used in the NFDRS equations. The ECPC fire danger indices are calculated on 100 km fuel model and slope grids, and then interpolated to 60 km grids for comparison to the atmospheric RSM indices. The fire danger indices calculated from RAWS observations are based on the WIMS descriptions of each RAWS site, not grids. Additional bias comes, of course, from consistent errors within the model itself.

Bias can interfere with measures of forecast accuracy that are based on a direct comparison of forecast and observational values such as the root-mean square error. In order to minimize the bias between the RAWS observations and RSM output, correlations between datasets are computed using anomalies (deviations from climatology) rather than the original forecast or observational values. At a weekly time scale, the RAWS overall daily maximum and average temperature indices are shown to correlate with the validating observations (RV) with a value of 0.7. The remaining temperature, relative humidity and precipitation elements have correlations closer to 0.5, with wind speed correlations closer to 0.4. Correlations between RAWS observations and the RSM forecasts (RF) at week 1 are not quite as high, with 0.6 for the maximum and average temperature elements, 0.5 for minimum temperature, and minimum and average relative humidity, 0.4 for maximum relative humidity and the precipitation elements, and 0.25 for wind speed. In all instances, the RSM validation versus RSM forecast (VF) atmospheric correlations are greater than the other two comparisons and greater than 0.6. Month 1 and seasonal correlations for the RF and VF comparisons drop

to values close 0.2 for most atmospheric indices, excluding minimum temperature in which both RF and VF correlations drop below 0.1 and wind speed in which the RF correlation is closer to 0.05. The RV monthly and seasonal correlations remain comparable to the weekly correlations for maximum, minimum and average temperature, and typically drop by no more that 0.15 for the other elements.

Both the RF and RV BI and IC indices have small correlations with RAWS observations, even in the first week (close to 0.2). ERC and SC correlate even lower at 0.15 and almost 0.12 respectively. In contrast, the overall VF week 1 correlations are 0.6 or higher for all four indices. RF and RV seasonal forecasts are comparable with the week 1 correlation for SC; lower by 0.1 for BI and IC and 0.05 for ERC. In contrast, the VF correlations are greater for all fire danger indices at week one with a value of 0.6 and seasonally with a value of 0.25 or 0.3.

Wilks (1995) suggests that a correlation of 0.6 or higher is preferred for forecasts to be considered useful in a quantitative sense. While it is clear that the RF seasonal (and some of the week one) correlations do not reach this 0.6 lower limit, this does not necessarily mean that the forecasts are absent of skill entirely. In most cases (except for wind speed and minimum temperature), the RF seasonal correlations in the atmospheric and fire danger indices are still higher than the weekly means after week 3. This indicates that there is skill in the seasonal forecasts of these elements.

For modelers, these results are additional encouragement that fire danger indices can be skillfully forecast by this RSM at seasonal time scales, even if the current skill is not high. These results also serve as a useful contrast of RSM skill when compared to RAWS observations rather than the validating observations. The skill when compared to

RAWS is much lower than when compared to validation, especially for the precipitation, wind speed and fire danger indices. However, as discussed in Chapter 6, even indices with lower overall correlation may have high correlation in specific locations, especially during a given season. For instance, seasonal wind speed correlates with values at or above 0.6 in southern California and Arizona during the winter, and in parts of Washington, Oregon, New Mexico and Colorado during the summer. The results for the RSM forecasts versus RSM validation comparison are comparable to studies performed at ECPC for the fire danger indices (Roads, 2003b). The VF precipitation correlations in this study are slightly higher than the correlations found in a similar study at ECPC (Roads 2003a).

For a land manager, it is recognized that fire danger indices are only one component of strategic planning and deployment of resources in relation to fire suppression, prescribed fire and fire use. Knowledge of the local area and available resources are very important in any fire management decisions. Used in conjunction with this knowledge, the RSM model output can be useful for land managers and fire weather meteorologists. The one-week forecasts of the atmospheric indices, especially temperature, show significant skill and could likely be incorporated into short-range fire weather forecasts. Seasonal forecasts of atmospheric indices and fire danger ratings show low skill as an overall average, but can have much higher skill in specific regions and during specific seasons. For instance, the spatial analysis in Chapter 6 indicates higher correlations of seasonal forecasts in all indices for southern California, Arizona and Nevada. While management decisions in these regions will still be based partly on

factors like experience, the seasonal forecasts there could be considered skillful indicators of future fire danger.

Specific recommendations

Modelers:

- Re-evaluate the algorithm used to output fire danger indices, focusing on elements like fuel moisture and carry-over values.
- Incorporating RAWS into the initialization of the model (perhaps even as part of the NCEP/NCAR operational analysis or reanalysis), would likely aid in the upgrading model skill with reference to RAWS.

Fire Managers:

- The skill of most of the week-one forecasts of atmospheric indices (especially temperature) is very high. These values should be useful in making short-term management decisions.
- While seasonal skill as an overall average is low, especially for the fire danger forecasts, most indices still show some potentially useful regional skill during the summer and winter. A land manager could note which indices correlate highest in the region of interest and use those indices as part of long-term management decisions.

Future work on this topic might include a more in-depth examination of the large biases and low overall correlation between the RAWS observations and the ECPC forecasts. Also, performing a similar study between the ECPC GSM forecasts and RAWS observations would be helpful. Generating fire danger indices locally from ECPC forecasts of weather elements and comparing them to the fire danger indices

output by ECPC would be beneficial. Upgrading the GSM and RSM to the latest incarnations of each would hopefully improve the forecasts of precipitation and wind speed; with possible increases in fire danger forecast skill as a result. It may also be of additional benefit to fire management to examine the potential of this RSM to forecast for specific RAWS.

This study should provide modelers with a useful comparison of RSM skill as compared to another set of observations. It shows seasonal periods and spatial locations where the model forecasts can be improved. Additionally, this study provides seasons and locations when and where these forecasts would be most useful in fire management applications.

References

Anderson BT, Roads JO, Chen S-C, Juang H-MH (2000) Regional Simulation of the Low-level Monsoon Winds Over the Gulf of California and Southwest United States. *Journal of Geophysical Research-Atmospheres* **105** (D14), 17,955-17969.

Anderson BT, Roads JO, Chen S-C, Juang H-MH (2001) Model Dynamics of Summertime Low-Level Jets over Northwest Mexico. *Journal of Geophysical Research-Atmospheres* **106** (D4), 3401-3413.

Anderson BT, Roads JO (2002) Regional Simulation and of Summertime Precipitation over the Southwestern United States. *Journal of Climate* 39pp (in press).

Bradshaw LS, Deeming JE, Burgan RE, Cohen JD (1983) 'The National Fire-Danger Rating System: Technical Documentation.' USDA Forest Service General Technical Report INT-169, 44pp.

Burgan RE (1988) '1988 Revisions to the 1978 National Fire-Danger Rating System.' Res. Pap. SE-273. Asheville, NC: U.S. Department of Agriculture, Forest Service, Southeastern Forest Experiment Station. 39 pp.

Caplan P, Derber J, Gemmil W, Hong S-Y, Pan H-L, Parrish D (1997) Changes to the 1995 NCEP operation medium-range forecast model analysis-forecast system. *Weather Forecast* **12**, 581-594.

Chen, F, Mitchell K, Schaake J, Xue Y, Pan H, Koren V, Duan Q, Betts A (1996) Modeling of land-surface evaporation by four schemes and comparisons with FIFE observations. *Journal of Geophysical Research* **101**, 7251-7268.

Chen S-C, Roads JO, Juang H-MH, Kanamitsu M (1999): Global to regional simulation of California's wintertime precipitation. *Journal of Geophysical Research* 104 (**24**) 31517-31532.

Chen S-C, Roads JO, Wu M (2001) Seasonal Forecasts for Asia: Global Model Experiments. *Journal of Terrestrial-Atmospheric-Oceanic Sciences* 12 (**2**), 377-400.

Chou M-D, Suarez MJ (1996) 'A solar radiation parameterization (CLIRAD-SW) for atmospheric studies', NASA Technical Memorandum no. 104606, v. 3, 102pp.

Deeming JE, Lancaster JW, Fosberg MA, Furman RW, Schroeder MJ (1972) 'National Fire-Danger Rating System.' Res. Pap. RM-84. Fort Collins, CO: U.S. Department of Agriculture, Forest Service, Rocky Mountain Forest and Range Experiment Station. 165 pp.

Deeming JE, Burgan RE, Cohen JD (1977) 'The National Fire-Danger Rating System-1978.' Gen. Tech. Rep. INT-39. Ogden, UT: U.S. Department of Agriculture, Forest Service, Intermountain Forest and Range Experiment Station. 63 pp.

Han J, Roads J (2002) US Climate Sensitivity Simulated with the NCEP Regional Spectral Model. *Climate Change* (submitted)

Hong S-Y, Pan H-L (1996) Nonlocal boundary layer vertical diffusion in a medium-range forecast model. *Monthly Weather Review* **124**, 2322-2339.

Hong S-Y, Leetmaa A (1999) An evaluation of the NCEP RSM for regional climate modeling. *Journal of Climate* **12**, 592-609.

Juang H, Kanamitsu M (1994) The NMC nested regional spectral model. *Monthly Weather Review* **122**, 3-26.

Juang H, Hong S, Kanamitsu M (1997) The NMC nested regional spectral model. An update. *Bulletin of the American Meteorological Society* **78**, 2125-2143.

Kalnay E, Kanamitsu M, Kistler R, Collins W, Deaven D, Gandin L, Iredell M, Saha S, White G, Woolen J, Zhu Y, Leetma A, Reynolds R, Chelliah M, Ebisuzaki W, Higgins W, Janowiak J, Mo KC, Jenne R, Joseph D (1996) The NCEP/NCAR 40-Year Reanalysis Project. *Bulletin of the American Meteorological Society* **77**, 437-471.

Kanamitsu M (1989) Description of the NMC global data assimilation and forecast system. *Weather Forecasting* **4**, 335-342.

NWCG (2002) Gaining an Understanding of the National Fire Danger Rating System. Eds., P. Schlobohm and J. Brain. NFES 2665, PMS 932, Boise, Idaho, 78 pp.

Pan, H-L, (1990) A simple parameterization of evapotranspiration over land for the NMC medium-range forecast model. *Monthly Weather Review* **118**, 2500-2512.

Pyne SJ, Andrews PL, Laven RD (1996) *Introduction to Wildland Fire*. John Wiley & Sons, Inc. 769 pp.

Roads JO, Ueyoshi K, Chen S-C, Alpert J, Fujioka F (1991) Medium-Range Fire Weather Forecasts. *International Journal of Wildland Fire* **1**, 159-176.

Roads JO, Chen S-C, Fujioka F, Kanamitsu M, Juang H (1997) Global to Regional Fire Weather Forecasts. *International Forest Fire News (BAHC)* **17**, 33-37.

Roads J, Chen S, Kanamitsu M, Juang H (1999) Surface water characteristics in NCEP global spectral model reanalysis. *Journal of Geophysical Research* **104**, 19307-19327.

Roads JO, Chen S-C (2000) Surface Water and Energy Budgets in the NCEP Regional Spectral Model. *Journal of Geophysical Research-Atmospheres* **105**, 29,539-29550.

Roads JO, Chen S-C, Fujioka F (2001) ECPC's Weekly to Seasonal Global Forecasts. *Bulletin of the American Meteorological Society* **82**, 639-658.

Roads J, Brenner S (2002) Global Model Seasonal Forecasts for the Mediterranean Region. *Israel Journal of Earth Sciences* 51 (**1**), 1-16.

Roads JO (2003a) Experimental Weekly to Seasonal, Global to Regional US Precipitation Forecasts. *Journal of Hydrology* (submitted)

Roads JO, Fujioka F, Burgan R (2003b) Fire Danger Forecasts. *International Journal of Wildland Fire* (submitted)

Roads J, Chen S-C, Kanamitsu M (2003c) US Regional Climate Simulations and Seasonal Forecasts. *Journal of Geophysical Research-Atmospheres* (in press).

Schlobohm P (2003) 'NDVI-derived Green-up Date for the National Fire Danger Rating System.' Master's Thesis. University of Nevada, Reno.

Schwarzkopf MD, Fels SB (1991) The simplified exchange method revisited: An accurate, rapid method for computation of infrared cooling rates and fluxes. *Journal of Geophysical Research* **96**, 9075-9096.

Takle ES, Gutowski Jr. WJ, Arritt RW, Pan Z, Anderson C, Silva R, Cayan D, Chen D, Christensen JH, Hong S-Y, Juang H, Katzfey J, Lapenta W, Laprise R, Lopez P, McGregor J, Roads J (1999) Project to Intercompare Regional Climate simulations (PIRCS). *Journal of Geophysical Research* **104**, 19, 443-19,449.

Troen I, Mahrt L (1986) A simple model of the atmospheric boundary layer: Sensitivity to surface evaporation. *Boundary Layer Meteorology* **37**, 129-148.

Wilks DS (1995) *Statistical Methods in the Atmospheric Sciences*. Academic Press, 467pp.

Appendix

Acronyms used in this paper:

AC – Anomaly Correlation
BI – Burning Index
CAPE – Convective Available Potential Energy
DJF – December January February
ECPC – Scripps Experimental Climate Prediction Center
ERC – Energy Release Component
FWI – Fire Weather Index
GDAS – Global Data Assimilation System
GOES – Geostationary Operational Environmental Satellite
GSM – Global Spectral Model
IC – Ignition Component
JJA – June July August
KBDI – Keetch-Byram Drought Index
MRF – Medium Range Forecast
NCAR – National Center for Atmospheric Research
NCEP – National Centers for Environmental Prediction
NFDRS – National Fire Danger Rating System
NOAA – National Oceanic and Atmospheric Administration
NWCG – National Wildfire Coordinating Group
RAWS – Remote Automated Weather Station(s)
RF – RAWS observations versus ECPC forecast values
RMSE – Root-Mean Square Error
RSM – Regional Spectral Model
RH – Relative Humidity
RV – RAWS observations versus ECPC validating observations
SC – Spread Component
SD – Standard Deviation
UTC – Coordinated Universal Time
VF – ECPC validating observations versus ECPC forecasts
WIMS – Weather Information Management System
WRCC – Western Regional Climate Center